Out of the darkness and into the light: The quest for fluorescence-based soil tracers

Robert Hardy

Lancaster Environment Centre

Lancaster University

Submitted for the degree of Doctor of Philosophy

September 2016

Abstract

This thesis explores the use of fluorescent tracers to monitor the redistribution of soil at high temporal and spatial resolutions. Soil redistribution happens on a second by second basis with individual particles moving millimetres at a time. There are few, if any, existing tracing methods which permit the monitoring of soil movements at temporal and spatial scales that are commensurate with the scales at which these movements happen. This thesis charts the development of new tracing technologies that allow for the movement of soil to be monitored at high spatial and temporal resolution, resolutions which are commensurate with the movement of individual particles. This will allow for deeper insight into how soil moves and has a range of applications for fundamental soil movement studies to applied agricultural investigations. In order to study the movement of clay a novel fluorescent clay tracer was created along with fluorescent imaging techniques which allowed for the movement of this tracer to be captured. The movement of larger soil particles is also important and by using a commercially available fluorescent tracer combined with fluorescent videography it was possible to track the movement of individual soil particles across a soil surface during a simulated rainfall event. The movement of these particles was captured 50 times a second with sub-mm precision. A similar system was then developed for use in the field environment and was demonstrated at field scale by monitoring the redistribution of a tracer across a soil surface as a result of tillage. It was also possible to monitor the vertical redistribution of the tracer within the soil profile by digging soil pits. The methods detailed here show that it is possible to gain much information about the redistribution (i.e. change in location) of soil across a soil surface without the inconvenience, expense and system perturbation that is caused by traditional sampling. Overall these methods demonstrate that it is possible for soil tracing to operate in a data rich environment providing new opportunities to develop, parameterise and evaluate soil movement models.

Acknowledgements

I would like to thank all those that were involved with the construction of this monstrosity. Jackie Pates, John Quinton, Mike Coogan and Mike James for the hours they spent listening to my crazy ideas. Thanks also for all those that have put up with me during my time at Lancaster, of which there are too many to list. It goes without saying that without Beth Penrose this thesis would have never come to see the light of day.

Declaration

Except where reference is made to other sources, I declare that the work in this thesis is my own and has not been previously submitted, in part or in full, to any institution for any other degree qualification.

Chapters 1, 2 and 3 were drafted by Robert Hardy and finalised after discussion with and comment from my supervisors (primarily Jackie Pates).

Chapter 4 has been published in a peer-reviewed journal. The work was carried out by Robert Hardy under the supervision of Jackie Pates, John Quinton and Mike Coogan. The manuscript was drafted by Robert Hardy and finalised after discussion with and comment from my supervisors as well comments from the external reviewers.

Chapter 5 has been submitted peer-reviewed journal and accepted subject to minor revisions. The laboratory work and data processing were carried out by Robert Hardy under the supervision of Jackie Pates, John Quinton and Mike James. The manuscript was drafted by Robert Hardy and finalised after discussion with and comment from my supervisors as well comments from the external reviewers.

Chapter 6 has been prepared for submission to a peer-reviewed journal. The laboratory work was carried out by Robert Hardy under the supervision of Jackie Pates, John Quinton and Mike James. The field work was carried out in collaboration with John Quinton and Peter Finer's team (Ausburg University, Germany). Data processing was conducted by Robert Hardy The manuscript was drafted by Robert Hardy and finalised after discussion with and comment from my supervisors.

Chapters 7 and 8 were drafted by Robert Hardy and finalised after discussion with and comment from my supervisors (primarily John Quinton).

Statement of authorship

Authorship of the work in this thesis and the results described therein have been collected and written as acknowledged in the declaration.

R. Hardy

J. Pates

J. Quinton

M. Coogan

M. James

Table of contents

Table of figures

Table of tables

Chapter 1: Thesis introduction

1.1 Thesis overview

The overarching aim of this thesis is to develop tracing tools to help understand how soil moves in the natural environment, and more specifically to understand the movement of material (particularly clay) over the surface of soil. Existing methods for exploring the movement of soil have significant limitations, which include limited temporal and spatial resolution, high cost (in terms of time and money) and poor (or unknown) ability to mimic the natural behaviour of soil. Therefore, with the aim of reducing or removing some of the current limitations, particularly relating to temporal and spatial resolution, new methods to understand how soil (specifically clay) moves, were designed, tested and evaluated.

1.2 Global soil erosion

Soil erosion is a global problem, with global average loss estimated to be 0.38 mm of soil per year, most of which is a result of human activity (Yang et al. 2003). Water is a major driver of soil erosion; it is estimated that water induces soil erosion on 1.1 billion ha of land with 68% of that being severely affected (Lal 2003). It is expected that soil erosion will become an increasing problem in the future as a result of climate change and land use change (Yang et al. 2003). Around 90% of the world's agricultural land suffers from erosion problems with 80% being moderately to severely affected (Pimentel et al. 1995).

Soil erosion is a problem for a variety of reasons, centred on both the eroded land and the receiving water bodies. Arable land plays an important part in food production, and in some cases, soil erosion has led to land abandonment due to loss of soil fertility (Wood and Armitage 1997). Fertility loss due to erosion results from a collection of mechanisms, including physical loss of soil and leaching of nutrients. Transport of soil into surface water bodies has been shown to increase the likelihood of flooding due to siltation (Yin and Li 2001), while increasing turbidity, which reduces the amount of light able to penetrate the surface, and hence reducing primary production (Cloern et al. 2014). Eroded sediment can also act as a vector for other types of pollution, which are bound to the surface of the transported particles. Examples of these pollutants include metals (Quinton and Catt 2007), pathogens (Tyrrel and Quinton 2003) and phosphorus (Sharpley et al. 1984), the last of which is known to cause eutrophication in surface water bodies (Catt et al. 1998, Haygarth et al. 2005).

1.3 Regional erosion variability

Erosion rates vary on global and local scales. Using water-induced erosion as an example, on the Brabant Plateau in central Belgium it was found that soil erosion rates were on average 6 Mg ha^{-1} yr^{-1}. However, over 30% of the arable land studied had an erosion rates of over 10 Mg ha^{-1} yr^{-1} and erosion rates as high as 50 Mg ha^{-1} yr^{-1} were found in certain areas (Van Rompaey et al. 2001), highlighting the variation present within a relatively small area (850 km^2). While the average rate may not be considered a threat to land sustainability, the higher erosion rates certainly are. It was noted that most of the erosion happened as a result of high intensity showers, which resulted in water flowing over the soil surface, transporting pesticides and nutrients into the local watercourses. In other words, the erosion was largely event-driven, rather than a steady process. Although water erosion has been used as an

example here, there are also other drivers for soil erosion, such as wind, ice and human activity (Sumner 2000).

1.4 Soil and its movement

Soil erosion can be thought of as the detachment and subsequent transport of soil particles away from the bulk soil (Morgan 2005). Generally, erosion on hillslopes is either transport limited, meaning the erosion rate is limited by the amount of material that can be moved away, or detachment limited, where the erosion rate is limited by the rate at which material can be detached from the bulk soil (Pelletier 2012). Bare earth hillslopes are often transport limited, as the energy needed to detach material is low, whereas slopes that are vegetated are often detachment limited. Nonetheless, in both cases detachment must occur before transport can take place. There are a number of mechanisms which lead to detachment including: mechanical (including tillage), aeolian, and hydrological processes (e.g. rain splash and overland flow) (Pimentel et al. 1995). It should also be remembered that soil redistribution happens on a second by second basis with individual particles moving millimetres at a time.

Soil consists of a number of different fractions, some of which are defined by the size of the particles (Table 1.1). Energy is required to both detach and transport soil particles and, for non-cohesive sediments, the amount of energy that is required is related to the size of the particle; generally smaller particles will be eroded more easily that larger particles.

Table 1.1 Classification of soil fractions by particle size (Sumner 2000)

Coarse soils	**G** GRAVEL	Coarse	20 - 60 mm
		Medium	6 - 20 mm
		Fine	2 - 6 mm
	S SAND	Coarse	0.6 - 2.0 mm
		Medium	0.2 - 0.6 mm
		Fine	0.06 - 0.2 mm
Fine soils	**M** SILT	Coarse	0.02 - 0.06 mm
		Medium	0.006 - 0.02 mm
		Fine	0.002 - 0.006 mm
	C CLAY		< 0.002 mm

The clay fraction represents the smallest particle sizes (< 2 µm; Table 1.1) and as one of the smallest particles found in soil, it is also one of the most easily transported (Sumner 2000). However, clay exhibits a number of unique properties, such as a tendency to flocculate and aggregate. This tendency results in clay moving in a different way than would be expected based solely on particle size, and therefore when the clay fraction of soil moves, it is possible that the transport of this is dictated by the size of the clay aggregates, not the individual particles. In addition to being highly mobile, clay is an important vector for the transport of a variety of other materials owing to its high surface area to volume ratio and its ability to sorb ions. These materials include a wide variety of chemical nutrients (Syers et al. 1971), heavy metals (Quinton and Catt 2007) and organic compounds (Homenauth and Mcbride 1994). The exact nature of the ions which a clay particle will sorb relates to the structure of the clay.

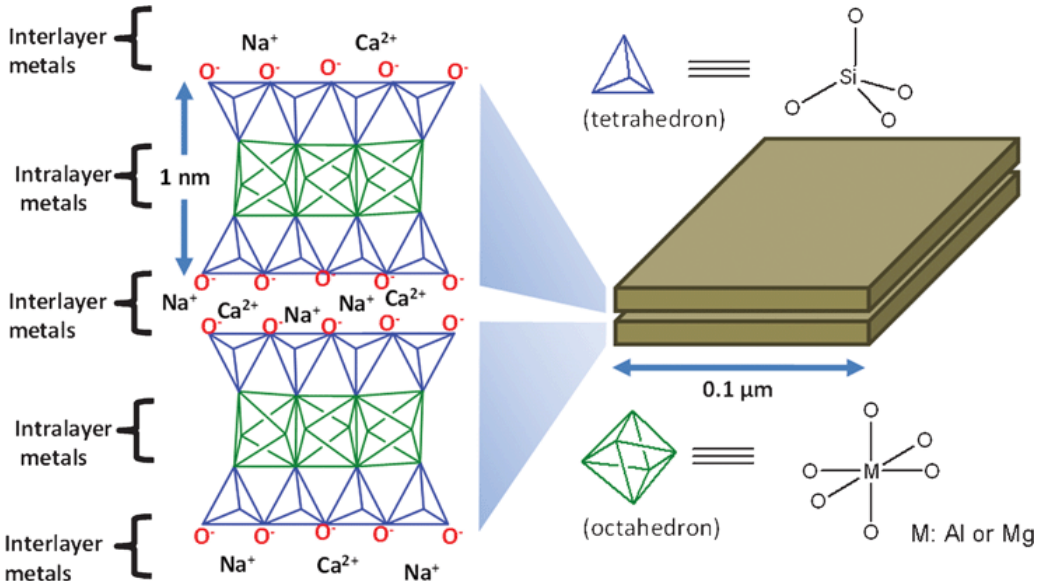

Figure 1.1 The generic structure of clay (Zhu et al. 2012)

Isomorphic substitution, which is the exchange of an interlayer ion in the clay matrix for another of a different (and often lower valance) ion, often results in clay gaining a net negative charge (Sumner 2000). In order to balance the charges, cations tend to become associated with the clay, a process which is facilitated by clay's large surface area and multitude of binding sites. Due to clay being an important vector for contaminants, understanding the movement of this soil fraction is of particular importance, and there are few tracers available which are able to do this successfully. Developing a tracer for the clay fraction is therefore a focus of this thesis.

1.5 Why are tracers important?

Directly studying soil movement is challenging, as soil is made up of many small and similar looking particles which cannot be uniquely identified. Tracers, however, can be easily identified from the bulk soil, often either chemically or visually.

Traditionally, bulk movement measurements have been used, for example, to measure the total amount of soil that leaves a field in a given time. However, these measurements lack detail about the pathway and velocity at which the soil particle has travelled. For example, very little is known about how individual soil particles move over a soil surface as a result of

rainfall. Specifically, there is virtually no information about the pathway a particle takes and the speed at which it travels in response to rainfall.

It is possible to obtain information about the pathway and speed of motion of individual soil particles and identify when they are in motion using soil tracing methods. However, no current tracing techniques, to my knowledge, have been extensively used to measure this at a high resolution in the field.

1.6 Why fluorescence could be useful?

Fluorescent tracers are used in this thesis as they offer a number of advantages over existing tracing methods. They are easy to detect with both the human eye as well as instrumentation (such as a camera). There are many known fluorescent compounds and therefore it should be possible to select compounds that have the desired properties. As cameras are capable of detecting fluorescent compounds it may be possible to take advantage of a camera's capacity to offer highly spatially and temporally resolved data.

1.7 Range of scales

Many existing methods are designed to function at limited spatial scales, for example either in the laboratory or in the field, but few that are capable of operating effectively from the micro to macro scale. Having a technique that can operate at varying scales would allow a more direct comparison between micro and macro scales, as well as reducing the potential for method bias causing differences between experiments that are conducted at different scales. It could also simplify erosion studies by allowing the same study to obtain data (and therefore study soil processes) at a range of temporal and spatial scales. These scales could range from, for example, second to day and millimetre to metre scales. In this thesis I aim to look at soil movement from a 50^{th} of a second to tens of minutes, and hundreds of microns to tens of metres.

1.8 Thesis motivation and rationale

This thesis presents the development of tools which will allow for deeper insights into how soil moves, through the use of tracers. Of particular interest is the movement of clay across a soil surface, as there is currently a lack of existing tracing methods which allow for this fraction of soil to be studied. During the development of this thesis it also became apparent that there was a lack of tracing solutions able to investigate individual particle movements over small temporal and spatial scales. It was also noted that there was a lack of technologies which could operate over a wide range of temporal and spatial scales. As such, this thesis aims to present a technology which is flexible, and therefore can be adapted to suit the needs of many different studies, which may operate at different resolutions.

As stated in Section 1.4, soil erosion happens on a second by second timescale, with individual particle of soils often only moving a few millimetres. Currently there are few, if any, tracers that allow for studies to be undertaken at this resolution. Studying soil movement at a scale and resolution which is commensurate with the scale and resolution at which soil movement takes place at is likely to give deeper insights into soil movement than investigations which do not.

The tools that are developed in this thesis are not designed to solve a particular problem or issue, although many examples are given showing how they can be used (see Chapters 4, 5 and 6). As a more explicit example, soil erosion models, such as MALARHAM (Wainwright et al. 2008), allow for the generation of temporal and spatial resolved data, but there is a lack of empirical data (of matching temporal and spatial resolution) which can be used to evaluate and parameterise these type of models. This thesis presents methods which allow soil tracing to be undertaken in different forms and at different resolutions than are currently possible. This should allow for the formation of a more complete picture of how and why soil is transported. For example, the development of a tracer which would allow for the high

resolution tracing of soil under dynamic conditions would allow a deeper understanding of what happens under these conditions than is currently possible.

Once it became clear that it would be possible to monitor the movement of clay across a soil surface at moderate temporal and spatial resolutions (Chapter 4) the work was extended to encompass larger sized soil fractions. This gives the techniques presented here larger scope by enabling them to be used to investigate more types of soil, for example those that do not have a significant clay component.

In this thesis, much reference is made to rainfall driven erosion, mainly due to the large amount of literature which exists about the topic, and as rainfall driven erosion is likely to be a significant erosive force in study areas within easy reach of the university. However, efforts were made to demonstrate that this technique is not only applicable to the study of soil due to rainfall, such as in Chapter 7, where the influence of tillage on soil is considered.

Chapter 2: A critical review of existing tracer methodologies

2.1 Easy to observe but hard to measure

"Easy to observe, but hard to measure" is how Polyakov and Nearing (2004) described the process of soil erosion. Mass balance studies, soil and hydrological modelling and soil tracing are some of the techniques available for the understanding of soil erosion in the short to medium term. Tracing generally involves adding an easy identifiable substituent (tracer) to soil or sediment. Tracers allow for the acquisition of empirical data regarding the pathways that soils take during an erosion event and they can be used to show deposition of soil over a large area, both of which are unobtainable using other methods such as modelling and mass balance techniques. This review will focus on existing tracers and their associated methodologies with the aim of elucidating the characteristics which the perfect tracer (and

associated methodology) would have. Basic information relating to how soil erosion operates can be found in Section 1.4, and Section 1.5, which highlights why tracers can be useful in understanding erosion processes. Although the perfect tracer almost certainly does not exist, understanding the features that the perfect tracer might have can go a long way towards trying to design better tracers.

2.2 The perfect tracer and tracing methodology

2.2.1 Fundamental limitations with current tracing methodologies

The relative advantages and disadvantages of various tracing techniques have been described at length in the literature, e.g. (Parsons and Foster 2011, Guzman et al. 2013, Mabit et al. 2013). Basic background information about some of the most commonly used tracing techniques can be found in later sections of this chapter; radionuclides (Section 2.3.1), magnetic tracers (Section 2.4) and rare earth elements (REE; Section 2.5). However, there is little literature describing the overarching limitations of current tracing methods. Here, some of these limitations are explored in more detail, with the aim of understanding how they affect the progress of soil science.

2.2.2 Characteristics of the perfect tracer.

The perfect tracer: behaves exactly the same as the material that it is tracing; is straightforward and cheap to manufacture (if required); is easy, cheap and rapid to detect; and works on a variety of scales and resolutions (both temporal and spatial) (Zhang et al. 2001, Guzman et al. 2013). In many ways, the ability to detect the tracer is the most important feature; after all, the tracer may be perfect in every other way, but if it cannot be identified then it is of no use. Tracers can generally be classified into two groups, native or applied, with the difference being that native tracers already exist within the environment, whereas applied tracers have been added, generally intentionally.

2.2.3 Tracer likeness

In many ways, the ideal tracer would be a perfect mimic of the material which it was trying to trace; most current tracers are reasonably deficient in this respect. For example, if trying to trace clay movement, current options include radionuclides such as ^{137}Cs (which is liquid metal at 28 °C), trace heavy metals (REE such as Nd and Y) and plastic or magnetic beads. The base materials of many tracing methods (such as heavy metals or plastic) do not bear much resemblance to soil. However, they are often processed in an attempt to make the differences between the tracer and the soil less pronounced. For example, REE are often ground to a fine powder which makes them a similar size to clay particles, but their density is higher than clay and they do not have the same physical and chemical properties, such as cation exchange capacity (CEC), shape, and tendency to aggregate. Magnetic or plastic beads not only have different chemical and physical properties, such as CEC, shape and aggregation tendency, but additionally are extremely different in terms of size and shape to soil particles. In the case of ^{137}Cs tracing, ^{137}Cs itself bears little resemblance to soil but when added to soil should have negligible impact on the soil properties, as the amount of ^{137}Cs present in terms of mass is extremely low and the adhesion process is natural. However, as previously discussed, the method relies on the assumption that the soil and the ^{137}Cs remain irreversibly bound (see Section 2.3.2), which may not always be the case (see Section 2.3.2.2). For the times when this assumption is not correct (i.e. when the ^{137}Cs can move independently from the soil) then there would need to be evidence that ^{137}Cs has similar properties to soil when it is not attached to soil. Given that ^{137}Cs is an extremely reactive metal that is liquid at room temperature there is little reason to believe that ^{137}Cs and soil share physical or chemical properties. Therefore, how closely the ^{137}Cs tracer mimics the movement of soil is therefore linked to how much of the time it remains absorbed onto soil and how far ^{137}Cs can travel without being attached to clay. Overall it can be concluded that ^{137}Cs itself is a poor mimic for clay however, ^{137}Cs labelled clay, which is the material that is really being traced, is a

good mimic. Some tracers have been designed to accurately mimic the natural properties of the substance which they are trying to trace (e.g. the marine tracer Partrac Ltd., Black et al. (2013)). This tracer is designed to be used in the sea to trace the movement of sand, and is based on a natural sand core. This sand has been coated with a thin, hard, smooth layer of fluorescent pigment, which adds to the diameter of the particle (but often not significantly), while retaining some of the properties of the sand from which it is made, e.g. there is little change in density or size of the particles.

Armstrong et al. (2012) baked natural clay to enhance its magnetic signature, and used it as a tracer for clay movement. As both the tracer and the substance that is being traced were similar initially, the tracer could be considered a close mimic to the clay it traces. However, the conditions used to bake the clay are far more extreme than ordinarily found in nature (i.e. > 100 °C, under reducing conditions). These conditions may cause the removal of organic material, which is naturally associated with the clay, and will alter the properties of any organic material present. However, this 'baked' clay is likely to be more similar to natural clay than any metal or plastic substance.

2.2.4 Sampling

Almost all current tracer methodologies require physical collection of material. This requirement presents one of the most significant limitations to the usefulness of soil tracers. The sampling density of studies is highly variable (Guzman et al. 2013), and is always a balance between maximising the information obtained about soil movement with the cost and effort of collecting, transporting and processing the samples. Therefore, it appears that the practicality of sampling affects the spatial resolution of the tracer techniques. Similar considerations can also impact the temporal resolution of a study. For example, cost of travelling to the field site may be a limit to the number of events (such as summer thunderstorms or winter storms) after which samples can be collected. Across all the

literature reviewed here, the most time-resolved studies were event-based. There was no evidence of any methodology that has be used to monitor the spatial redistribution of soil on short timescales (< 1 minute).

Another issue with physically sampling the study site is that it can perturb the system which is being studied. This is because removing material from the sample site often impacts on the processes being studied. It is also highly impractical to physically sample during many events, such as a thunderstorm. Therefore, if highly temporally resolved data is desired, then any method which requires physical sampling would be hard to successfully implement. Even removal of minimal amounts of material often involves walking over the site which will impact the study. As an example, walking over a recently tilled field is likely to compress it and create local depressions which may collect runoff, therefore altering the process that would normally occur in a field.

Overall these issues make physical sampling seem very unattractive, yet almost all tracing studies make use of physical sampling, as there are few alternatives currently available. Only a few studies have used *in situ* methods to determine tracer concentrations in the field. Caesium-137 can be determined *in situ* (Mabit et al. 2008), however the equipment is expensive, not very portable and has much poorer detection limits than laboratory-based methods. Consequently, none of the large-scale (with a study area greater than 100 ha) ^{137}Cs-based studies included in the review by Guzman et al. (2013) used *in situ* measurements. Depending on the desired outcome of the study, *in situ* monitoring of ^{137}Cs may be sufficient, however it is not able to operate at resolutions which are commensurate with the scales at which soil erosion takes place at, i.e. small (< 1cm) movements of individual particle happening on a second by second timescale.

Magnetic properties can be determined *in situ* and Armstrong et al. (2012) used this property to study the movement of magnetically-enhanced clay. They were able to evaluate

the redistribution of clay by comparing the magnetic susceptibility (high and low frequency) and remnant magnetisation (natural and anhysteretic) of a given area before and after a simulated rainfall event. Partrac Ltd. distributes tracers containing iron oxides, giving them a strong magnetic signature, which can be sampled using a magnetic susceptibility sensor (Black et al. 2013). Both these techniques require the user to hold the sensor within a few millimetres above the ground, which, in the case of a field site, means that researchers need to walk over the field site in order to collect measurements, which may impact on the process being studied. As with the collection of samples, taking point measurements is also limited by the time and personnel available for the study.

Overall, it is clear that sampling limits the temporal and spatial resolution of a technique, and is a barrier to understanding soil redistribution on short-term timescales and under highly dynamic conditions. Although there are some techniques in existence which do not require sampling, uptake of these techniques has been poor and the time and expense these techniques require are likely to be barriers to adoption. Therefore, there is still a need for a tracing methodology which does not require the removal of material from the study site.

2.2.5 Uncertainties

Many tracing methods have a poor handle on the magnitude of uncertainties associated with them. One of the clearest examples is the ^{137}Cs method; the method assumes that the spatial deposition of ^{137}Cs is relatively uniform, however there is reasonable evidence that this is not the case. It is worth noting that is it is very hard to truly measure the magnitude of the resulting uncertainty and this issue extends to other tracers, such as REE. For example, there are often unknown, variable concentrations of naturally-occurring tracers present in soil. Therefore, when these tracers are applied to soils, and subsequently analysed, it can be difficult to discern what concentrations of the tracers are attributed to the applied tracer, and which were present before the application. In the case of ^{137}Cs, this is due to the fact

that the material was deposited over a number of rainfall events and the local intensity of these events, along with the amount of ^{137}Cs deposited per event is unknown (Parsons and Foster 2011). The obvious solution to this issue is to conduct "pre-sampling" before studies are undertaken, which would allow the concentrations present to be determined, though this "pre-sampling" can interfere with soil processes, and therefore results may not be representative of what would happen in a natural area (i.e. one that had not undergone pre-sampling). One solution to issues associated with determining background levels of pre-existing tracer material is to create a tracer that does not already exist in the environment, and therefore can be easily discerned from the background.

2.2.6 Tracer availability

A tracer must be affordable both to manufacture (if required) and to analyse. Most commonly used tracers are inexpensive, although there are some more exotic tracers which can be quite expensive, such as fluorescent microspheres. However, in terms of being a fundamental limitation to soil science, the cost of a tracer is largely irrelevant, it simply constrains the scale or replication level of a study. Methods that are based on the natural properties of soils (such as the ^{137}Cs concentration or the magnetic signature) are only possible in places where these properties occur, thus limiting their availability.

2.2.7 Temporal scales and their influence on 'perfect' tracer methodology

The temporal and spatial scales at which a study is operating have a major effect what properties are desirable in a tracer. Guzman et al (2013) calls for the use of ephemeral tracer where that the lifetime of the tracer is matched to the lifespan of the study which prevents having tracers present in the soil for long periods of time after the study has been completed. . In relation to temporal scales, and as a minimum, the tracer must exist in sufficient quantities to be detectable for the duration of the study. For example, if the study of long term soil movement is desired, and is therefore going to operate over tens of years,

then the tracer must exist for at least that length of time, ideally without degradation of the tracer. If degradation of the tracer does occur, then ideally this would happen via a well-defined and easily modelled pathway. Caesium-137 (see Section 2.3.2 for more details) is a good example of this as it has a well understood decay profile which is unaffected by environmental factors and the decay of the tracer is easily modelled. Conversely, if a study of a short-term soil process such as response to an individual rainfall event is required, then the tracer only needs to be detectable for the short time required (hours to days) for the event to occur plus the amount of time required for it to be analysed. In terms of spatial scales, the ideal tracer and tracing methodology would operate at the spatial scale required for studying the desired process. For example, splash erosion often results in soil particles being moved small distances (mm to cm) therefore millimetre resolution would be helpful, however this process can occur over large spatial area such an entire field; an ideal tracer and methodology would be able to observe this.

2.2.8 Concluding remarks

Fundamentally, the most important aspect of a tracer and its methodology is that it can investigate the desired soil process in sufficient detail within operational constraints. Sufficient detail would give understanding of the soil process at adequate temporal and spatial scales and resolutions. Operational constraints would include factors such as time (e.g. the time to set up or decommission the study, time to analyse the samples), manpower, equipment availability, logistics and environmental factors such as temperature, wind speed and rainfall

2.3 Existing methodologies

There are several existing tracing methodologies, most have been described at length in existing literature and reviewed recently by Guzman et al. (2013). Therefore, a detailed

review will not be repeated here, although a brief introduction to some of the most widely used tracing methods has been included. The aim of this review is to explore the limitations of existing tracer methodologies (both practical and theoretical) and relate these back to the ideal characteristics that a tracer should have (see Section 2.2)

2.3.1 Radionuclides

Radionuclides are the most commonly used type of tracer, accounting for over 40% of all tracer studies (Guzman et al. 2013). Many radionuclides have been used as soil tracers (Walling 2003, Mabit et al. 2008), including ^{210}Pb (half-life = 22.3 years), which is a naturally occurring product of the uranium decay series, and ^{7}Be (half-life = 53.22 days), which is a naturally occurring cosmogenic radionuclide, and ^{137}Cs (half-life = 30.2 years), an anthropogenic radionuclide, which, in this context, largely resulted from atmospheric nuclear weapons testing. Radionuclides are generally easy to detect and quantify, although this process can be time consuming.

As ^{137}Cs is the most commonly used of these radionuclides, there is extensive literature relating to its use and well documented methodologies for its use. Therefore, ^{137}Cs will be the focus of this section, although many of the issues identified are relevant to other tracer radionuclides.

2.3.2 The ^{137}Cs tracing methodology

Caesium is the most electropositive element making it highly reactive, leading to strong and rapid binding with soil particle surfaces (especially to clay and organic matter) after its deposition on a soil surface (Ritchie and McHenry 1990). Moreover, caesium's chemical similarity with potassium means that, over longer time-scales, it readily undergoes isomorphic substitution, resulting in long-term and irreversible incorporation into the clay matrix (Mukai et al. 2016). To use ^{137}Cs as a tracer, soil samples are collected from the field and a profile of the concentration of ^{137}Cs with depth is created. This profile is then

compared to an undisturbed soil profile with differences between profiles being attributed to soil movement. There are two basic assumptions that the tracing method is built on. Firstly, it is assumed that the distribution of ^{137}Cs on the soil surface is spatially uniform. Secondly, it is assumed that ^{137}Cs and the soil are both being re-distributed by the same physical processes, and that other mechanisms (e.g. biological and chemical) have no significant role in re-mobilising or preferentially removing the ^{137}Cs. The validity of these assumptions is discussed below.

2.3.2.1 Initial uniform distribution

Parsons and Foster (2011) published a critical review of the use of ^{137}Cs in soil erosion studies, which raises some fundamental questions about the assumptions the tracing methodology is based upon, critically arguing that the assumption of initial uniform distribution is incorrect. An initial uniform distribution relies on spatially uniform fallout from the atmosphere, spatially uniform transfer to soil and no redistribution taking place during transfer from rainwater to soil; Parsons and Foster (2011) argue that none of these conditions are met. Rainfall is a significant vector for the transport of ^{137}Cs from the atmosphere to the ground and Parsons and Foster (2011) present rainfall maps showing areas of higher and lower rainfall as evidence that fallout of ^{137}Cs from the atmosphere is non-uniform. Caesium-137 tracing is undertaken on a variety of scales and it is likely that the rainfall will be reasonably uniform over a small scale, e.g. within a field, but it is very unlikely to be uniform on a large scale, e.g. over a catchment. Parsons and Foster (2011) also present evidence that during rainfall events the rainfall rate can be greater than the infiltration rate, which could lead to puddling and runoff, which they identify as evidence that there is non-uniform transfer to soil once water containing ^{137}Cs has been deposited on the soil surface. This could lead to localised areas of high ^{137}Cs concentration within a field, as puddles rich in ^{137}Cs containing water could have formed and subsequently this ^{137}Cs would be absorbed into the soil. The combination of these factors can lead to micro and macro variation in ^{137}Cs

concentrations which are not related to soil movement and the extent of these variations will affect how useful ^{137}Cs is on any given scale. Similar issues are likely to be present for most tracers where the initial distribution of the tracer is not mapped at high resolution. One possible solution to this issue is to have a tracer than can be mapped at high spatial resolutions with easy.

2.3.2.2 ^{137}Cs biological redistribution

Advocates for using ^{137}Cs as a soil tracer (e.g. Guzman et al. (2013)) state that biological uptake of ^{137}Cs is negligible, and therefore imply that biological processes have little effect on the redistribution of ^{137}Cs in soils. However, this assumption has been challenged by Parsons and Foster (2011), who argue that biological uptake of ^{137}Cs is substantial, suggesting that the role of biological processes on ^{137}Cs distribution may largely invalidate the use of ^{137}Cs as a tracer for soil movement. This debate highlights the usefulness of having a tracer that can be shown not to be subject to biological redistribution. If the a given tracer is subject to biological redistribution then then it is desirable to have this happen in a well-defined manner, in order for the effect of biological redistribution to be accounted for in a tracing study.

2.3.2.3 Is there enough ^{137}Cs left?

More fundamental, *a priori,* reasons exist for starting to develop other tracing methods that do not rely on ^{137}Cs. One of the most compelling is that there simply is not much ^{137}Cs left. The majority of ^{137}Cs deposition happened in the early 1960s as a result of the atmospheric testing of nuclear weapons (Guzman et al. 2013), which is over 50 years ago. As ^{137}Cs has a half-life of 30.2 years, around two thirds of this ^{137}Cs has decayed away. As a more explicit example, only 30% of the ^{137}Cs that was deposited in 1966 remains. The accident in Chernobyl (Ukraine, 1986) added additional ^{137}Cs, but this material was mostly deposited regionally (i.e. across Europe; Smith and Beresford (2005)), and furthermore was 30 years

ago, meaning half of that ^{137}Cs has now decayed away. The more recent incident in Fukushima (Japan, 2011) has also deposited some ^{137}Cs, but terrestrial deposition has principally been confined to Japan (Yasunari et al. 2011). Finally, in many areas of the world, insufficient ^{137}Cs has been deposited (from any source) to enable it to be used as a tracer.

The use of ^{137}Cs as a tracer has developed opportunistically, exploiting the presence of ^{137}Cs in our environment. However, there is a need to avoid situations whereby future widespread contamination occurs, and so inevitably this method will become obsolete in the future. To some extent, improved detection methods could extend the working life of ^{137}Cs methods, but these improvements a mitigating measure against decreasing amounts ^{137}Cs in the environment, rather than dealing with the primary issue.

2.3.2.4 Concluding remarks

Mabit et al. (2013) published a reply to Parsons and Foster (2011) stating that it is possible to use ^{137}Cs as a tracer and the fact that some authors have failed to consider some of the limitations of the method is not evidence for the method being invalid overall. All tracing methods make assumptions and it is important to understand how these assumptions affect the conclusions that can be drawn from a given study. In general, it can be said that most assumptions fall into two broad categories; I) assumptions relating to the input of the tracer, and II) assumptions relating to how the tracer moves in comparison to the soil. Much can be learnt about future tracer design based on the experience that has been gained from ^{137}Cs tracing methods. Regarding assumptions, I) it can be concluded that knowing the location and concentration of initial deposition of the tracer is important and for assumption II), it is important for that tracer and the soil to move in the same way. For both assumptions I) and II) understanding the extent to which a tracing method deviates from these ideals will help in understanding the uncertainties related to a method.

2.3.3 Temporal resolution of radiotracers

The temporal resolution of radiotracers is limited by their half-lives, the shorter the half-life the greater the potential temporal resolution. Commonly used tracers, such as ^{137}Cs (half-life 30.2 years) and naturally-occurring ^{210}Pb (half-life 22.3 years) are usually used to determine erosion and sedimentation rates on medium timescales (tens of years; (Mabit et al. 2008)), although measurements of up to 100 years are possible. As ^{137}Cs did not exist before the 1940s, when nuclear weapon development began, it cannot be used to look at sediments or soils older than this date. The only commonly used radionuclide for studying truly short-term soil movement is the naturally occurring ^{7}Be (half-life 53.22 days), which can resolve soil movements on week to month timescales (Blake et al. 2002, Mabit et al. 2008). There are a number of technical difficulties with using ^{7}Be as a tracer, including its short half-life (meaning samples must be analysed rapidly) and the problems in determining the distribution of pre-existing ^{7}Be before the start of a study (Walling et al. 1999, Mabit et al. 2008).

2.3.4 Spatial resolution of radiotracers

An important aspect of any tracing method is its spatial resolution, both in the theoretical and practical sense. It is not possible to achieve a greater resolution that the theoretical limit, which for radiotracers such as ^{137}Cs is likely to be determined by the amount of ^{137}Cs which is required to allow for meaningful measurement of this radionuclide. This affects the maximum resolution as give volume of soil will need to be recovered and it is common to acquire larger volumes of soil by increasing the soil core diameter. As an example, for ^{137}Cs tracing, a depth profile of ^{137}Cs at each sampling site is required. As gamma detection is reasonably sensitive, the amount of material needed is often reasonably small. This often allows for core with a diameter of 5 cm or greater to be sufficient. Therefore, ^{137}Cs tracing offers the potential for moderate to high resolution data. On a practical level achieving this resolution is likely to be difficult as, at plot or field level, this would involve collecting

thousands of samples, which in turn will take months to years to analyse. Perhaps more importantly, having high spatial resolution for a ^{137}Cs study will not be of great benefit as it could be argued that the accuracy of the data is low, as at higher resolutions, the assumptions discussed above start breaking down. For example, at high resolution there is often unknown and presumably non-uniform deposition of ^{137}Cs as well as (see Section 2.3.2.1) with the potential for biological redistribution (see Section 2.3.2.2). Therefore, sampling at high resolution would result in having a highly resolved, but low accuracy, map of soil redistribution which is unlikely to be worth the extra effort required to produce it.

There are a variety of other radio tracers available, such as ^{210}Pb and ^{7}Be. Both ^{210}Pb and ^{7}Be are naturally occurring radionuclides and therefore are not subject some of the issues that ^{137}Cs is, such as the fact that most of the ^{137}Cs present in the environment will decay away in the next few decades. In other ways, ^{210}Pb and ^{7}Be radiotracers are similar to ^{137}Cs. For example, both have a limited spatial resolution due to the time taken to collect and analyse samples. The short half-life of ^{7}Be (53.22 days) further complicates this as the samples must be analysed quickly (within a couple of months) or most of the ^{7}Be will have decayed away.

2.4 Magnetism

There are two main ways that magnetism is used in erosion studies. Firstly, the naturally-occurring magnetic properties of soil can be used as a tracer for the movement of soil. Secondly, magnetic material can be added to soil and the redistribution of this material can be monitored.

2.4.1 Naturally-occurring magnetism

Different soils have different magnetic properties due to variations in type and content of minerals within the soil. Dearing et al. (1986) demonstrated that it is possible to use these natural magnetic properties of soil to trace its movement. Royall (2001) utilised these magnetic properties to assess redistribution of soil at the plot/field scale in Alabama (USA).

Quantification of the amount of soil that has moved is difficult using natural magnetic properties, and bias may be introduced due to differences in speed or pathway taken between the magnetic or non-magnetic material (Guzman et al. 2013). There has also been some success in enhancing the natural magnetism of soil and using the enhanced soil to investigate soil movement in small soil boxes (Armstrong et al. 2012). Armstrong et al. (2012) created magnetically-enhanced soil by baking it at high temperature, which alters the structure of the soil. Furthermore, the use of natural magnetism is limited to soils which have appropriate magnetic properties and therefore cannot be undertaken in many environments.

2.4.2 Addition of magnetic particles

Incorporating magnetic material into soil and using changes in magnetism to map soil movement is also possible (Guzman et al. 2013). Examples include Parsons et al. (1993) who added crushed magnetite, and Ventura et al. (2001) who added magnetic beads to help trace soil movement. However, using incorporated magnetic material to trace soil movement is generally only successful where the natural magnetism of the soil is low and uniformly distributed.

2.4.3 Sampling of magnetic particles

Sometimes it is possible to use magnetic properties to trace soil *in situ* without sampling the soil, however these techniques tend to be qualitative rather than quantitative. Spatial resolution is theoretically limited by the size of the sensor, but in practise is limited by the amount of time available to spend making measurements.

2.5 Rare earth elements (REE)

Guzman et al. (2013) estimated that around 13% of all tracing studies use REE. Generally tracing with REE involves incorporation of an REE into a soil in discrete patches before the experiment is started. REE have been used on a variety of temporal and spatial scales. REE

have been used for studies on multiple timescales, from studies operating on week timescales (Zhang et al. (2001), Zhang et al. (2003)) to multi-year studies (Kimoto et al. 2006). While most REE studies have been carried out on small spatial scales (plot or flume scale) (Guzman et al. 2013), there are examples of studies on much larger scale, such as Mahler et al. (1998) who studied the movement of sediment in the Klast catchment in the USA. REE can be detected in very low concentrations (PPB) using INAA (instrumental neutron activation analysis) or ICP-MS (inductively coupled plasma-mass spectrometry). INAA generally offers better detection limits than ICP-MS, however most studies use ICP-MS (Guzman et al. 2013) because it is cheaper, more widely available and the detection limit is adequate. Both methods of analysis are slow and expensive, especially when sample collection and preparation are considered, which tends to limit the scale and/or resolution of studies. It should also be considered that REE are not that rare and often exist in detectable concentrations in many soils around the world, which can give an unknown and variable background concentrations of the REE, further complicating analysis.

2.6 Fluorescent tracers

The use of fluorescent tracing has been reasonably limited, though there are some examples of its use. These include the use of fluorescent microspheres (which are spherical, fine silt-sized plastic beads) in soils (e.g. (Burkhardt et al. 2008, Nielsen et al. 2011)) and in watercourses (e.g. (Tauro et al. 2012)). Other examples include the use of sand-sized fluorescent particles, mainly in marine and estuarine environments such as those developed by Black et al. (2013). There have been efforts to develop *in situ* fluorescent tracing techniques for use in oceanography. For example, Tedetti et al (2011) developed a technique which used fluorescence to track anthropogenic pollutants around the Mediterranean coast. Although there are some examples of use of fluorescent tracers in soil movement studies, little or no work has been done which allows for *in situ* high resolution measurement of

tracer (and therefore soil) movement to be obtained. Furthermore, fluorescent microspheres often have a different density than that of the material that they aim to trace. For example, Burkhardt et al (2008) used fluorescent microspheres to trace colloidal material, despite the disparity between the density of the fluorescent microspheres and the colloidal material they aimed to trace. In addition to the literature reviewed here, there have been a number of studies on tracing in marine environments, such as Gerino et al (1998), Bradshaw et al (2006), and excellent reviews including Black et al (2007).

2.7 Ideal characteristics of new tracing technologies

It may seem that, so far, the aim of this thesis has been to undermine existing tracing techniques, particularly ^{137}Cs. However, this was not the goal, rather by looking critically at the fundamental strengths and weakness of a tracer, it is hoped that a framework for creating better tracers can be developed. Caesium-137 has been examined more extensively that other tracers simply because it is one of the most widely used, and therefore has more documentation of the methodology. Also, it is reasonable to assume that it is widely used because it had the most advantages when compared to other available methods.

2.7.1 Easy to identify tracer while being a good mimic

Though the core concept behind the use of ^{137}Cs as a tracing technique is sound, the execution of it is poor. This may be a result of the tracer methodology being developed opportunistically from a collection of unfortunate events, rather than by a well-designed and executed plan. However, the ability to label soil (or a fraction of soil) with a very small amount of a substance that makes that soil easily identifiable, but does not significantly alter its properties, is potentially very useful. The gamma photons emitted by ^{137}Cs are easily detected and identified, using a gamma detector. If an alternative, less harmful, but easily detected material could be used, then this may offer a useful way of labelling soil fractions.

Using an easily detectable part of the electromagnetic spectrum (like gamma photons) to detect the tracer could be useful for future tracing methods. Visible light (wavelength ~400-750 nm) is readily detected by the human eye. There are variety of are detectors available to aid the quantification of visible light. These range from simple photoresistors to complex complementary metal oxide sensor (CMOS) arrays found in modern digital cameras. There are no significant hazards associated with the use of visible light.

One source of visible light with a relatively well-defined and unique electromagnetic signature is fluorescence. Fluorescence requires the excitation of fluorophore with a specific wavelength of light, which is generally different from the wavelength that is emitted. There is a vast range of chemicals that are known to fluoresce under particular conditions. Fluorescence can be measured very precisely, and thus offers extremely high sensitivity, even allowing the detection of single molecules (Sauer et al. 2011). As these chemicals can be detected in small quantities they would only need to be added to soil in small amounts. If the appropriate chemical be found and added in the appropriate way, then this could result in soil that is fluorescent but retains many, if not all, of the properties of "normal" soil. Therefore, developing new tracers with fluorescent properties could be advantageous.

2.7.2 Tracer stability

Much criticism of the use of ^{137}Cs as a tracer stems from the fact that it might not stay bound to the soil, so a new tracer should ideally avoid this problem. Expecting any material to be completely irreversibly bound to all different types of soil is unrealistic, especially when one considers the wide range of conditions that can be present in soils around the world. If creating a tracer that binds to all types of soil proves impossible, understanding the extent to which the soil and the labelling material are likely to dissociate would be useful. As assessment of every possible soil type is likely to be highly time consuming, it may be better

to have a general testing method which can assess the extent of dissociation between the materials that make up the tracer.

2.7.3 Tracer availability

Tracers that are in frequent use need to not only be stable and easily identified, but also readily available. For example, REE, which are reasonably widely used, are obtained through mining, and can be purchased as a fine powder. Generally, they are mixed into the soil and assumed to bind to some of the soil material. Caesium-137, which has been distributed in the environment due to weapons testing and nuclear accidents, has been integrated into soil by dissolved ^{137}Cs in rainwater binding with soil fractions such as the clay montmorillonite (Bostick et al. 2002). Some other, more exotic, tracers (e.g. ceramic prills, fluorescent microspheres) have failed to gain widespread adoption, which might be related to the more complex nature of their manufacturing process which can result in high costs. It is desirable to have a tracer that, in addition to having similar properties to soil (see Section 2.2.3), is simple, cheap and easy to manufacture, or requires no manufacturing at all. Therefore, future tracing methods need to use materials that are easily available and without great expense.

2.7.4 We are all on a budget

There have also been calls, for example from Guzman et al. (2013), for the development of tracer and tracing techniques which are inexpensive. This is unsurprising as although many tracing technologies have existed for an extended period of time (tens of years), very few can be considered cheap. Therefore, the ideal tracer system would have minimal start-up and running costs.

Radionuclide-based techniques generally rely on gamma spectroscopy (e.g. Zhang et al. (2016)) and require a gamma spectrometer and associated electronics, which are reasonably expensive. Additionally, in order to function, the gamma detector must be cooled using

liquid nitrogen which adds to the running cost. Similarly, REE studies generally rely on some type of destructive spectroscopy like ICP-OES (inductively coupled plasma optical emission spectroscopy) and/or ICP-MS (inductively coupled plasma mass spectroscopy) (Deasy and Quinton 2010). Both of these instruments are expensive to purchase, with ICP-MS potentially costing millions of pounds. The requirement of both of these techniques to generate a plasma, through the use of argon gas, also add considerably to the running cost.

2.7.5 Limits of optimisation and the need for new methods

As previously discussed, there are a number of tracing methods available, and optimisation of these may be the approach to combat their associated limitations. Most existing methodologies have been around for a number of years and have evolved over time, however there are limits to how much a method can be optimised. For example, if a method is only 10% optimised then there is still a lot of room for further optimisation, and increasing the optimisation by 20% (to 30%) is often easily achieved. However, increasing optimisation from 95% to 100% is much more difficult, as there are fewer opportunities for further optimisation, for example increased resolution, reduced cost or increased accuracy. Exactly how much room for optimisation there is in existing methods is unclear. However, easy, 'low hanging fruit' optimisation of frequently-used, historical methods is likely to have already been achieved. Given that there has been very little change in the last ten years in the way many tracers (e.g. ^{137}Cs, REE) have been used and measured suggests that the point of diminishing returns regarding optimisation may have been reached, unless a paradigm shift in measurement technologies is achieved. This contrasts with fluorescence-based techniques, which have also existed in some form for many years, as the last 10 years has seen major changes in the way that fluorescence can be detected. This is due to the widespread availability of photodetectors which can operate at very high spatial and temporal resolutions (see Section 2.7.7 for more details).

Most existing methods of soil tracing work within a paradigm where large investments in sample collection and processing are expected, high levels of uncertainly are accepted and poor resolution is the norm. Existing methods allow for marginal gains in one area, but often at the expense other area. For example, resolution can be increased by sampling more, but sample processing time is greatly increased as a result. Moving away from this existing paradigm may give us the opportunity to produce a tracing method that is cheap, has high resolution and has low associated uncertainty, as well as allowing data to be collected that was simply not possible before. As very few methods exist which allow soil tracing to occur without sampling, this is potentially a good area in which to develop methods.

2.7.6 Mitigate or redesign?

Based on existing methods, and anecdotal experience, it would appear that there is a tendency to try to find a "work-around" to allow for existing methodologies to be used in new ways or at different resolutions. These "work-arounds" are generally mitigation strategies to circumvent method limitations. A classic example of this is the tendency to collect more and more samples in order to study something in more detail or over a greater area. Collecting more and more samples, with a method that is not designed for large sample volumes, may not be the easiest way to acquire the desired data. While doing so may work, at least to some extent, it may be better to redesign the method based on the data required rather than adding mitigation steps. Examination of existing tracing methodologies shows that instrumentation used in current methods often has a high cost per sample, and therefore adding samples results in a requirement for many more resources. The extra resources used to allow for greater resolution have to come from somewhere and this reduces the amount of resources available for other studies. As the environment is highly varied and complex, it is probable that more studies rather than fewer are likely to produce a

better understanding of the systems being studied. This causes any method requiring large numbers of samples to be processed at great expense to be self-defeating. Within current financial constraints, it is not possible to obtain detailed spatial and temporal data from the number of large number of studies required. One solution is to create alternative methods that are designed to produce data of the desired quality and resolution without the expense required by many current methods

2.7.7 Sampling without removing material

Removing the need to physically sample soil would be a significant step towards changing the current paradigm within which soil tracing currently operates. Steps have been made in this direction (such as those detailed in Section 2.4.3), but so far have failed to truly break free. Current methods generally require the user to be physically close to the soil they are sampling (generally within millimetres) and still require a lot of time to take multiple measurements. In order to sample without removing material from the site, the tracer must be detectable from some distance and ideally without disturbing the sampling area when setting up measurement equipment. Digital photographic imaging, which can be performed without disturbing sampling areas, offers the ability to record spatially-resolved data at high temporal rates (typical video cameras run at 50 frames per second and still photographs can be captured in a fraction of a second). These data can subsequently be easily analysed using computers.

Modern digital cameras record visible light, and are capable of detecting very low levels of light using CCD (charge coupled device) or CMOS detectors. The detectors are sensitive to all visible light and some infrared light. To allow for the camera to detect different colours, filters are present over certain sections of the array which only allows certain colours of light to pass through and subsequently be detected. These filters create 3 separate colour

channels, namely red, green and blue. Thus, digital camera technology can be used to record the intensity of light at given bandwidths, and the images produced can be analysed quantitatively. Digital imaging could be a cheap, quick and well-resolved technique to track soil movement. However, in order to be able to quantify the movement of a soil tracer using this technology, the tracer would need to be identifiable against the background soil. Fluorescence is a process where light of a given wavelength is absorbed and the light of another (generally longer) wavelength is emitted. Each chemical fluoresces at a fixed wavelength, and if these wavelengths are in the visible range, they may be detectable using a digital camera. If illuminated, these chemicals will fluoresce, potentially allowing them to be imaged. Multiple images can be taken over time, and the movement of the tracer can be tracked spatially and temporally.

2.8 Knowledge gaps

2.8.1 A clay tracer and imaging system

The lack of a soil tracer which can be detected via an imaging system is currently a barrier to progress in understanding and managing erosion. While there are tracers which are capable of being detected by camera (such as the tracers developed by Partrac; see (Black et al. 2013)), there seems to be lack of tracing systems that make use of digital imaging. Furthermore, these existing tracers do not cover the full range of particle sizes. In particular, the clay fraction of soil has proved hard to trace, and therefore a tracer suitable for clay tracing coupled with an ability to image the tracer at high spatial and temporal resolutions would be an asset to soil science. There is also a lack of information about how to manufacture a good clay tracer, the lighting environment which is optimum for imaging the tracer, and which camera settings produce useable images.

2.8.2 An image analysis package for fluorescent photographs

Once a tracer has been imaged at high temporal and spatial resolutions, a method for extracting useful information from the acquired images must be developed. Due to the volume of data generated by high temporal and spatial resolution imaging, automated analysis packages would be a valuable asset. As an example, if one image of an area of soil is acquired every 10 s (moderate-high temporal resolution) then 360 images would be collected per hour. Additionally, modern cameras are easily capable of acquiring 10 mega pixel images meaning 1 hour's-worth of images (at 10 s intervals), would result in the production of 3.6 trillion data points (pixels). Processing this many pixels to identify those which represent tracer and those that do not would be extremely time consuming if done manually. Therefore, the creation of an automated system for the identification of pixels that contain tracer (as opposed to pixels that do not contain tracer) is required. This data then needs to be displayed in a user-friendly manner.

2.8.3 Lack of high resolution tracers

Currently, there are few high resolution tracers, due to the current requirement for almost all tracing methodologies to physically sample the soil. There has been a long history of studies into stochastic soil movement (e.g. Ellison (1944) quoted in (Ma et al. 2008)), Nearing and Bradford (1985) and van Dijk et al. (2002)) and there has been a recent revival in this area including empirical studies at a very small scale (Furbish et al. 2007, Furbish et al. 2009, Katsuragi 2011, Long et al. 2014), and new modelling work (Ma et al. 2008, Tucker and Bradley 2010).

Currently, empirical studies relating to the movement of individual soil particles operate at small scales and study highly simplified systems. Conversely, soil movement models involving individual particles are required to operate at large scales and are required to model realistic systems, in order to be useful in modelling real-world soil erosion. Therefore, the scales

involved in empirical studies are not consummate with those required by soil erosion models.

In short, most empirical studies which have observed individual particle movement use highly simplified systems and very small scales e.g. <7 cm^2 (Long et al. 2014), whereas successful models of real world situations tend to work at plot or larger scales (Morgan et al. 1998, Wainwright et al. 2008, Wainwright et al. 2008, Wainwright et al. 2008, Cooper et al. 2012). Simplifications of the soil erosion process used in empirical studies include: using single raindrops, the use of homogeneous media (often sand) and the use of flat surfaces (Furbish et al. 2007, Delon et al. 2011, Long et al. 2014). However, questions remain as to how applicable these studies are to real soil surfaces, which are heterogeneous, exhibit strong local micro-topography and incur multiple raindrop impacts over short time spans (seconds). The relationship between plot size and sediment yield is complex and it is often found to be non-linear e.g. Sadeghi et al. (2013). Sadeghi et al (2013) found that a plot 20 m long was needed to accurately parameterise a model of the small catchment they were investigating, while parameterisation using a shorter plot (5 or 10 m) did not produce useful results. This raises questions as to the suitability of very small scale experiments, such as those conducted by Furbish et al (2007), for anything other than understanding process dynamics.

The introduction of a tracer with both high temporal and spatial resolution would be a significant step towards gaining data suitable for model validation. Currently almost all laboratory-scale experiments are conducted under constant (rather than intermittent) and non-varying simulated rainfall. The development of high resolution tracers, particularly those that do not require physical sampling, may allow soil movement to be studied under dynamic conditions.

2.8.4 Is current literature part of the problem?

When investigating a given problem in environmental science, it is common to consult the existing literature. For example, if one wants to investigate a soil movement problem then a reasonable first step would be to consult literature reviews on tracing methods. Reviews regarding tracing methods, with Guzman et al. (2013) being a prime example, tend to focus on the comparative advantages and disadvantages of various methods. However, little focus is placed on the overarching limitations which exist; for example, almost all methods are simply too expensive, have poor temporal and spatial resolution, and understanding of the uncertainties surrounding the data is poor. It could be argued that the vast majority of the tracing methods which are currently used have these issues, and therefore they are just a feature of this type of study. However, I suggest that this need not be the case, but the lack of literature about these issues has resulted in a lack of awareness and therefore, until now, a lack of solutions. For this reason, some overarching issues regarding tracing have been discussed in Section 2.2, for example the need to sample material (2.2.4) and the resolution at which tracers operate (2.2.7).

2.8.5 Overall comments

It is recognised that the perfect tracer does not exist. However, by exploring the limitations of existing tracers, I have been able to identify barriers to progress and, where possible, suggest ways in which these barriers can be overcome. It appears that current understanding of soil movement could be enhanced by the creation of a fluorescent clay tracer as well as an imaging system capable of detecting the tracer which is operating at moderate to high temporal and spatial resolutions. Validation of models that include the movement of individual particles could be improved by having empirical measurements of these particles' movement. Therefore, the creation of a system capable of tracking the movement of multiple soil particles under rainfall conditions at high temporal and spatial resolutions could be of benefit to soil science.

2.9 Thesis aims

2.9.1 Thesis aims

The overarching aims of this thesis are to:

- I) develop *in situ*, non-destructive fluorescence-based methods for the identification of tracer on a soil surface;
- II) test these methods in both laboratory and field-based scenarios;
- III) investigate the motion of individual particles on a soil surface under simulated rainfall conditions at very high temporal and spatial resolutions.

2.9.2 Thesis objectives

These aims will be achieved through the following objectives:

- I) review current tracing technologies with the aim of identifying barriers to progress and, where appropriate, suggest ways to overcome these problems (Chapter 2).
- II) create a clay tracer which accurately mimics the physical and chemical properties of clay, is easy to distinguish from native clay, and is capable of being sampled without the need to physically remove soil (Chapter 4).
- III) identify or create a tracer for larger particle sizes (~50-400 µm) capable of yielding quantitative results and create a methodology that will allow the use of this tracer without the need to physically remove soil (Chapter 5)
- VI) identify or create a tracer which allows the motion of individual particles to be tracked (Chapter 5);
- V) create an imaging system which allows the motion of particles to be recorded on a sub-second timescale (Chapter 5);
- VI) produce an analysis toolkit for the processing and visualisation of data relating to the motion of individual particles (Chapter 5)
- VII) demonstrate the methods in the laboratory (Chapter 4 and 5) and in the field (Chapter 6)

2.9.3 How aims and objectives link to current knowledge gaps.

Several limitations to current tracing methodologies were identified in Section 2.7, and several knowledge gaps were identified in Section 2.8. The aims and objectives described in

Section 2.9 attempt to overcome several of obstacles. Aim I, which is achieved through objective II, addresses the need for an easily identifiable tracer which is a good mimic for soil properties (Section 2.7.1) by creating a new tracer which is has very similar characteristics to the clay fraction of soil. Details of this can be found in Chapter 4, including the development of a basic image processing package which helps fill the knowledge gap identified in Section 2.8.2. Chapter 4 also gives a laboratory-based example of how the technique can be used to track clay at high temporal and spatial resolutions, fulfilling part of aim II and objective VII, as well as beginning to address the need for high resolution tracers (Section 2.8.3).

Chapter 5 fulfils part of aim II and III by completing objective III, IV, V and VI. The image processing package developed as part of this chapter allows extremely high temporal and spatial resolution images to be analysed and therefore begins to address the knowledge gaps presented in Sections 2.8.2 and 2.8.3. The tracer that is used is commercial available and, so far, has been shown to be highly stable in a number of environments which go some way to addressing the issues identified in Sections 2.7.2 and 2.7.3.

Chapter 7 demonstrates how the tracer could be used in the field to investigate a specific issue, in this case soil movement as a result of tillage. In doing so it allows for part of aim II to be completed by fulfilling objective part of objective VII. Section 2.8.3 states that there is a lack of high resolution tracing systems, and this chapter demonstrates that progress has been made in alleviating this issue.

Chapter 3: Technical background relating to fluorescence and image processing

3.1 Introduction

This thesis uses a collection of technologies and ideas which are not commonly used in soil science. This chapter aims to give a brief overview of these ideas and technologies, in order to put them into a broader context. Firstly, an introduction into fluorescence will be given, where the key concepts relating to fluorescence and practical implications of these concepts will be discussed. Secondly, an introduction into imaging and image processing will be given, with the focus being on the ideas and techniques that have been employed in the development of the methodology used in this thesis.

3.2 Fluorescence in a nutshell

Sauer et al (2011) produced an excellent textbook about fluorescence and imaging which gives a much deeper treatment of the topic than is possible here and is an excellent resource should further information be required. Simplistically speaking, fluorescence can occur when a photon interacts with a material and its energy is transferred into an electron. The excited electron then falls back to its ground state emitting a photon without the emission of heat (Figure 3.1).

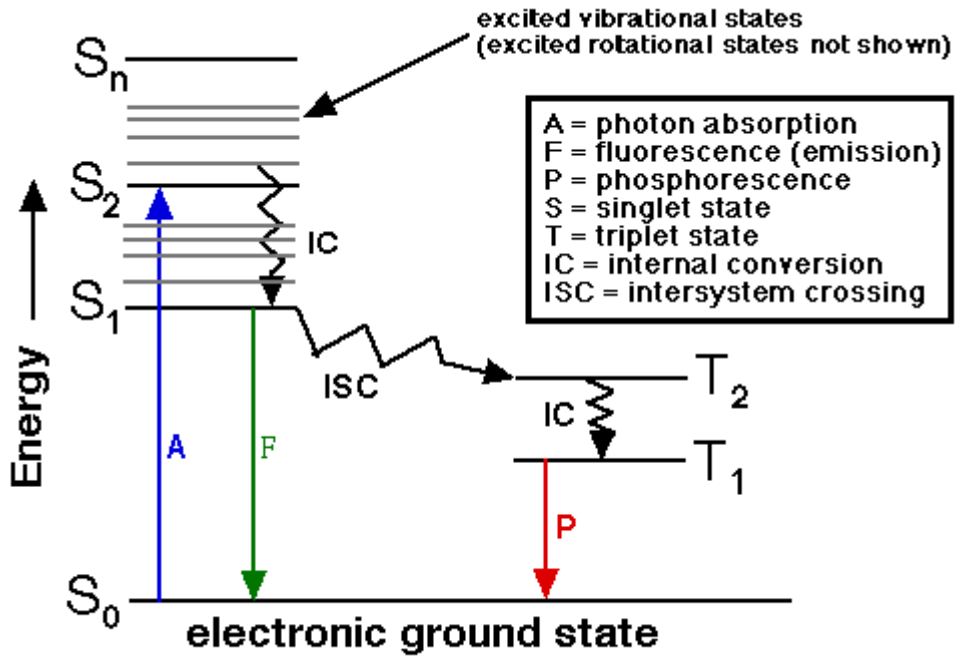

Figure 3.1. Electron energy levels relating to key fluorescence processes . (Chasteen) http://www.scimedia.com/chem-ed/quantum/jablonsk.htm

In the strictest sense, fluorescence only truly occurs when the emission of light is caused by an S1 to S0 transition of an electron, whereas an emission of light from a triplet state (T1) causes phosphorescence, although both result in the emission of light. However, due to the applied nature of this thesis, I shall consider a material to be fluorescent if it is capable of absorbing and re-emitting electromagnetic radiation without the emission of heat. For example, the exact decay mechanism for the Partrac tracer (used extensively in Chapters 5 and 6) is unknown, and therefore may be fluorescent, phosphorescent or combination of the two. Identifying whether the decay mechanism of the Partrac tracer used in Chapters 5 and 6 is fluorescence or phosphorescence is unimportant (and therefore has not been investigated), as I found that light must be constantly supplied to the material in order for light to be emitted. This contrasts with classical phosphorescent material which can often be seen to glow for many seconds after the light source has been removed. It is likely that majority of light emitted from the tracers used in the methodology I have created is a result of fluorescence as the fluorophores (fluorescent chemicals) are organic. They lack a heavy

metal atom which would help facilitate intersystem crossing permitting population of the triplet excited state and allow for phosphorescence to occur. I have therefore used the word 'fluorescence' to describe this decay process throughout this thesis.

It is possible that an electron can fall from the S1 to S0 state without the emission of a photon. This process is called quenching and happens when the electron in the S1 state returns to the S0 state without the emission of light. There are many different mechanisms by which this non-light emitting decay can occur. The key component is that energy is capable of being transferred from an excited electron to somewhere else, often in the form of heat.

3.3 Some practical implications of fluorescence

3.3.1 Stokes Shift

Fluorescent materials do not generally absorb all frequencies of light equally well and will generally have a 'preferred' wavelength that they absorb most efficiently, known as the absorption maximum. The most readily emitted wavelength for a material is known as the emission maximum. Generally when materials fluoresce, the light that is emitted is of lower energy and therefore of longer wavelength, than the light that is absorbed, causing a shift towards the red end of the spectrum. The difference between the absorption maximum and emission maximum is known as the Stokes Shift. The Stokes Shift for a given material is more or less fixed, as are the wavelengths of light that the material is capable of absorbing and emitting. Almost all surfaces reflect some light, and in a practical sense the Stokes Shift allows the differentiation of reflected light, which is the same wavelength as the excitation source, and light emitted by fluorescent material, which is of a longer wavelength. Therefore, is it not possible distinguish between the emitted light from a fluorescent tracer and the reflected light from the surface of wet soil.

3.3.2 The use of visible light

Visible light was used in this thesis for a variety of practical, safety and cost reasons. From a safety point of view using visible light is advantageous as humans have an innate tendency to blink and or look away when exposed to visible light bright enough to damage their eyes. Using non-visible light would mean that the user of the methodology would have no innate way of knowing if they were being exposed to dangerous levels of light, which could lead to burns or eye damage. On a practical level, it is useful as the light used to illuminate the fluorophore can also be used by the user to see the environment they are working in. Additionally, it allows the user to see the fluorescence of the material they are working with, as the light emitted is also within the visible spectrum. There is a much bigger market for devices which emit light that can be seen by humans than light than cannot; for example, lasers and LEDs emitting light visible to humans are generally cheaper than those that do not. The same is true for devices that can record light visible to humans (e.g. digital cameras). These are more common than devices that record light outside the visible spectrum, as we prefer cameras that mimic the way we see the world rather than those that operate at different wavelengths. There is also a larger market for these types of devices.

3.3.3 Fluorescent spectroscopy

Much of this thesis makes use of classic spectroscopic ideas and theories, however these ideas have been adapted to suit the aims of the thesis. Much of spectroscopy focuses on recording detailed emission and excitation spectra and interpretation of these data. Spectrometers generally use a monochromatic light source, which is used to excite a small sample of a fluorophore. A spectroscope, a device capable of recording detailed information about the intensity and wavelength of the light, is then used to analyse the emitted light. Spectroscopy is widely used in environmental studies and is often described as being non-destructive and inexpensive (Rossel et al. 2006, Xia et al. 2007), making it ideal for use in tracing studies. However, traditional spectroscopy has extremely limited spatial resolution,

often with information being collected about an area which is less than 1 cm^2, and is therefore little use in larger scale tracing studies.

3.3.4 Adaption of traditional fluorescent spectroscopy

There have been attempts to use cameras as low-tech spectroscopes (Long et al. 2014, Debus et al. 2015) although much of the work has focussed on biological systems. Though it is difficult to make digital cameras true spectroscopes, where the wavelengths are quantifiable within small bandwidths, standard cameras are already crude spectroscopes as they divide the incoming light into three broad wavelength groups, i.e. colour channels. For the purpose of detecting the tracers used in this thesis on a soil surface, these broad bandwidths were found to be sufficient, and the camera's ability to record the intensity of incoming light allowed potential quantification of the amount of tracer that was present. Cameras also have the advantage of being able to resolve spectral information spatially as well as temporally, giving the potential to image large areas rapidly and repeatedly.

In order to undertake spectroscopy, a light source is usually needed, which is classically supplied by a broadband lamp. This light is then filtered using a monochromator. The combination of the lamp and the monochromator allows great flexibility in the wavelength, bandwidth and intensity of light illuminating the sample, which is useful in laboratory applications, due to varying analyte (i.e. the substance being analysed) properties. However, for the purposes of detecting a single fluorescent soil tracer, the light source does not need to be able to emit multiple wavelengths of light. For a single fluorescent soil tracer, fixed wavelength light sources such as LEDs and lasers, offer an alternative means of exciting the tracer. To create a single image of a large area, the area must be uniformly illuminated; the wide lighting angle often found in LEDs can aid uniform illumination.

3.3.5 Uniform lighting

Uniform lighting aids image acquisition as it prevents areas of high and low light intensity, and therefore allows cameras to take higher quality images. Cameras cannot deal with areas of high and low light as well as the human eye due to their limited dynamic range. This is why photos of people with the sun behind them tend to look silhouetted. For scientific imaging for fluorescent material, uniform light simplifies the process of quantifying the emitted light from the fluorescent material. The amount of the light that a sample emits is often related to the amount of light that it is exposed to. If the fluorophore behaves in a quantitative manner a fixed percentage of the excitation light is converted into emitted light. This is known as the quantum yield of a material. Having a uniform lighting environment may allow for measurements taken from anywhere within that environment to be comparable, assuming the measurement are taken in the same manner. If the lighting environment is not uniform then corrections may need to be made depending on the severity of the heterogeneity present in the lighting

3.3.6 LED and laser lighting

There are many different devices capable of generating monochromatic light. Two examples used in this thesis are lasers and LEDs, however there are some differences in the properties of the light generated. The bandwidth of lasers tends to be smaller than that of LEDs, as does the area that is illuminated. The intensity of laser light can vary hugely and there are some extremely powerful lasers in existence, however the cost of these is generally high. A single LED tends to produce moderate amounts of light but they are very cheap and easily grouped to allow for higher intensity LED-based lamps to be produced (Chapter 5).

During the development of the methods presented in this thesis it was found that the use of diffusers was important in allowing a uniform lighting environment to be created. Diffusers work by scattering light from a point source in order to spread it more evenly over a surface.

As laser light often comes as a single narrow beam then an extremely high quality diffuser is required to scatter the light in a uniform way. LEDs, by contrast, tend to emit light in a much wider arc and this allows for lower quality and therefore cheaper diffusers to be used.

3.3.7 Processing spectra

A spectrum is the wavelengths of light that are emitted from an object. There are various scientific instruments that are able to record this light, for example a spectrometer. It is common for spectra to be displayed graphically (i.e. using a graph with wavelength against intensity). These spectra are often interpreted by eye, for example the analyst may look for the presence or absence of distinctive peaks in the spectra to indicate the presence or absents of certain molecular moieties. As an example, in Infrared spectroscopy a strong absorption at 1700 cm^{-1} is indicative of a carbonyl, whereas the absence of this is reasonable good evidence that there is no such moiety. There have been moves to automate this process, often in the area of disease diagnostics (Ollesch et al. 2013), probably due to the high number of samples needing to be processed. One reason that I was keen to use a technique that has based interpretation of spectra, was that it has already been shown to be possible to automate the analysis process. This suggests that it may be possible to use a similar process for the tracing of soil movement.

3.4 Image analysis

3.4.1 Some details on how camera function

It quickly became clear that if large amounts of images were going to be acquired then there would need to be an automated way to extract meaningful data from them. In order to develop a technique which would allow for automated image processing, some prior knowledge of how digital cameras function is required. Here, some background information relating to how modern digital cameras function is provided to give some context as to how useful data was extracted from images. This section aims to give the reader a background

into the ideas and techniques which are used in the methodology described in this thesis, and identifies some issues surrounding them. It is not intended to be a review of image processing, as there are many textbooks are a far better resource than this could ever be.

In simple terms, when a camera records an image it does so using three colour channels: red, green, and blue. Each channel has a series of small, light sensitive sensors which record the intensity of light to which they are exposed. Each one of these sensors returns a numeric value, which is akin to a number of counts, and is referred to as a pixel. The range of values that a pixel can have varies depending on the file format used; for example, for JPEG this range is 0-255. The camera uses internal software to convert the number of counts into a value between 0 and 255 using a mathematical function, which is not necessarily linear and therefore can result in interval data, i.e. a value of 20 might not be twice 10. In some cameras, it is possible to get the direct count outputs from the sensor without processing, which is generically known as RAW format. RAW format images are not in a defined file format and many different camera manufactures use their own format. However, it is normally required to process the image before it can be viewed. This gives the user great control over the final image, often permitting corrections for under or over exposure. However, it does greatly increase the file size and adds a level of processing before the images can be viewed. Cameras which are capable of recording RAW images also tend to be more expensive than those that cannot. This method focuses on the use of JPEG images rather than RAW images as they are smaller and come in a recognised file format. Small scale trials have found that the increases in data quality achieved by using RAW images compared to other file formats (e.g. JPEG or TIFF), do not outweigh the increases in complexity of processing the images and storage demand.

3.4.2 Image processing software

An off-the-shelf program capable of analysing the images of the nature of those which result from this methodology could not be found. ImageJ was probably the closest program for undertaking the analysis required and was used for some initial trials as it has a graphical user interface. There may be some high-end software available, however due to limited funds, there was little exploration of expensive software. Closed source programming languages, like Matlab, were also avoided as these require licenses and therefore limit the availability of the technology to those than can afford the licence. It became clear that writing scripts to extract information from the images would allow greater flexibility, speed and reproducibility. It should be noted that it was expected that hundreds if not thousands of images were going to require processing, so finding an efficient and automated way of doing this was key to the success of the project. An image can be deconstructed into three colour channels and each channel can be displayed as a matrix which can then be manipulated by the user. Initially these manipulations were carried out using the "licence free" language R (see Chapter 4). This is an open source language derived from S and has a collection of large array of packages which can be used to extend the capabilities of the language. R provided a useful platform to perform simple image manipulations, such as thresholding, in a rapid and perfectly reproducible way. Thresholding is a basic image segmentation technique which can be used to separate area of an image based on colour intensity (Shapiro and Stockman 2001). By defining an intensity threshold it was possible to determine which areas of the image had tracer in them. The location of these areas could be determined by using the pixel's coordinates. By using these coordinates and the intensity threshold, it is possible to extract quantitative data about the tracer location (e.g. 4.6, Chapter 4).

The aim of "Using real time particle tracking to understand soil particle movements during rainfall events" (Chapter 5) was to identify and track individual particles as they moved in response to water. As the particles being tracked in "Using real time particle tracking to

understand soil particle movements during rainfall events" (Chapter 5) were larger than those in "A novel fluorescent tracer for real-time tracing of clay transport over soil surfaces" (Chapter 4), an alternative way of extracting information from the soil images was required. When tracking clay, as in "A novel fluorescent tracer for real-time tracing of clay transport over soil surfaces" (Chapter 4) there were many clay particles within a single pixel, whereas in Chapter 5 there were multiple pixels for a single particle. In order to limit the quantity of data to a reasonable amount, a method of identifying where the centre of a given particle was, was needed. No user-friendly package could be found in R, however a Python library (trackpy) was found which was able to identify small round particles against a contrasting background. The Python library trackpy searches using Gaussian filtering among other techniques. In this chapter use is made of a number of image processing algorithms which are freely available online at from the github repository (Trackpy 2010). Additional software was developed and this is described in Chapters 6 and 7. The most important aspect of this toolkit, is that it can effectively locate the trace particles in an image (Chapter 5 Figure 5.1). The same basic particle location techniques were used in Chapter 6.

One previous use of this toolkit was to track the motion of small particle in a fluid using images acquired using a microscope. The toolkit uses a Gaussian-based search to identify the location of spherical objects which are different in brightness to the background. As the images that I have used have bright spots (caused by the fluorescent tracer) against a dark background the software was easily able to detect the fluorescent particles. The algorithms appear to be quite stable in their ability to detect particles, even with slightly blurred images. The stability is probably due to the extremely high contrast between bright particles (tracer) and the dark areas containing no tracer. It should be noted that the algorithms work best when the density of particles is low enough so that no particles are touching. Detailed information relating to this is available in Section 6.4.3. In many ways, this is ideal as it means that the amount of tracer can be kept low which reduces the cost of the trials. The Gaussian-

based search algorithm used in trackpy is highly sensitive and can often find false positives. The number of false positives can be greatly reduced by pre-processing the images. This was achieved by removing non-relevant information, such as the red and blue colour channels (the tracer is green), and reducing the background noise. This was done by a technique akin to thresholding. Generally thresholding results in a binary image however this would result in loss of information which is useful in determining the centre of the particle. Therefore, highpass thresholding was carried out whereby all the pixels which were less than a certain value were set to 0 and all others were left as they were. For a given set of images one high pass thresholding value was determined by trial and improvement using a small subset of the images to test the value. This value is not the same for every set of images as it is depending on the many factors which can vary from study to study, such as camera type and location, lighting location and intensity and camera parameters. This process was inspired by the way that JPEG compression operates. In this process area of similar colour values are grouped together and treated as if they are all the same colour. This is way much of the information that is low intensity noise is removed leaving a cleaner background. Although pre-processing the images takes time, the amount of time needed for locating particles is reduced, and therefore the process takes less time overall. Trackpy also outputs data into a standard Python data frame format (PANDAS) which allows for it to be accessed and manipulated with ease. SPYDER (Scientific PYthon Development EnviRonment) is an excellent development platform which has many Matlab-like libraries such as matplotlib which allows for easy creation of graphs. These have been used extensively throughout Chapters 5 and 6. The ability to interface general purpose programming with reasonably high quality scientific graphics is one of the reasons that Python and particularly SPYDER were chosen for this thesis.

Once information was extracted and placed in a PANDAS dataframe, further processing was undertaken, in a similar way to how data is processed in traditional spreadsheet packages

(e.g. Excel). Due to the huge size of these dataframes, they cannot be displayed graphically on a screen, so processing must be manipulated using command line code. However, as many of the processing methods are simple mathematical operations (e.g. averaging), they could have been executed in more familiar (to some users) spreadsheet packages (e.g. Excel) if the dataframes had been smaller.

Chapter 6 aims to build on the work carried out in Chapter 5, while working at larger scales and adding in additional methods. Chapter 5 deals mainly with the fine scale detection and tracking of particles whereas Chapter 6 starts to apply these techniques to look at larger scales. For example, Chapter 6 details how located particles can be counted in order to give an impression of tracer concentration without the need to physically sample the soil (see Section 6.4.1). Other methods of estimating tracer concentration, such as using the average brightness of a given area as a proxy for tracer concentration (see Section 6.4.3) are also developed in Chapter 6.

3.4.3 Image analysis

Recent advances in image analysis have allowed scientists to examine the physics of erosion processes in more detail. Model systems, based on the measurement of single raindrop impacts on a bed of sand-sized particles, have allowed some insights to be gained into the likely effects of a raindrop impact. Much work has focused on developing a detailed understanding of the formation of splash craters and associated physics (Delon et al. 2011, Katsuragi 2011, Nefzaoui and Skurtys 2012). More recently, Long et al. (2014) investigated the ejection of particles from a single raindrop impact, showing that the vast majority of ejected particles have low velocity and a high ejection angle, resulting in a small displacement, while less than 3% ejected particles have a low angle and high velocity resulting in larger travel distances (Long et al. 2014). Although not intended to mimic natural systems and working with single drops at small (< 1000 mm^2) scales, this work suggests that

soil particles are likely to be displaced via a series of small movements with intermittent larger movements. Extending this type of work to systems which are a better mimics of the natural world may allow for a deeper understanding of soil particle movement to be gained.

3.5 Conclusions

Overall a large component of the imaging processing techniques that are used here are not new. They are techniques that have been used extensively but have seen limited application in soil tracing technologies. Much work was involved in the adaption of these techniques to suit the wide variety of studies that are likely to be relevant to soil tracing. As a result, the techniques are designed to operate over a range of temporal resolutions (from 1/50s to minute scales) and over a variety of scales (from sub mm to m). Efforts were made to strike a reasonable balance between cost, user friendliness, adaptability and resolution of the imaging techniques and associated software.

Chapter 4: A novel fluorescent tracer for real-time tracing of clay transport over soil surfaces

Robert A. Hardy[1], Jacqueline M. Pates[1], John N. Quinton[1], Michael P. Coogan[2]*

[1]Lancaster Environment Centre, Lancaster University, Bailrigg, LA1 4YQ

[2]Chemistry Department, Lancaster University, Bailrigg, LA1 4YQ

* Corresponding author: j.quinton@lancaster.ac.uk

KEYWORDS Clay; tracing; soil erosion; diffuse pollution; fluorescence; tracer.

4.1 Abstract

Clay is an important vector for the transport of pollutants in the environment, including nutrients, pesticides and metals; therefore, the fate of many chemicals in soil systems is closely linked to that of clay. Understanding the mechanisms responsible for clay transport has been hampered by the lack of a suitable tracer. Producing a tracer that accurately mimics clay transport is challenging, due to the small size of the particles and their unique physical properties. Here I describe the design and synthesis of a tracer using natural clay particles as a foundation, exploiting the natural ability of clay to sorb molecules to coat the clay with a thin layer of fluorophore. Application of the tracer has been demonstrated through the collection of real-time images of the tracer moving over the surface of a soil box during a rainfall event. These images allow, for the first time, clay to be tracked spatially and temporally without need to remove soil for analysis, thus resulting in minimal experimental artefacts. Custom written software has been used to extract high resolution data describing tracer movement and extent throughout the experiment.

4.2. Introduction

Clay is a key component of many of the world's soils. Its ability to sorb nutrients, such as phosphorus (Syers et al. 1971, Sharpley et al. 1984, Sumner 2000), potassium (Petrofanov 2012), metals (Quinton and Catt 2007) and organic pollutants (Homenauth and Mcbride 1994, Sumner 2000), and its ease of transport in flowing water makes clay an important vector for contaminant transport. Clay particles are moved by both overland flow (Quinton et al. 2001, Quinton and Catt 2007) and by subsurface flow (Mccarthy and Zachara 1989), which may connect with rivers and lakes. Although studies have developed an empirical understanding of clay movement (Quinton et al. 2001, Quinton and Catt 2007) and there have been attempts to model clay transport over and through soils (Jarvis et al. 1999, Jomaa et al. 2010), deriving spatial and temporal distributions of clay movement in response to rainfall has proved elusive. In this paper I describe a methodology, which, for the first time, allows the tracking of clay in time and space across a soil surface.

4.2.1 Tracing clay movement

Tracing clay movement has proved very challenging (Armstrong et al. 2012). One aspect of this challenge is the small size of the particles being traced. For larger particles (grains of sand size) there has been success in mixing a dye with a binding agent and then applying this mixture to the surface of the particles (Black et al. 2007). However, this technique has limitations for particles that have a diameter of a few microns, as the coating significantly alters the size and density of the particles. Therefore, for clay an alternative method of tracing is required.

This has led researchers to develop a range of techniques for tracing clay, including the use of fluorescent microspheres (Burkhardt et al. 2008, Nielsen et al. 2011), rare earth oxides (REOs), which, strictly speaking, are fine silt particles (Zhang et al. 2001, Stevens and Quinton 2008), and the labelling of clay particles with organic molecules (Selvam et al. 2008). The

majority of methods require sampling (via physical removal of material) of the soil after the experiment to determine the tracer concentration (Parsons and Foster 2011, Mabit et al. 2013). However, it is desirable to understand how a process changes over time requiring the collection of dynamic data. Sampling interferes with detachment and transport processes, limiting the use of existing techniques for process studies. Therefore, a method that does not require removal of material is required if progress is to be made in understanding the dynamics of these processes. Additionally, there are significant density differences between tracers (such as microspheres and REOs) and native clay particles, which are likely to affect their transport. Therefore, a clay tracer with the same physical and chemical properties as the native soil clay, and that can be manufactured easily and analysed using a non-invasive, non-destructive and in-situ analysis technique operating at moderate to high temporal resolution, is desirable. Some progress has been made in the nano-particle community with the creation of florescent nano-clays, however, no environmental application of the material has been reported (Diaz et al. 2013).

4.2.2 Fluorescence

Fluorescence detection often allows for a high signal to noise ratio permitting single molecule detection (Lakowicz 2006). This sensitivity enables minimal fluorophore to be used in tracer production, resulting in negligible modification of the coated particle. Traditionally, fluorescence is measured on discrete samples using a fluorimeter, providing detailed spectral information. Two previous studies have captured images of fluorescent tracers using film cameras. In the first, silt and sand-sized glass particles (44 to 2000 μm) labelled with uranium salts, which fluoresce under UV light, were monitored on a 10 m slope inclined at 5.5% (Young and Holt 1968). Later, fluorescently-labelled pesticide granules (size unknown) were detected in soil, with each photograph imaging 0.63 m^2 (Woods et al. 1999). This work assessed how soil tillage methods affect incorporation of pesticide granules into soil; no effort was made to acquire images of the pesticide moving.

4.2.3 Fluorophore selection

Four principal criteria were used to select the fluorophore. It should: bind strongly to clay; fluoresce at a wavelength different to the auto-fluorescence of soil; be well characterized; and be detectable using a CMOS (Complementary Metal Oxide Sensor) detector in a digital camera. Successful binding relies on matching the fluorophore to the clay of interest; in general the fluorophore should carry the opposite charge to the clay and be lipophilic. Soil auto-fluorescence, due, in part, to the large quantity of organic aromatic acids that are present (excitation maximum at 465 nm, emission maximum at 517 nm) (Milori et al. 2002, Rinnan and Rinnan 2007), can result in high background fluorescence and therefore interfere with detection of the tracer. Therefore, to reduce the impact of natural fluorescence a fluorophore that excites between 520 and 600 nm was desired. Having a well-characterized fluorophore allows more rapid progress to be made as its chemical properties are already well described. Finally, I wanted to use a CMOS detector array, commonly found in consumer grade cameras, as they acquire images within the visible range (400-700 nm). A fluorophore that fluoresces in this range was therefore required.

Rhodamine B was selected as the fluorophore, because: it binds to clay, e.g. Rhodamine B has been shown to bond organically-modified montmorillonite (Diaz et al. 2013), and sodium montmorillonite has been shown to be a successful remediation method for water contaminated with Rhodamine B (Selvam et al. 2008); it typically has an excitation maximum around 570 nm and emission maximum of around 590 nm (Beija et al. 2009), avoiding the most intense soil auto-florescence; and it fluoresces within the range detectable by a CMOS detector. Many derivatives have been synthesized, which could allow fine tuning of the clay tracer's fluorescent properties (Beija et al. 2009), and it is commercially available and inexpensive.

4.3. Materials and Methods

Here I describe the materials and methods used to produce the clay-sized fluorescent tracer, tests of its stability and its application to a laboratory scale erosion experiment.

The instruments used were an Agilent Technologies Cary Eclipse fluorescence spectrometer and an Agilent Technologies Cary 60 UV/vis absorbance spectrophotometer. Disposable plastic cuvettes were used throughout (Fisher Scientific). The water used was deionized water, unless otherwise specified, and Rhodamine refers to Rhodamine B from Acros Organics (132311000).

4.3.1 Tracer production

The tracer was produced by sorbing Rhodamine onto the surface of clay particles. Twelve grams of montmorillonite (69904 ALDRICH) was ground to a fine powder, and sonicated for 30 minutes in water. Rhodamine (0.2 g) was added and the volume made up to 1 L. The mixture was sonicated for a further 45 minutes, stirred for 2 hours, then allowed to settle. The supernatant was clear and colourless, and a vivid red-purple powder was visible at the bottom of the beaker. Excess supernatant was decanted off and the powder collected using vacuum filtration through two Whatman #5 filters. The filtrate was clear and colourless to the eye. The tracer was then thoroughly rinsed using a 50:50 mixture of saturated NaCl and ethanol and then repeatedly with water. The resulting tracer was dried at room temperature in a desiccator and protected from light. If required, the tracer was gently disaggregated by hand before use.

4.3.2 Tracer stability

Stability tests were carried out to ensure the tracer would not degrade over the duration of the trial (less than 24 hours). One gram of tracer (equivalent to 16.7 mg Rhodamine) was placed into 100 mL of solvent (either High Ionic Activity Solution (HIAS) or distilled water), and stirred to mix. The HIAS was prepared by combining 25 g NaCl, 4.1 g Na_2SO_4, 0.7 g KCl,

11.2 g $MgCl_2.6H_2O$ and 2.3 g $CaCl_2.6H_2O$ with deionised water to give a final volume of 1 L (Sverdrup et al. 1942). The aim was to produce a simulated natural water of high ionic activity with respect to the major elements. The concentrations used in this solution are extreme compared to those normally found in terrestrial waters; if the tracer is stable under these conditions, I assume that it will be stable in the vast majority of soil environments.

After a period of time (> 40 h), during which the tracer was allowed to settle, 3 mL of the supernate was placed in a plastic cuvette to assess desorption of Rhodamine from the tracer, using UV/vis absorbance spectrophotometry and fluorescence spectrometry. No attempt to separate the tracer from the water was made, as any particles remaining in suspension were too fine to remove by filtration.

To make calibration standards, first a stock solution was prepared by dissolving 18.2 mg Rhodamine in 100 mL deionised water. Standards for UV/vis spectrophotometry and fluorescence spectrometry were prepared by diluting the stock 1:250 for fluorescence measurements and 1:125 for UV/vis measurements, using either HIAS or deionised water. Thus, the UV/vis standards contained 0.144 mg Rhodamine per 100 mL, and the fluorescence standards contained 0.072 mg Rhodamine per 100 mL. These are the concentrations that would be achieved had 1% or 0.5% Rhodamine dissolved off the tracer during the stability experiments.

4.3.3 Physical properties of tracer

A Leica confocal microscope was used to record images of clay and tracer particles. Images were taken using a 63x optical lens under oil. The size range of particles was measured using a Malvern Mastersizer 2000.

4.3.4 Acquiring fluorescent images

Images were acquired using a Canon 500-D DSLR camera mounted on a tripod. (See Supplementary Information (SI) 1: Camera setup, for further details of the camera settings and filters). A ~75 mW, 532 nm (green) laser was used to illuminate the soil box, after passing through a rotating diffuser (SI 2: Laser lighting setup, SI: Figure S1). Achieving uniform illumination is critical to producing accurate images (Waters 2009). Visual and photographic assessment of the light showed an acceptable degree of uniformity (SI: Figure S2).

4.3.5 Soil box

Perspex soil boxes (350 mm by 500 mm), with drainage holes in the base, were filled with 4 cm fine gravel, landscape fabric membrane, 3 cm sand and 4 cm soil (screened to 4 mm) to simulate natural infiltration conditions following Armstrong et al. (2012) method. The soil was a clay loam soil of the Wick 1 association from Lancaster, Lancashire, United Kingdom. A 150 x 50 x 5 mm section of soil was removed, mixed with 4 g of tracer and then replaced (Figure 4.1). To bring them to near saturation, the soil boxes were immersed in water, to a depth 1 cm above the soil-sand interface, for 22 hours. The box was then drained for one hour and exposed to rainfall, while set at a slope of 4%.

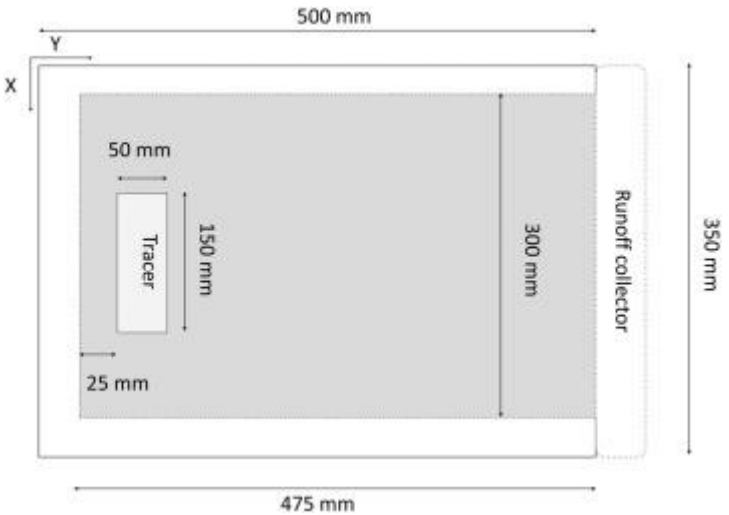

Figure 4.1. Schematic of the soil box used showing starting location of tracer. The grey area is the imaged area.

4.3.6 Rainfall

A gravity-fed rainfall simulator was used to deliver rainfall with an intensity of 42 mm h^{-1} using reverse osmosis (RO) grade water (Armstrong et al. 2012).

4.3.7 Runoff testing

Runoff was collected from the run-off collector (Figure 4.1), with the container receiving the run-off changed every 5 minutes. Runoff collected from between 30 and 45 minutes after rainfall has commenced was bulked and vacuum filtered using two Whatman #5 filters to remove the particulates.

4.4. Results

4.4.1 Tracer stability

In order for a tracer to be useful it must remain intact for the duration of the study. The most likely route of tracer degradation is desorption of Rhodamine from the clay surface. To investigate this possibility, UV/vis absorbance and fluorescence spectrometry were used to characterize the loss of Rhodamine upon exposure to HIAS or distilled water (over 40 hours).

The supernate showed virtually no absorbance of light in the UV/vis range due to solution phase Rhodamine, as demonstrated by the lack of a peak at ~ 560 nm (Figures 4.2a and b). Figure 4.2a shows a raised baseline attributed to fine, colloidal-sized particulate matter (the tracer) remaining in suspension scattering the light, a hypothesis supported by the lack of specific absorption bands. The small peak at ~ 590 nm is assigned to Rhodamine as no other component absorbs in that region. However, the wavelength maximum does not match that of the Rhodamine standard, which suggests that the Rhodamine responsible for this peak is modified compared to the standard. An interaction between Rhodamine and montmorillonite, either through chemisorption onto the surface, or simple protonation (the

montmorillonite used is pH 3), could account for this shifted wavelength. The absence of a raised baseline in HIAS (Figure 4.2b) suggests that there are no tracer particles present; I propose that the high ionic strength of HIAS encourages flocculation and hence precipitation out of the clay tracer (Elimelech 1995).

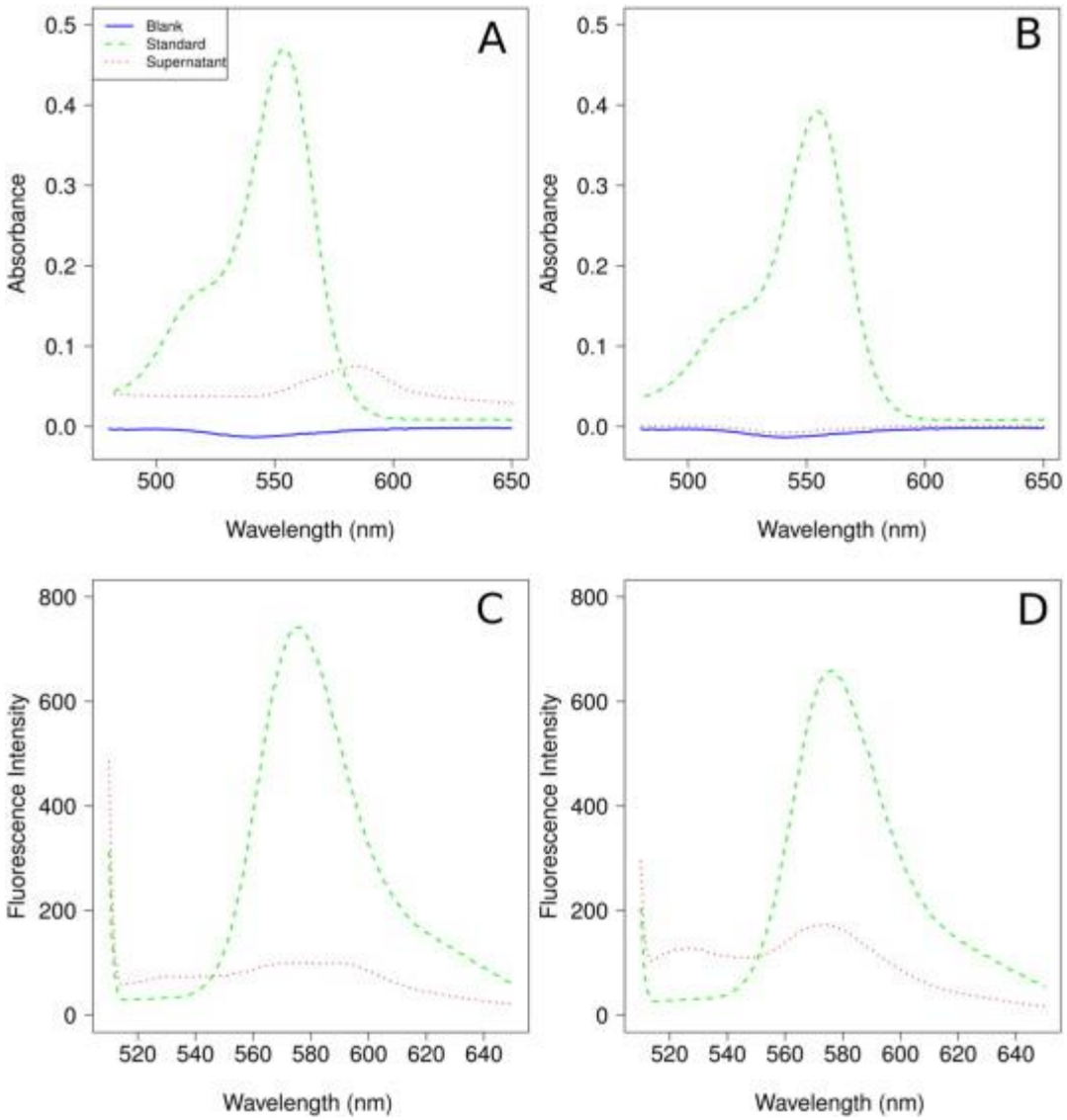

Figure. 4.2. UV/vis (A and B) and fluorescence spectra (C and D) of supernatant solutions. The tracer was mixed with either deionized water (A and C) or high ionic activity solution (B and D) and the supernatant separated after more than 40 h, to test for desorption of Rhodamine.

Fluorescence measurements showed a peak with a maximum emission at 575 nm, attributed to dissolved Rhodamine, in the HIAS solution (Figure 4.2d). In order to estimate the amount of Rhodamine lost from the tracer during the experiment, linearity between the sample and

standard was assumed and the following equation used to estimate the amount of Rhodamine lost: (standard concentration / fluorescence intensity of standard) x fluorescence intensity of sample. This relationship suggests that approximately 0.022 mg Rhodamine was lost from the tracer, i.e. 0.13% of the total amount used in the experiment. A broader and flatter peak is seen in the deionized water sample (Figure 4.2c), indicative of minimal desorption from the tracer. The greater desorption of Rhodamine in HIAS is probably due to the high ionic strength of the solution, whereby the HIAS ions compete with the Rhodamine for binding sites on the clay forcing the latter to desorb. However, HIAS has a much higher ionic strength than water soil mixtures, where the tracer will be deployed; therefore it is reasonable to assume that desorption will not readily occur during soil transport experiments.

4.4.2 Physical properties of tracer

Comparing the particle size distribution of the tracer and the clay from which the tracer was made, it was found that 55% of the tracer had a size of less than 2 µm, compared to 51% of the montmorillonite. Furthermore, the size distribution of the particles before and after treatment with Rhodamine was consistent (SI 3: Tracer size). Confocal microscope images show that the particles retain their irregular sizes and shapes (Figures 4.3a and b). The Rhodamine appears to be uniformly distributed over the particle surface, without disturbing surface texture (Figure 4.3c). The appearance of more rings around the clay in the phase contrast image of the tracer is consistent with the hydration of the clay during synthesis of the tracer.

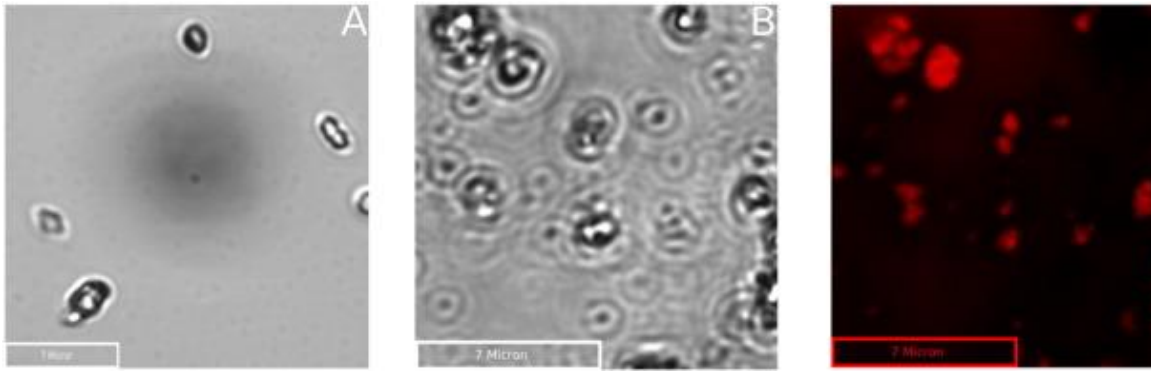

Figure. 4.3. Confocal micrographs of clay tracer: A) phase contrast before treatment with Rhodamine; B) phase contrast after treatment with Rhodamine; and C) false colour fluorescent after treatment with Rhodamine. Note that the clay retains its size and shape after treatment and that the fluorescence appears quite uniformly on the clays surface.

4.4.3 Tracer movement images

The images show, for the first time, clay movement over a soil surface in real time under continuous simulated rainfall conditions (Figure 4.4 and SI 4: Images). The movement of tracer across the whole soil box was recorded every 7 s from a distance of ~ 2 m. The sample area is 2431 x 1769 pixels (0.135 m^2), which equates to approximately 31 pixels per mm^2. As no soil was physically removed from the box during the experiment, there was no external disturbance to the system, resulting in fewer sampling artefacts. By increasing the light input (by increasing the camera aperture and moving the light source closer to the target) and sensitivity of the CMOS detector (by increasing the ISO setting), the soil box was imaged on the sub-second time scale (every 0.8 s), although increased noise was present (SI 5: Rapid imaging).

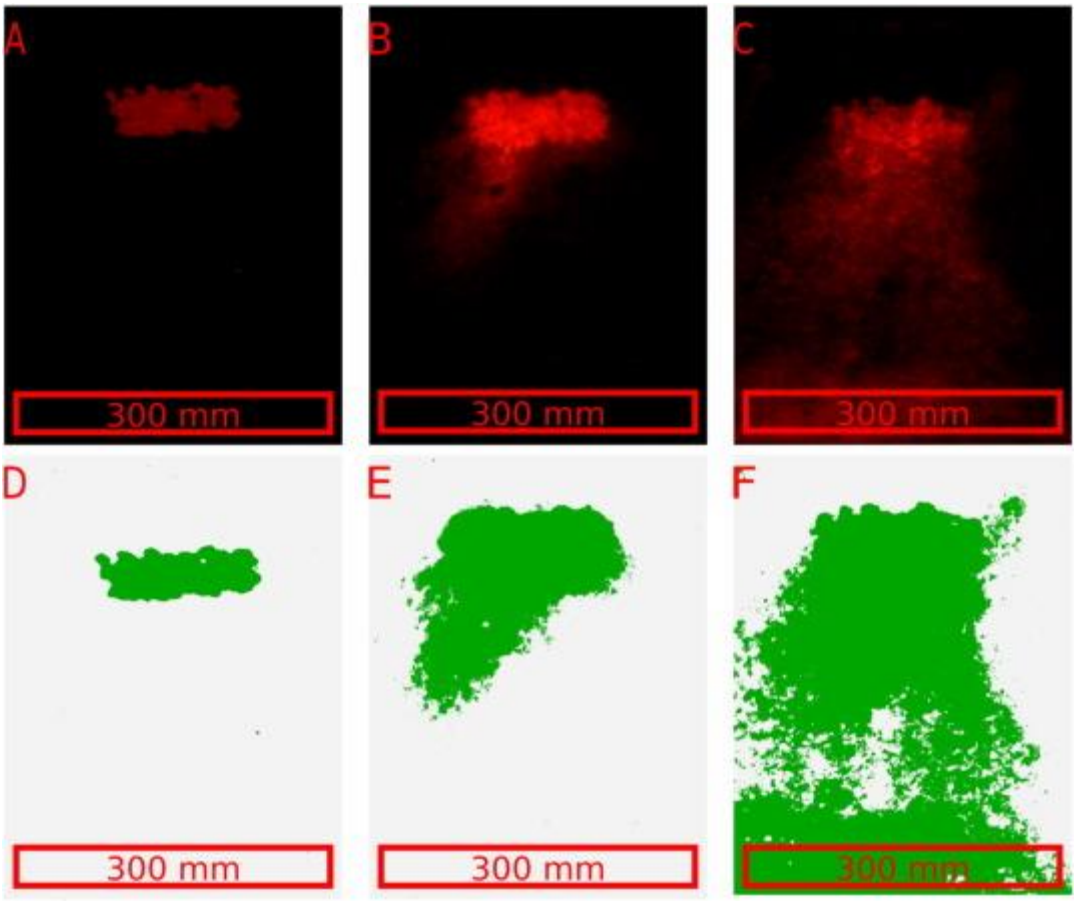

Figure 4.4. Images of soil box (top of box at top of image) showing tracer location at various times. A to C are true colour images and D to F are false colour images produced using [R]. A and D were before exposure to rain, B and E are after 262 s of rain and C and F are after 2252 s. After 0 s the tracer was constrained to the area where it was applied. After 262 s the tracer had moved down the box and spread laterally, further movement and lateral spreading continued until the experiment was ended at 2252 s. Transport pathways of clay from the top of the box to the bottom can be observed together with a depositional area which formed at the bottom edge of the box.

4.4.4 Image processing

Although it is possible to view the images without post-processing, much can be gained from doing so. Using [R] (Polzehl and Tabelow 2007, Team 2013, Urbanek 2013, Hijmans 2014), the images were converted to false colour with noise suppressed (Figure 4.4). Further details of the image processing methods can be found in SI 6: Image processing. These images were easier to analyse visually, as they show presence of tracer in green and the absence in white. The file size of the images is approximately 100 times smaller than the original images. Images of this nature were then compressed (Cinepak codec by Radius, quality 100) into a

time-lapse video using VirtualDub (version 1.10.4) allowing the whole event to be reviewed in less than a minute.

The intensity of fluorescence from the tracer, in the solid state, is independent of the concentration of tracer. This type of behaviour is symptomatic of self-quenching, which involves the rapid exchange of energy between molecules and de-excitation via non-radiative processes, typically relaxation to the ground state through vibrational levels. Due to the close spatial proximity of the Rhodamine molecules to one another when bound to clay and the small Stokes shift (and therefore overlap of excitation and emission bands), this type of behaviour is neither unusual nor unexpected (Lakowicz 2006). As the amount of light emitted from the tracer is not a function of the tracer concentration, the intensity of light cannot be used to quantify the amount of tracer at a given point. Nonetheless, the true-colour images shown (Figures 4.4a-c) have some qualitative properties, as areas that are much more intensely coloured are likely to contain more tracer that those that are less intensely coloured.

I have confidence that interference due to autofluorescence was not a problem as I have used constant illumination and the initial images (Figures 4.4a and 4.4d) show intense colour where the tracer was applied and virtually no colour anywhere else.

4.4.5 Runoff testing

In order for the tracer to be useful it must remain intact throughout the experiment, which can be evaluated by recovering the tracer afterwards. Particulate material recovered from the runoff, was dried and photographed on a black (non-fluorescent) background (Figure S4). The colour and intensity seen in Figure S4 (SI 9:Runoff) are very similar to the colour and intensity seen in Figure 4.4, suggesting that the tracer has remained intact throughout the experiment.

The filtrate was a reddish brown to the eye, which were attributed to fine particles, given that they are illuminated when a ~ 1 mW (532 nm) laser beam is passed through the suspension (an effect not seen in particle-free solutions). The filtrate was centrifuged at 15000 rpm for 99 minutes, the supernatant decanted and then imaged on a non-fluorescent background, using standard image acquisition and processing parameters. No fluorescence was seen (Figure 4.5), in contrast to a solution containing 2 µg/L Rhodamine, which could be readily detected. I am therefore confident that the images in Figures 4.4 a, b, c are images of the Rhodamine-labelled clay rather than Rhodamine in solution.

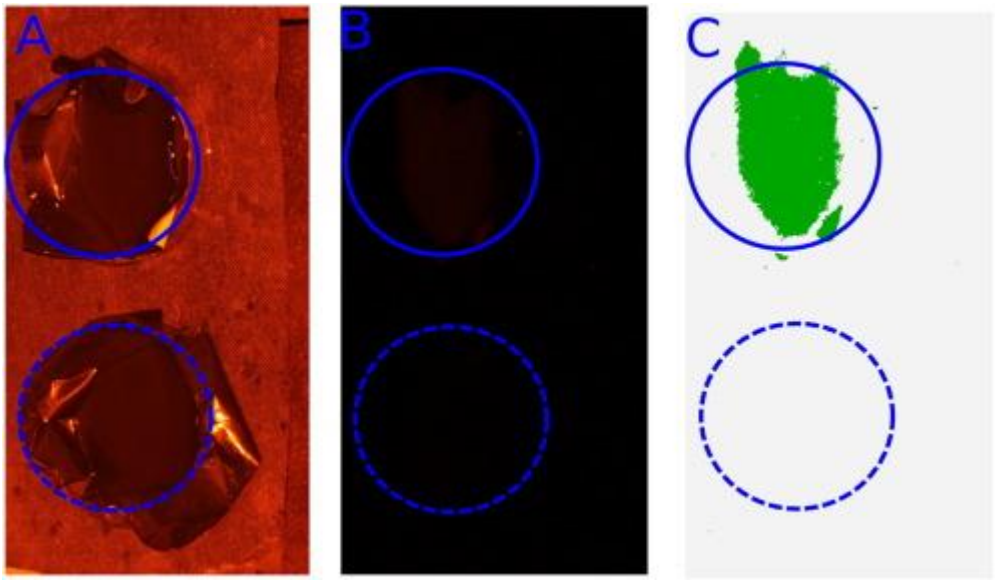

Figure 4.5 Comparison of soil-box runoff in a Petri dish backed with black plastic after filtration and ultra-centrifugation with a Rhodamine standard. The solid circles show the location of the standard (2 µg/L) while the dotted circles show the filtered and ultra-centrifuged soil-box runoff. A is a true colour image captured under typical room lighting with a 570 nm long pass filter on the camera, B is a recorded using 532 nm lighting and a 570 nm filter, and C is a false colour image process using R. The standard is clearly detectable in C but not the runoff.

4.4.6 Demonstration of application

In order to demonstrate how high temporal and spatial resolution data can be used in the study of soil erosion processes, the tracer front was mapped against time (Figure4. 6a). The

data were extracted from 312 images using a custom written function in [R] (SI 10: Tracking tracer spread). The effect of rain-splash was analysed by looking at how the tracer front moved up and down the box (Figure 4.6a), which demonstrates the dynamic nature of both the upper and lower tracer fronts. As expected the movement down the box is more rapid than that up the box. The lower tracer front moves rapidly to begin with, slows and then moves rapidly again. I attribute this behaviour to changes in soil microtopography, akin to a dam bursting, allowing overland flow to connect with the bottom of the box and rapidly deliver the tracer. The spike at approximately 1000 s is attributed to an artefact in the data. Lateral spreading of the tracer was also noticed in the images so a plot correlating the width of the tracer band to time was also produced (Figure 4.6b), as well as the changing tracer area over time (Figure 4.6c). The development of the tracer area can viewed dynamically in the online version of the paper http://www.sciencedirect.com/science/article/pii/S034181621630056X.

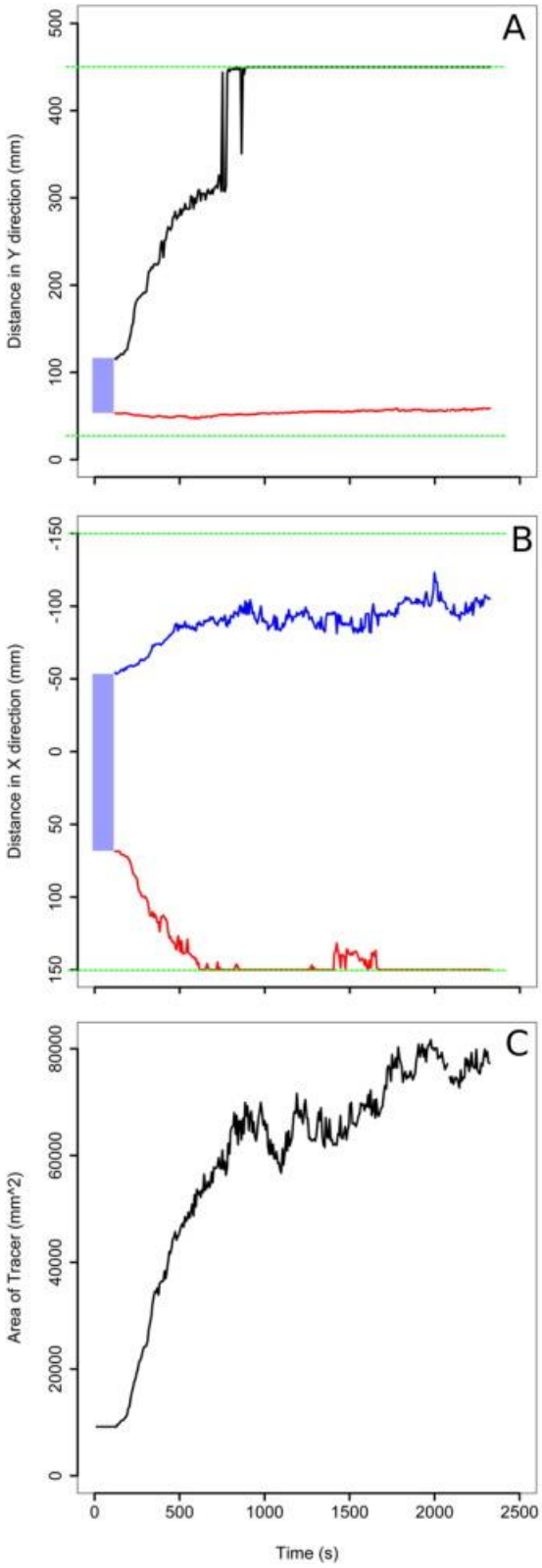

Figure.4.6. The movement of the tracer over time. The imageable area is bounded by the dashed green lines and the blue box represents the original location of the tracer. A shows the movement of the tracer in direction Y (the primary direction of water flow), B shows the lateral spread of tracer in direction X (orthogonal to the primary direction of water flow), and C shows the total area that the tracer occupies. All changes are shown against time.

4.5. Discussion

I have developed a tracing and imaging method that, for the first time, allows clay movement to be traced, with mm precision in two dimensions with a time-step of approximately 1 s, under simulated rainfall conditions without the need to stop the experiment to take samples. This is a major advance over previously reported techniques. Previous work has focused on the use of exotic particles and elemental tagging in soil tracing; examples include fluorescent microspheres (Pryce 2011), ceramic prills (Plante et al. 1999, Duke et al. 2000), plastic magnetic beads (Ventura et al. 2001) and REOs (Deasy and Quinton 2010). These methods have been criticized as the tracers have different physical properties, such as size, shape and density, to the target soil (Zhang et al. 2003). By using natural particles as the basis for this tracer I believe that I have minimised or avoided many of these problems; physically, the tracer retains the same size and density characteristics as the native clay and aggregates in the same way as the untreated clay.

The second advantage over existing methods is to ability to capture spatial information, without the need to destructively sample the experiment, and temporal information throughout the experiment, allowing highly dynamic changes in tracer distribution to be captured. Other than work utilizing magnetic susceptibility (e.g. Armstrong et al. 2012), experimenters have largely relied on destructive sampling at the end of an experiment in order to understand surface processes. Destructive sampling has limited spatial resolution, because of the size of samples required (typically > 2 cm^2), is laborious, and for many tracers requires subsequent analysis. The temporal and spatial resolution of this tracing method will allow insights into the controls on colloidal detachment and transport to be gained, and have the potential to enable the spatial testing of distributed models of size-selective erosion processes (Heng et al. 2011).

The system I have described is limited in scale to a 0.5 m x 0.4 m soil box, constrained by the field of view of the camera as well as the area that can be illuminated with the laser. Larger fields of view could be used to expand the area that can be imaged; however, this would reduce the resolution of the system. Working on larger study areas will require a brighter laser for illumination and either multiple cameras to capture multiple images, which could be stitched together in post-processing, or a super-camera with a large frame area and high density of pixels, for example the qG (Aqueti Inc.), which is 250 megapixel camera with a 50 by 24 degree field of view.

This new tracing methodology will open up new opportunities to understand clay transport and associated pollutants and nutrients, helping us to develop a better understanding of these dynamic processes. There is potential to develop the system further to provide a tracer and detection method for field-based deployment and the quantification of tracer concentrations, opening up new possibilities for understanding the fate and behaviour of sediment and contaminants in the environment.

Supporting Information. Diagrams relating to equipment design, camera and lighting conditions, computer code, runoff testing and demonstration of application can be found in the Supporting Information. This information is located in Appendix 1.

Acknowledgments

R.H. is funded by a joint U.K. Natural Environment Research Council – Analytical Chemistry Trust Fund studentship (NE/J017795/1). Thanks to Mike James for his support with image processing and Debbie Hurst for microscope images.

Chapter 5: Using real time particle tracking to understand soil particle movements during rainfall events

Robert A. Hardy,[1] Michael R. James,[1] Jacqueline M. Pates,[1] and John N. Quinton[1]*

[1]Lancaster Environment Centre, Lancaster University, Lancaster, LA1 4YQ, U.K.

* Corresponding author: John Quinton (j.quinton@lancaster.ac.uk)

Highlights:

- Real time tracing of soil particles under rainfall conditions.
- Sub-second and sub-millimetre accuracy in particle location.
- Visual and numerical data interpretation toolkit developed in Python.

Key words: Particle tracing; soil erosion; fluorescent imaging; fluorescence; tracer

5.1 Abstract

Very little is known about how individual soil particles move over a soil surface as a result of rainfall. Specifically, there is virtually no information about the pathway a particle takes, the speed at which it travels and when it is in motion. Here I present a novel technique that can give insight into the movement of individual soil particles. By combining novel fluorescent videography techniques with custom image processing and a fluorescent soil tracer I have been able to trace the motion of soil particles under rainfall. The system is able track multiple sub-millimetre particles simultaneously, establishing their position 50 times a second with sub-millimetre precision. An analysis toolkit has been developed enabling graphical and numerical analysis of the data obtained. For example, I am able to visualise and quantify parameters such as distance and direction of travel. Based on my observations I have created a conceptual model (Stop, Hop, Roll) which attempts to present a unified model for the movement of soil particles across a soil surface. It is hoped that this technology will open up new opportunities to create, parameterise and evaluate soil models as the motion of individual soil particles can now be easily monitored.

5.2. Introduction

“Transfer soil material into a plastic tray for air drying”. This statement was taken from page one of *Procedures for Soil Analysis* ISRIC (Reeuwijk 2002) and succinctly illustrates how traditional soil science is conducted. In short, one goes into the field, collects a sample and then brings it back to the laboratory for analysis, which inherently limits the amount of information that can be collected about a given location. Firstly, sampling involves perturbation to the system being studied, and the more a system is studied the more perturbation occurs, leading to a delicate balancing act between the number of samples to be collected (and therefore the amount of data available) and need to limit the unwanted perturbation to the system. Secondly, soil is known to be a highly heterogeneous, both temporally and spatially, as are the erosion processes that redistribute soil particles and deliver them to surface waters (Armstrong et al. 2011).

To address the constraints introduced by sampling, and the costs associated with sample processing and analysis, there has been a growth in proximal soil sensing (PSS) to collect in field measurements of soil properties. These methods include the development of near-infrared spectroscopy for carbon measurements (Dhawale et al. 2015) and the use of hand-held x-ray fluorescence for metal determinations (Vanhoof et al. 2004). Such measurement techniques are generally much faster and cheaper than traditional methods, as there is no need to collect samples and data are generally acquired in digital form. As a result, more data can be collected with the same amount of resources. PSS methods are also often complementary to more traditional techniques and can be used, among other things, to inform targeted sampling. Here, I focus on a new PSS method, which can help inform our understanding of soil erosion.

To date, work on soil erosion processes has included seminal studies of splash erosion (Hudson 1965, Bollinne 1978), concentrated flow erosion (Knapen et al. 2007) and the interaction of

splash erosion processes with shallow overland flow (Kinnell 1988). These studies have led scientists to develop process-based modelling approaches to the prediction of soil erosion, such as WEPP (Nearing et al. 1990), EUROSEM (Morgan et al. 1998, Heng et al. 2011) and MAHLERAN (Wainwright et al. 2008, Wainwright et al. 2008, Wainwright et al. 2008).

Most soil erosion process studies have focused on bulk soil properties, deriving empirical relationships between soil properties and the erosive agent. For example, Bollinne (1978) related the kinetic energy of the rainfall to the mass of material ejected from a splash cup, and the relationships developed by Govers et al. (1986) to explain sediment concentration in overland flow related flow shear velocity to sediment concentrations. While these approaches have led to advances in our understanding of water-based erosion processes, our ability to progress beyond studies of bulk soil properties has been hampered by the availability of suitable methods.

Recent advances in image analysis have allowed scientists to examine the physics of erosion processes in more detail. Model systems, based on the measurement of single raindrop impacts on a bed of sand-sized particles, have allowed some insights to be gained into the likely effects of a raindrop impact. Much work has focused on developing a detailed understanding of the formation of splash craters and associated physics (Delon et al. 2011, Katsuragi 2011, Nefzaoui and Skurtys 2012). More recently Long et al. (2014) investigated the ejection of particles from a single raindrop impact, showing that the vast majority of ejected particles have low velocity and a high ejection angle, resulting in a small displacement, while less than 3% ejected particles have a low angle and high velocity resulting in larger travel distances (Long et al. 2014). Although not intended to mimic natural systems and working with single drops at small (< 1000 mm^2) scales,

this work suggests that soil particles are likely to be displaced via a series of small movements with intermittent larger movements.

Particle movement processes are beginning to appear in soil erosion models. Tucker and Bradley (2010) have proposed a particle-based model and there has been incorporation of particle based models into existing models such as MAHLERAN (Tucker and Bradley 2010, Cooper et al. 2012). This approach uses a 'marker in a cell' approach, which moves a marker (particle) through a series of cells. The cells contain hydrological information and the particles are passed through the cells. The model was tested using soil movement data from a single plot scale (13.75 × 6.5 m) ^{137}Cs tracer experiment. The empirical endpoints of the experiment were compared to the simulations of particle movements in the model. However no temporally-resolved data is available about the movements of individual particles throughout the experiment to allow validation of the model's movement of the particles. Instead validation can only be carried out based on the net movement of particles throughout the whole experiment.

Given the paucity of data on particle dynamics in response to erosion processes and the need to provide validation data for a new generation of particle-tracking soil erosion models, I set out to develop a simple and cost effective methodology that allows the motion of individual particles to be ascertained at high temporal and spatial scales. I demonstrate an experimental system that allows individual grains of a ~250 µm diameter fluorescent tracer to be tracked through time and space during a simulated rainfall event. A data set based on this work is presented and the potential for further work highlighted.

5.3. Materials and Methods

5.3.1 Experimental setup

5.3.1.1 Soil box setup

Following the methodology adopted by Armstrong et al. (2012), a soil box (0.2 × 0.3 × 0.15 m) was filled with 40 mm of gravel, followed by a fabric membrane, 30 mm of sand, and 40 mm of soil. The soil was sandy loam soil of the Oak 2 association from Calthwaite, Cumbria, U.K. (54.7544° N, 2.8281° W) and had been screened to 4 mm, prior to being packed carefully into the box in 1 cm layers with a bulk density of 0.9 g cm^3. A coated natural particle tracer (Partrac Ltd www.partrac.com) with a nominal diameter of 220 μm (250 μm after coating), consisting of a sand core and a green fluorescent coating, was applied to the surface of the upper area of the soil box. To produce a more natural pitted soil surface and to allow the particle tracer to become more integrated with the soil, the box was placed in water to a depth of 1 cm above the soil-sand interface for 24 hours following tracer application, the box was then exposed to simulated rainfall (40 mm h^{-1}) for 45 minutes, and finally drained for 1 hour before starting the experiment. The soil box was set on a slope of 5 degrees.

For the experiment, the box was initially covered to prevent rain from impacting on the soil. It was videoed for 78 s before the cover was removed, and videoing continued for a further four minutes whilst the soil was exposed to rainfall (40 mm hr^{-1}).

5.3.1.2 Lighting set-up

Illumination to excite the fluorescent coating was provided by 20 high-power 450 nm (blue) LEDs in two arrays. The LED arrays were located ~2 m from the soil box and positioned just behind and either side of the camera to reduce shadowing on the soil surface. The laboratory was blacked out, so there was no natural light present. Background lighting (for safety) was provided by

another 450 nm LED array in the middle of the laboratory, pointing at the ceiling. To prevent fluctuation in lighting intensity, the LEDs were driven from a constant current and voltage source (12 V, 0.7 A), with excess heat removed through aluminium heat sinks and forced air cooling.

5.3.1.3 Video setup

Full HD video, 1920 × 1080 pixels at 50 frames per second, was captured using a Panasonic HC-X920 digital video camera in telemacro mode, at the maximum image brightness setting. The camera was located 2 m from the soil box and imaged an area of 96 × 54 mm, giving a nominal pixel footprint on the soil surface of 50 × 50 µm. Due to the non-orthogonal nature of the camera in relation to the soil box the size of the pixel footprint will vary in the x direction. In the current work, this error is expected to be small due to the relatively small distances over which the particles are being tracked. However, if the particles were to be tracked over larger areas then it may be important to consider the systematic error in pixel area in future. The camera was fitted with a 490 nm longpass filter (Thorlabs), which prevented almost all of the light emitted from the LEDs from entering the camera, whilst allowing the particle fluorescence to be captured. The camera, lighting and soil box were positioned as show in Figure S1.

5.3.2 Initial data processing

Data processing was conducted on a Dell Precision T3500 running Ubuntu 14.04 LTS. All frames were extracted from the video using ffmpeg 2.2.4 (Figure 5.1a) and saved at their native resolution in a JPEG format to keep file sizes small. Code to pre-process the images was written using Spyder (Scientific PYthon Development EnviRonment) running Python 2.7.10. This code removed the red and blue channels (as they contain no useful information) and then minimised noise by setting all pixels with an intensity value less than a threshold, to zero. The threshold value was selected to most effectively reduce the noise without adversely affecting particle

detection, through trial and improvement over a subset of the images. The threshold value, 110 in the example described here, was then applied to the image set (Figure 5.1b). These exact values are unlikely to be transferable to different sets of images as they are highly sensitive to many operational parameters, such as lighting and camera location, camera settings and tracer concentration. Determination of a threshold value is a relatively simple process once one has gained experience in doing so. In this study, the process involved selecting an image which was reasonably representative of the whole image set. A threshold value was chosen, experience suggests that 75 makes a good starting point, and then the image was processed using this value (as described below). The detected location of particles is compared to the location of particles which is determined by the human eye, which is easily achieved by overlaying the detected particle locations on the original image (Figure 5.1c). False positives suggest that the threshold value is too low and particles not being found suggest the threshold value is too high. Optimisation on a single image continues until an appropriate value has been found. This value is then checked using a selection of other images to ensure that it is appropriate for the whole image set, after which the whole image set is processed using the determined threshold value.

Each pre-processed frame was then searched for particles (Figure 5.1c) using the Python library trackpy (https://github.com/soft-matter/trackpy). Trackpy recognises a particle by identifying a small image region having a 2-D Gaussian-like distribution of pixel brightness, and determines sub-pixel coordinates of the brightness centroid, as well as other parameters.

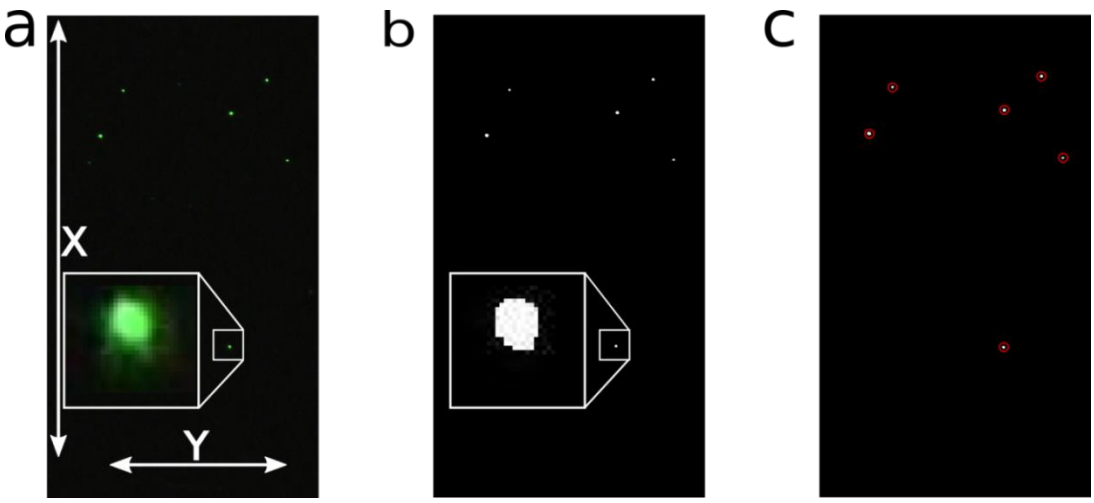

Figure 5.1. The identification of particles in the video frames. X is the up and down slope direction and y is across-slope. a) A raw frame extracted from the video footage (1920 × 1080 pixels, 96 × 54 mm). The inset shows an enlargement of a particle (original size 20 × 25 pixels enlarged to 80 × 66.6). b) The same frame after grey-scale and threshold pre-processing. The inset shows an enlargement of a particle (original size 20 × 25 pixels enlarged to 80 × 66.6). c) The particles (circled) identified using the trackpy routine.

5.3.3 Pathway location

A linking algorithm was used to match particles detected in different frames into pathways representing the movement of individual particles (Figure 5.2a). Each identified particle in a frame was linked to an identified particle in the subsequent frame, if it was located within a defined spatial range (75 pixels in this case) of the original particle location, with no prediction made of the particle movement direction. If there was no particle within the area, the algorithm searched forward through subsequent frames until one was found. If a maximum number of frames (50 in this case) was exceeded, then a pathway was ended. The resulting particle pathway (Figure 5.2a) was given a unique number (Pathway Number), which was stored along with other parameters. Sometimes a clearer impression of a pathway can be gained by visualising the discrete particle locations as a continuous line (Figure 5.2b); however, it must be remembered that the particle may not have followed this path explicitly and no additional data are created in

this process. The expected level of deviation from the shown pathway is expected to be low, as the particles are located 50 times a second, and should greater accuracy be required, then a camera with a higher framerate could be used.

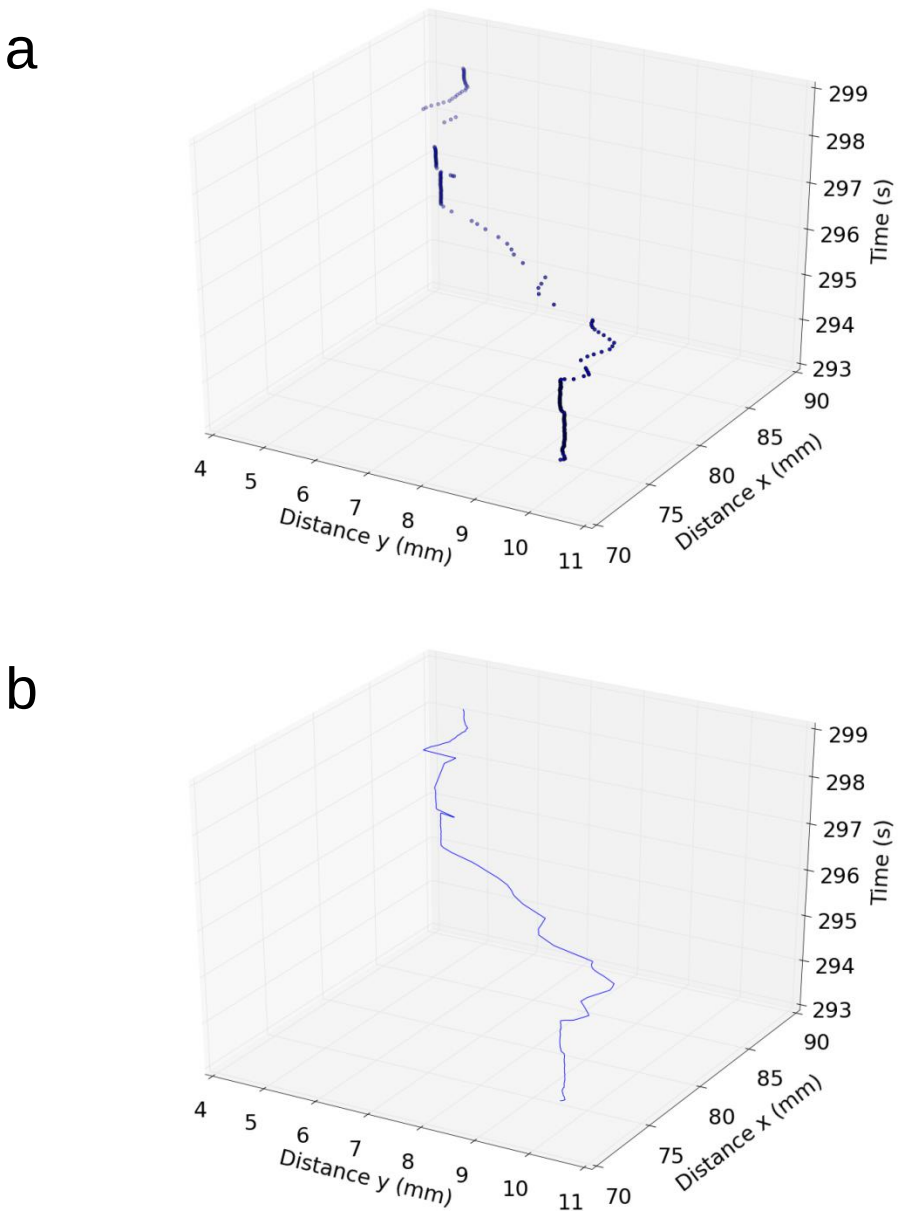

Figure 5.2. The movement of a single particle over 218 frames (4.36 seconds). a) The precise locations each time the particle was detected. b) The pathway created by interpolating between the locations given in a). The particle was detected in all but one of the 218 frames.

Further filtering was carried out by removing pathways lasting less than 25 frames (0.5 s) and pathways with a mean "signal" (a parameter determined by trackpy relating to the brightness of a particle) of <125. Data from the first 200 frames were removed due to camera shake; the rainfall simulator was turned off at frame number 15,000.

5.3.4 Data analysis tools

Bespoke visualization tools were used to display the position of the particles and their pathways in time and space. Functions (Table 5.1) were written in Python to assist with analysing the data produced from the images, and are available on request.

Table 5.1. Data analysis tools written to extract quantitative data describing the particles' movement.

Parameter or process (function name)	**Description**
Pathway length (displacement)	Calculates the summed displacement for a particle in x and/or y directions.
Net pathway length (displacement_net)	Calculates the net displacement of a particle, i.e. the straight line displacement between start and end positions.
Speed (speed)	Calculates the speed of a particle determined by dividing pathway length by time (measured in frames).
Average speed inside pathway (avg_speed_inside_traj)	Calculates the average speed of a particle over a given time interval.
Particle presence ratio (confidence_interval)	Calculates the fraction of frames in which a given particle is actually identified within its pathway. For example, if a pathway persists for 100 frames, but the particle is only found in 50 frames then the particle presence ratio (PPR) would be 0.5.
PPR filtering (confidence_filtering)	This function removes all trajectories with a PPR of less than a given value.

5.4. Results

When the experiment began, the high moisture content in the soil quickly led to visible shallow overland flow, which (visually) strengthened over the duration of the experiment. Of the particles applied, six were detected, and these were clearly observed to move within the video imagery. In the video frames, detected particles generally appeared as bright, near-circular features (Figure 5.1, insets) with diameters approximately 2.5 times those expected from the physical particle

sizes. This apparent enlargement is thought to be a camera effect (similar to blooming, and probably due to the high amplification required under the low light levels), but raised a question as to the precision of the particle locations derived.

5.4.1 Estimating uncertainty in particle location

Efforts have been made to understand the precision of the calculated particle locations. At the start of the experiment there were six particles which remained static for the first 78 s (3900 frames) as no rainfall was present. As the particles were static then net displacement should be zero and any deviation from this value was interpreted as an uncertainty relating the location of the particle. The particle presence ratio (PPR, Table 5.1) for each pathway was 1.00, indicating that each particle was found in each frame. This suggests that the system is very capable of detecting particles in a reproducible manner. The range of net displacements was 0.054 to 0.072 mm, and the mean was 0.065 mm. Thus, although sub-pixel particle coordinates were derived (given by the calculated brightness centroid), the measurement precision was ~1 to 2 pixels. Nevertheless, this precision compares favourably with the physical size of the particles (typically 0.13 mm or nearly 3 pixels). Therefore, despite the image blooming effect, it was possible to consistently locate particles and determine their position. Errors were smaller than the typical particle size and orders of magnitude smaller than expected travel distances (the total imaged area was 96 × 54 mm).

5.4.2 Particle movement

Figure 5.3a and Movie S1 (online version only) illustrate the movement of particles for the complete duration of the experiment and include the static period of 78 s followed by the rain event of 218 s. Six stationary particles (vertical lines in Figure 5.3a) can be seen at the start of the experiment. To avoid confusion, it should be noted that there are many more than six tracer

particles present in the soil box at the start of the experiment. It is expected that they are not visible as they are under the soil surface. As the soil moves these tracer particles may become present on the surface, in the same way that subsurface soil particle may move to the surface. Once the rain begins to fall (79 s) the particles start to move. It is clear that individual particles are not moving at all times, but when they do move that they tend to move in almost instantaneous hops or jumps, then roll. If the jump or roll intersects with a flow path the roll continues and the pathway is extended, but at a slower rate than those particles that have been ejected by a raindrop impact. Visually the pathways show some resemblance to those predicted by stochastic models (Lisle et al. 1998) as well as the more recent models by Tucker and Bradley (2010). The net direction of travel is mostly in a downslope direction (x), although many particles (e.g. Movie S1 particle in top right 4 min 20 s to 4 min 49 s) exhibit multiple uphill movements.

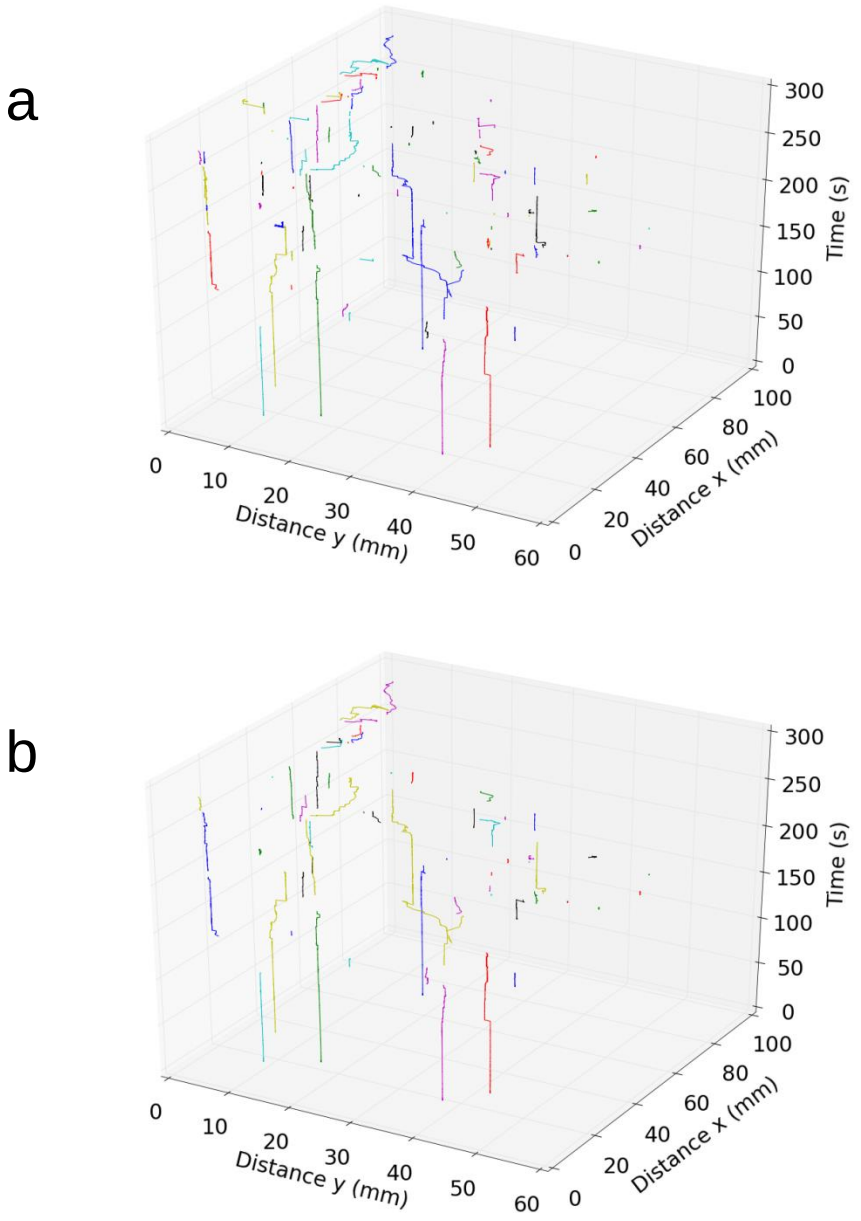

Figure 5.3. Particle pathways across a soil box during a simulated rainfall event (30 mm hr^{-1} starting at 79 s and finishing at 296 s) for: a) all particle pathways that have a lifetime > 0.5 s, and b) following the application of a filter based on a PPR of 0.95. Some particle pathways are truncated due to burial and/or submergence under water.

To improve the confidence that particle pathways are a true representation of the particles' movement a filter based on a PPR of 0.95 was applied (Figure 5.3b). This filter reduced the total number of trajectories from 94 to 61 (35%) and in practice meant that all the pathways described in Figure 5.4 have unknown particle locations for less than 5% of frames. Although the PPR is informative, it can be misleading as the particle location tool has the greatest chance of identifying a particle location while a particle is stationary and the particles are stationary most of the time. Therefore, it is possible that, when a particle is moving, proportionally fewer locations are returned when compared to it being stationary. As particles can spend a long time stationary a high PPR may be possible, but there may be limited information concerning the particle while in motion.

Figure 5.3 gives an excellent overall impression of the results; however it is difficult to examine the pathways of individual particles in detail. Using the bespoke visualization tools developed here, the trajectories of individual particles were extracted. Figure 5.2 illustrates this process for one particle; Figure 5.2a shows the particle location each time it was located on a given pathway and Figure 5.2b interpolates between particle locations to give an overall pathway. For this example, the PPR is 0.9908, meaning that the particle is present in over 99% of the frames.

Using the particle pathway illustrated in Figure 5.2, I can examine the movement of the particle in more detail. The total net displacement of this particle pathway is 23.5 mm, which is comprised of 17.99 mm of downhill travel (x axis) and 5.45 mm of movement to the left (y axis). The total pathway length was 28.4 mm, with 19.33 mm movement in x axis (up and down slope) and 9.01 mm in the y axis (across-slope). The mean speed of the particle was 6.50 mm s^{-1}, which is comprised of 4.43 mm s^{-1} in the x axis (up and down hill) and 2.07 mm s^{-1} in y axis (across-slope). The speed of the particle during its journey is highly heterogeneous (Figure 5.4);

movement is short lived and has speeds (based on 0.1 s averages) ranging from 0.04 to 45.15 mm s^{-1}.

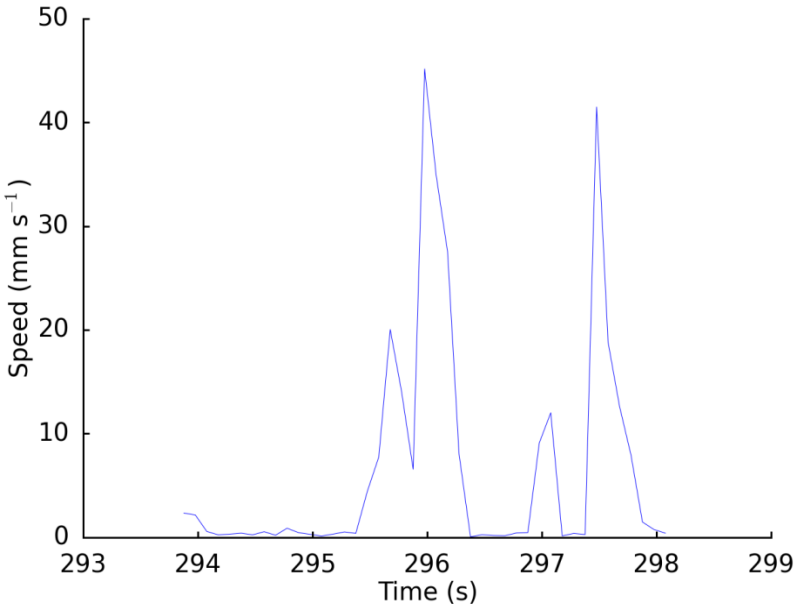

Figure 5.4. The speed profile of a single particle averaged over 0.1 s increments.

Using the filtered data displayed in Figure 5.3b I can explore the movement of multiple particles. There is a large range of average speeds and displacements (Figures 5.5 a, b). Most of the particles (68%) have displacements of < 2 mm, with the maximum displacement being 23 mm. No relationship was found between average speed and pathway length (Figure 5.6).

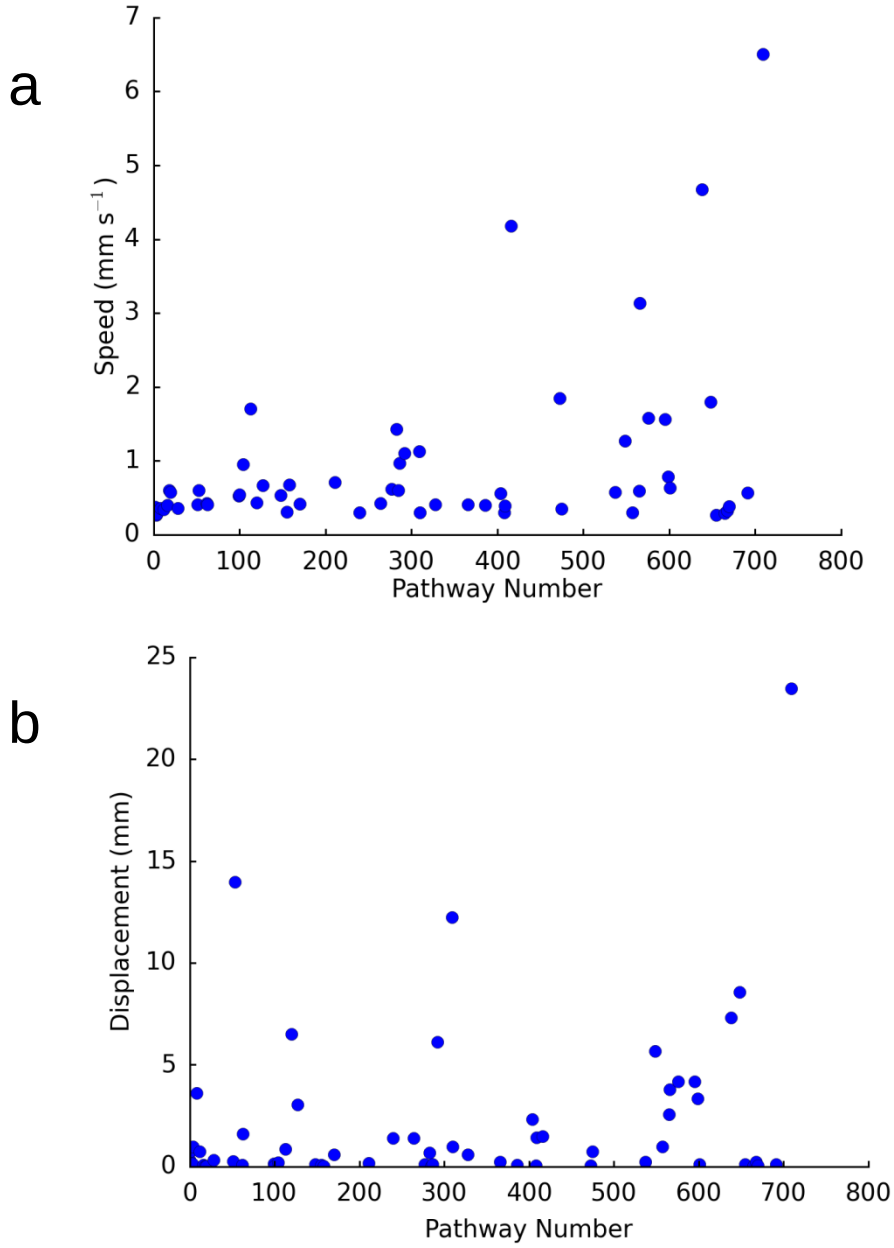

Figure 5.5. The range of a) speeds and b) net displacements for 61 particle pathways.

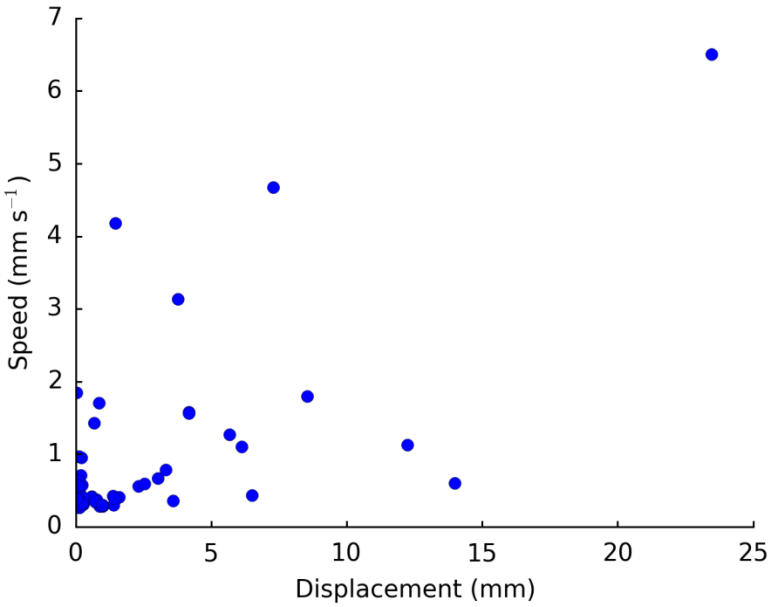

Figure 5.6. Comparison of particle speed and net displacement for 61 particle pathways. Note the lack of correlation between these two parameters.

The net displacement in x and y directions (Figure 5.7a, b) shows that most movement is in the downslope direction, with only a small amounts of uphill movement (Figure 5.7a). Out of the 61 pathways analysed, 38 had net downhill movement and 23 had net uphill movement. If the uncertainty in the particle location is considered (± 0.1 mm), then only 12 pathways show clear uphill movement, whereas 25 pathways show clear downslope movement. Furthermore, the maximum upslope displacement was 0.67 mm, while the maximum downslope displacement was 17.99 mm. As expected, movement across slope (Figure 5.7b) was more evenly distributed; 31 pathways showed net movement to the right whereas 30 showed net movement to the left. If uncertainty in the particle location (± 0.1 mm) is considered, then 17 showed movement to the left and 17 showed movement to the right and 27 showed no displacement.

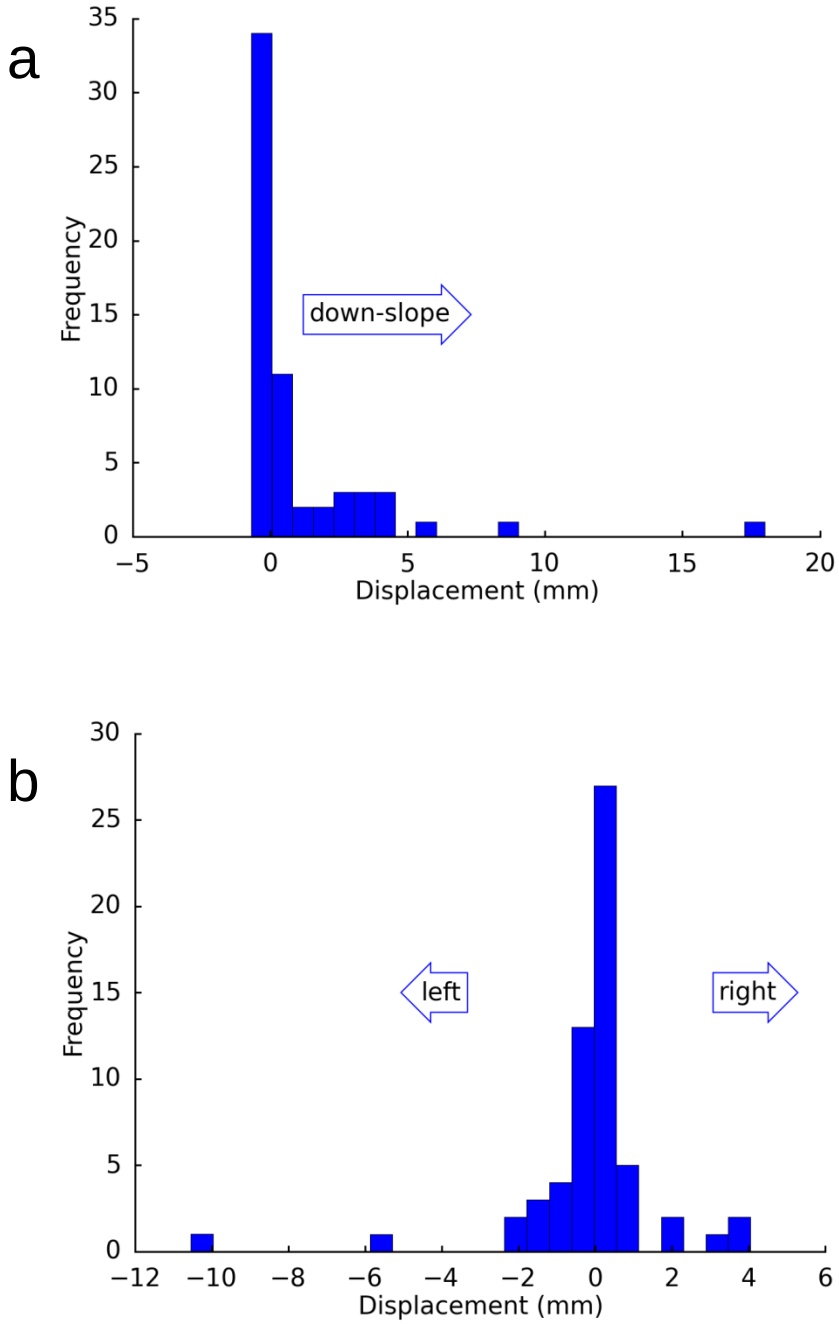

Figure 5.7. The frequency distribution of net particle displacement for 61 particle pathways: a) in the y direction (up-down slope) and b) in the x direction (perpendicular to the slope).

Overall, the average speed of the individual particles increases with time (Figure 5.8). Over the duration of the experiment, there are times when the average speed of all the particles is close to 0, but the range of average particle speeds increases with time. This apparent increase in speed over time could be linked to the increased overland flow that occurred as the experiment progressed.

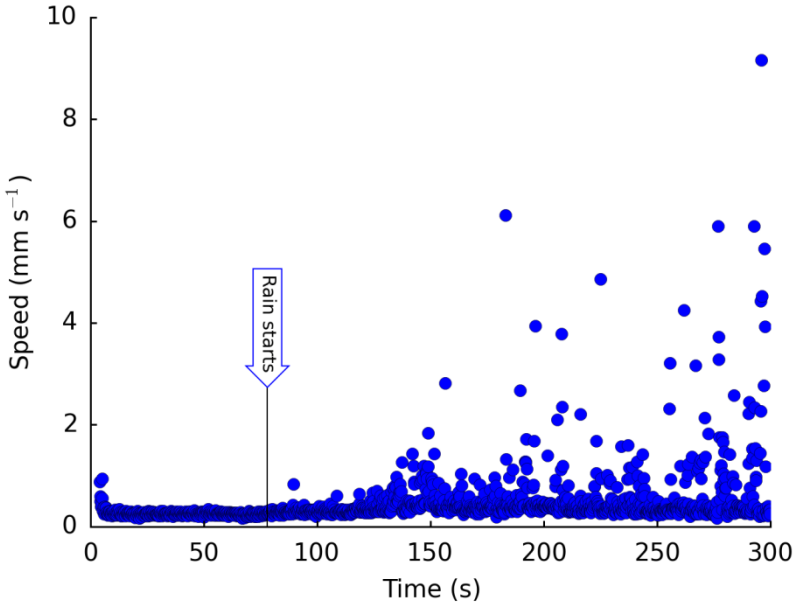

Figure 5.8. Average speed (0.1 s time steps) for all the particles detected.

In the video frames, evidence of "hops" taking place is represented by a particle apparently appearing in two places at the same time (Figure S2), suggesting that the particle is moving rapidly from one place to another. At one location, the particle image becomes duller, whilst at the other, it becomes brighter, and there is a streaking of the image in the direction of travel. Although the ejection of particles from granular media due to a single raindrop impact has been extensively studied (Nefzaoui and Skurtys 2012, Long et al. 2014), I believe that this is the first time that the hops of multiple particles in response to multiple impacts has been captured in real-time, under continuous rainfall conditions.

5.5. Discussion

To date, measurements of soil particle movements have been static, i.e. following a single raindrop impact. Here, for the first time, I have described a method for the collection of soil particle movement data at high temporal and spatial resolution under continuous rainfall conditions. The method allows the motion of many particles to be recorded and investigated under conditions similar to the natural environment. By removing the need to physically sample soil to obtain data, or to stop the experiment to sample, this method offers a step change in the way that data relating to erosion processes can be collected. Equally, by reducing the amount of time, money and resources needed to collect, process and analyse soil and sediment samples, this method allows more resource to be focused on developing our understanding of soil processes.

5.5.1 Model parameterization

Our approach is an important step since a new generation of erosion models is being developed that simulate particle transport and rely on an empirical base. However, as Wainwright et al. (2008) point out, there are "no physically based derivations of detachment, entrainment and travel distance" which are key parameters for these types of models. The method I propose here offers the potential to deliver the empirical evidence to parameterize and evaluate these new approaches to soil erosion modelling, such as those proposed by Wainwright et al. (2008). For example, Wainwright et al.'s (2008) MAHLERAN model approximates particle velocity, u_p, by using v_p (virtual transport rate), which they suggest can be parameterized by empirical observation of distance moved by a sediment particle per unit time, although these observations have proved difficult to obtain until now. However, my data suggest that particle speed (which is related to, but not identical to v_p) cannot be used as a proxy for displacement (Figure 5.6).This is not to suggest that the MAHLERAN model is incorrect (or in fact correct), as it does not use v_p as

a proxy for displacement. However, it does highlight the difficulties that can be encountered when using empirical data to parameterise models and that extreme care must be taken to ensure the appropriate parameter is selected for use in the model. This observation may be explained by the varying length of times that the particles remain still and the tendency for particles to stop moving. For example, take two particles, which both travel the same distance: particle A remains stationary for 1 second before moving 10 mm and is then buried; particle B remains stationary for 100 s before moving 10 mm and is then also buried. Particle A will have a speed of 10 mm s^{-1}, whereas particle B will have a speed of 0.1 mm s^{-1}. Furthermore, there appears to be a large spread of average particle speeds; the data presented in Figure 5.6b varies over four orders of magnitude (0.00061 - 2.15 mm s^{-1}) for the 61 pathways recorded. The distributions of both speed and displacement are strongly skewed, with very few particles moving fast or far. This observation may make it challenging to use a single number to parameterize v_p even in a controlled environment. It may be more useful to utilize the distribution of v_p and adopt a probabilistic modelling framework.

5.5.2 Overland flow as a driver for movement

It is clear from my results that the movement of soil particles is highly complex. Tucker and Bradley (2010) discuss "Ballistic Versus Near-Ground Motion". Ballistic motion refers to the movement of a particle through the air whereas near-ground motion refers to motion at or near the soil surface (like rolling). There is strong evidence in my experiments that both of these processes take place. Figure S2 clearly shows ballistic motion and particles can be seen exhibiting near-ground motion (rolling) in Movie S1. Tucker and Bradley (2010) imply that near-ground motion is linked to the gradient of the soil surface. There have also been large scale studies linking steeper slopes with increased erosion rates (Bakker et al. 2005), while others have suggested that overland flow occurs in greater volume on steeper ground (Akbarimehr and

Naghdi 2012). In this experiment, the slope of the soil surface remained more or less constant, however the speed at which the particles moved increased through the experiment. Although the magnitude of the observed overland flow was not measured, the observation that it appeared to increase as the experiment progressed, suggests that this was responsible for the increase in travel particle travel distances through time. The slope used in the experiment was shallow and particle rolling (non-local motion, Tucker and Bradley (2010)) seemed to be associated with particle transport in overland flow. I suggest that, in certain circumstances (such as the test conditions), it is the presence of overland flow that is the real driver for particle movement rather than the gradient of the slope. It could be considered that every particle that is not in motion is at a local energy minima and therefore in order for motion to be induced energy must be added. This energy could take the form of a raindrop impact which give the particle enough energy to overcome this local energy minima and therefore move.

5.5.3 Stop Hop Roll Model

This new understanding leads me to propose a simple conceptualization of splash and shallow overland flow transport of soil particles. Attempts at conceptualizing rainsplash-dominated transport are not new and include that of Kinnell (2005) who describes three types of Raindrop Impact Induced erosion, namely raindrop detachment splash transport, raindrop detachment with raindrop-induced flow transport, and raindrop detachment flow transport. However, Kinnell's approach tends to segment splash-induced transport processes suggesting that they tend to be seen separately from one another, and that there is a distinct point at which surface runoff begins.

When I examine the movement of multiple individual particles (on a sub-millimetre scale), I find that a particle will undergo a number of modes of transport within a very short time period.

Equally, at this scale, runoff is not simply present or absent, but surface water will alternately pond and flow, as it accumulates behind a barrier and then breaks through. There may be many of these pond and flow events over a small spatial area. Therefore I suggest that, at this scale, the movement of particles in response to a continuous rainfall event can be described simply as: stop-hop-roll-repeat.

"Stop" means that a particle is initially motionless and may remain this way; in Figure 5.2 particles remain stationary for extended periods of time. "Hop" is a rapid movement from one spot to another, and implies ballistic motion caused by the impact of a raindrop (Figure S2), when detachment of a particle from the soil surface occurs. The nature of this detachment is violent and abrupt, which results in the particle leaving the soil's surface. On shallow slopes hops are, on average, non-directional and result in no net soil movement. Leguedois et al. (2005) suggest that on shallow slopes splash is not an effective soil transport mechanism, but is important in detachment, which is in line with this papers findings and in keeping with this conceptual model. As an example, on a flat soil surface it would be expected the movement due to splash erosion in any direction would be, on average, equal. As a shallow slope is very similar to a flat surface, then it would be expected that any net directional component in soil movement would be minimal. This fits with the findings of this paper in that I do not attribute much of the soil movement to raindrop impact itself. Rather it is the raindrop impact that gives the soil particle the initial energy to become detached, or the "hop" stage of the model.

The "roll" step is responsible for most, if not all, of the net movement of soil; the net direction of movement is predominantly downslope and the travel distance is variable, see for example Movie S1 in the online version of this paper. Rolls start, on average, as non-directional transport with particles moving towards local depressions, for example a raindrop splash crater. However,

if during the course of the initial roll the particle interacts with flowing water then the particle will move with the water for a period of time until it stops. This study is not currently able to distinguish between different modes of transport in flowing water, i.e. bedload, saltating or entrained particles, but given the small scale of the flows and their transient nature I expect that most particles are rolling over the soil surface or saltating, probably a mixture of both. This conceptual model is cyclic and a particle often undergoes many cycles before it has moved any significant distance. Abrupt changes in slope or deep flowing water will cause the model to break down as the particle may no longer be able to hop in all directions or be subjected to raindrop impact.

5.6. Conclusions

This method gives, for the first time, data with a high temporal (1/50 second) and spatial resolution (< 1 mm) describing how soil particles move as a result of rainfall. The use of video and image analysis tools delivers rapid turnaround times for data analysis at low cost. Data on the recorded motion of particles generated using this methodology have the potential to parameterize and validate a new generation of soil erosion models to describe particle movement, allowing a deeper understanding of the motion of soil particles to be developed by giving clear empirical evidence of how these particles behave.

This work also highlights the importance of developing new technologies within geomorphology and soil science that take advantage of general advances in technology.

Acknowledgments and Data

R.H. is funded by a joint U.K. Natural Environment Research Council – Analytical Chemistry Trust Fund studentship (NE/J017795/1). Thanks to Mike Coogan for his insights into fluorescence and to Partrac Ltd (Glasgow) for supplying the tracer.

Supporting information

The supporting information relating to this chapter can be found in Appendix 2.

Chapter 6: Quantitative LED-induced fluorescence tracing (qLIFT): A laboratory based trial

Authors: Robert Hardy, John Quinton, Jackie Pates, Mike James

6.1 Abstract

Understanding the movement and fate of soil in the natural environment is of great important. One way that soil movement is often studied is by the use of tracers. Here, I present new techniques to allow for the use of a commercially available tracer to monitor the movement of soil across a soil surface in a laboratory setting. The two techniques presented here can be used to quantify the concentration of tracer in a given location without the need to physically sample the soil. One technique allows for the automatic enumeration of individual tracer particles, which works well at low concentrations, while the other uses the amount of light emitted from the tracer which allows for higher concentrations to be quantified. This makes the techniques rapid and cost effective as well as being complementary to existing techniques which require sampling. The theoretical bases for these techniques are described along with a lab-scale demonstration of the techniques and examples of the types of data that can be acquired. These techniques use monochromatic light from LEDs to illuminate the tracer, and a modified DSLR camera to sample the tracer. The images are then processed using custom written software (in Python) into user friendly outputs such as colour intensity maps of the area, showing the relative amount of the tracer.

6.2 Introduction

Soil erosion is a global problem, with the FAO stating that if soil erosion continues at its present rate, there will be a 10% reduction in global crop yield by 2050 (ITPS 2015). There has been a long history of studies in to both erosion processes and erosion control measures with these largely taking the form of monitoring sediment at the outlet of a field plot, hillside or catchment e.g. (Quijano et al. 2016, Zhang et al. 2016). These approaches have several

drawbacks: they only provide information at the sampling point, and reveal little about the transport pathways taken by the sediment. They may also disrupt the very system they are being used to study, by imposing boundaries and removing sediment and water from the system. Tracers offer a way to gain an insight into how soil erosion process operate. There have also been calls for the development of new tracing technologies (Stroosnijder 2005)

The most commonly used tracer in soil erosion studies is ^{137}Cs, a fall out radionuclide principally associated with atmospheric nuclear weapons testing and nuclear accidents (Guzman et al. 2013). Caesium-137 has a half-life of 30.2 years, which means that unless there are significant new releases, it will cease to be useful as a soil tracer in the near future. It should be remembered that this tracing methodology was created opportunistically and that ^{137}Cs was never designed as a tracer.

Alternative approaches to soil tracing have been developed and have included the use of rare earth oxides (Kimoto et al. 2006), magnetic minerals (Guzman et al. 2010), ceramic prills (Plante et al. 1999) , RFIDs (Radio Frequency IDentification) (Parsons et al. 2014) as well as rock (Poesen et al. 1997) and glass fragments (Young and Holt 1968). Such tracers have helped to identify sediment transport pathways, however, most suffer from a significant problem: in order to innumerate the tracer after the erosion event, samples need to be removed from the study site, which is costly and time consuming.

Physically sampling the soil has another major drawback: it disturbs the study environment, often affecting the process that is being studied. This means that assessing changes over time e.g. after multiple rainfall events, is difficult. Currently there are no routine techniques that allow the quantification of a soil tracer without the need for sampling. Although magnetic susceptibility measurements have been used quantitatively on small scale (Guzman et al. 2010), they cannot be used quantitatively unless the vertical distribution within the soil is known (or assumed). This requires sampling, due to the non-linear decay of the tracer signal

with depth. Therefore, there is an urgent need for a tracer that can be analysed, without the need to physically sample the soil, to generate soil movement information with greater temporal and spatial resolution, as well as reducing the cost and logistical challenges associated with sampling and analysis.

Fluorescent sediment tracers have been used to study the movement of sediments in estuaries (Gerino et al. 1998) and marine environments (Bradshaw et al. 2006), but these studies have relied on the use of sampling to determine tracer distributions. Within terrestrial systems there has been some interest in the use of fluorescent tracers, however there is still a tendency to rely on sampling (Woods et al. 1999). Here I develop a novel method, qLIFT (Quantitative LED-Induced Fluorescent Tracing) that utilises LED light to induce fluorescence in a sand-sized tracer, which is then detected using CMOS (complementary metal oxide sensors) as it moves across a soil surface without the need for removal of soil material. I present two complementary but independent methods for quantifying the concentration of tracer from images. This paper focuses on the development of these techniques as well as giving examples of the type and nature of the data which the techniques are able to generate. For example, I show that the technique offers the ability to gain information relating to the movement of a tracer in response to simulated rainfall at very high temporal and spatial resolutions. It should be noted that this paper does not aim to offer any explanation of the processes which are responsible for tracer particle movement. Rather, it simply presents a technique that can allow for quantitative assessment of tracer particle concentration in the presence of rainfall without the need to physically remove material when sampling. It is hoped that this will allow for studies of dynamic processes, such as soil movement in response to non-steady state rainfall, to be investigated in greater detail than was previously possible.

6.3. Materials and methods

6.3.1 Experimental setup

6.3.1.1 Tracer

The tracer used throughout was a commercially available fluorescent tracer (Partrac Ltd), green in colour, consisting of natural quartz particles coated with a fluorescent pigment. In the laboratory studies, particles with a nominal diameter of 250 µm were used, whereas in the field study, a smaller tracer with a nominal diameter of 70 µm was used. The tracer has been used widely in estuarine and marine studies, and to a lesser extent in terrestrial environments, and is known to be stable in a variety of environments (Black et al. 2013, Collins et al. 2013). Partrac are capable of manufacturing a wide range of tracers with varying physical properties, such as size and density, and providing the appropriate tracer can be manufactured the tracer should be reasonably representative of the soil which it is designed to trace.

6.3.1.2 Lighting and image acquisition

Correct lighting is critical to successful image acquisition. The lighting must be uniform (both spatially and temporally), of narrow and fixed wavelength, and of the correct intensity. For field work, portability, ease of use and robustness must also be considered. Custom made lights using LEDs offered the best solution at minimal cost. Two LED lamps (nominal wavelength 450 nm) with diffusing plates fitted were used (details can be found in Supporting Information (SI Lighting)).

Images were recorded using the CMOS array inside a Canon 500D DSLR camera. A 490 nm longpass filter (Knight Optical) was fitted to the lens to prevent the camera from detecting the LED light. The Canon 500D DSLR was controlled manually with a wired shutter release. Images were recorded at the highest possible resolution in JPEG format, to ensure that the

data size was reasonable and easily accessible by a wide range of software. Post-processing was carried out using a custom written script in Python (Python 2.7, SPYDER[2]).

6.3.1.3 Image interpretation

I used two methods to analyse the amount of tracer in the images: an intensity-based method, similar to that of Hardy et al. (2016) and a particle counting method. The intensity-based method used the numeric pixel values from the green colour channel in the camera. Thus, each pixel is treated as an individual data point, which rapidly leads to the generation of large data sets. Therefore, there is a need to manipulate these matrices in different ways depending upon the task in hand. It may be possible for a single pixel to have more than one particle in it, however this does not affect the ability of the software to determine the concentration of tracer present when using the intensity based method. Having more than 1 particle in a pixel will simply result in that pixel having a higher value. Further details can be found in Hardy et al. (2016). If an average concentration of tracer was desired, the median or mean value of the whole matrix was used without regard for the position of each data point. Alternatively, if data regarding the total amount of tracer in a given area were desired, then the sum of all pixels in that area was used.

Often areas of the image must be selected for analysis, and selecting the appropriate area is key. In order to avoid overly complicating the process of area selection (and thus keeping it within the realms of a moderately-skilled user), areas were rapidly selected by eye and were not subsequently manipulated to “improve” the data. Areas consisted of a rectangle defined by the upper left and lower right corner coordinates, found using GIMP (GNU Image Manipulation Program, https://www.gimp.org/) by placing the cursor in the desired locations and noting the values displayed.

The second approach was to count the number of individual particles present in a given area, which is less sensitive to changes in lighting intensity and camera position than the intensity-

based approach. The particles were located using bespoke software, drawing on the Python trackpy library and detailed in Hardy et al. (2016). This software also returned a parameter relating to the intensity of the particles located, permitting filtering of false positives, which are common due to the highly sensitive search algorithm used. False positives can be reduced by more aggressive preprocessing of the images; however this may also result in missing some of the tracer particles. Therefore, it has been found that it is generally better to allow the false positives and filter later rather than attempt to remove them.

6.3.2. Validation of the intensity-based method

To gain a better understanding of how the tracing system performed, a laboratory experiment was conducted. A 1.1 x 1.3 m soil covered area was prepared in the laboratory to which soil-tracer mixtures were applied in small patches. The mixtures were created by sieving a loam textured soil to 1 mm and combining it with tracer in varying concentrations. Further details about the configuration of lighting and camera can be found in SI Laboratory setup.

A series of assumptions were established, namely:

i) For patches of the same concentration, there is minimal difference between patch intensities and the intensity of each patch is uniform.

ii) There are only small differences between different images of the same tracer surface.

iii) The variation in the intensity between patches of the same concentration is much smaller than the intensity variation between patches of different tracer concentrations, and the concentrations can be clearly differentiated.

iv) Tracer concentration can be expressed as a function of intensity.

To test assumptions (i) and (ii), 12 patches (20 x 20 cm) of soil-tracer mixture (100 g kg^{-1}) were applied to the soil surface and images acquired as described above. To test assumption (iii) and (iv), soil-tracer mixtures containing 3.97, 11.51, 19.85, 44.60 and 93.57 g kg^{-1} (concentrations A, B, C, D and E) were applied to the soil surface (~ 2.0 x 2.0 m) in patches (~ 25 x 25 cm) as a complete random block pattern (Figure 6.1).

D-1	A-6	C-11	E-16	B-21
B-2	C-7	E-12	A-17	D-22
D-3	C-8	E-13	B-18	A-23
E-4	D-9	B-14	A-19	C-24
A-5	B-10	D-15	E-20	C-25

Figure 6.1. The complete random block pattern layout used for testing hypotheses (iii) and (iv). Numbers are used to identify the block position. Letters refer to tracer concentrations, where A is 3.97, B is 11.51, C is 19.85, D is 44.6 and E is 93.57 g kg^{-1}.

6.3.3 Validation of the particle-based method

In order to test the ability of this method to accurately and reproducibly count particles, four test counting samples (TCS) were created by sprinkling a small amount of tracer onto a circular piece of Blu-Tack (~ 6 cm diameter) and gently pressing it into the surface of the Blu-Tack. When imaging the TCS, the setup was similar to Figure 6.2, but with the camera positioned 1.5 m from the TCS, which created a non-orthoimage. To determine the reproducibility of the technique, each TCS was imaged 11 times, and the total number of particles in each image was determined.

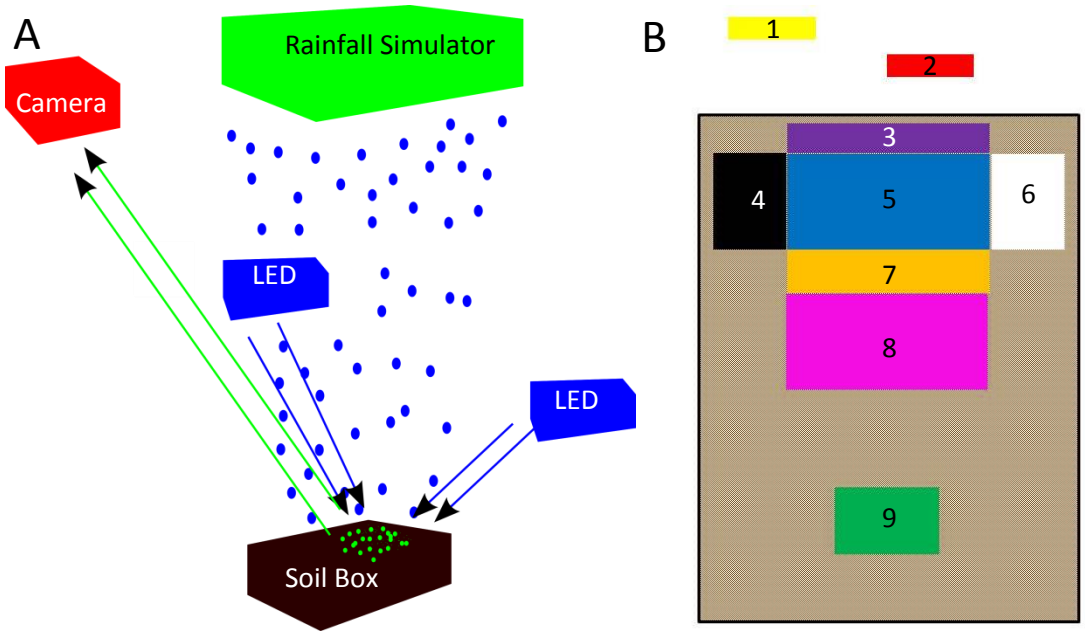

Figure 6.2. Schematic of the setup used to image the movement of the tracer. A) The blue arrows indicate the direction of the LED light and the green arrows show the pathway of the green light emitted by the tracer towards the camera. B) A schematic of the soil box surface. The numbered coloured areas represent image sampling locations: original tracer location (OTL) (5-blue), left (4-black) and right (6-white), above (3-purple) and below 1 (7-orange), below 2 (8-pink) and below 3 (9-green) the OTL. The yellow (1) and red (2) boxes are optical (OCL) control locations 1 and 2 respectively.

6.3.4 Quantitative real-time assessment of tracer movement

A 0.5 x 0.3 x 0.1 m soil box with drainage holes was filled with 3 cm of gravel, 1 cm of sand and 4 cm of an Oak 2 association sandy loam soil from Cumbria, UK. This soil had been sieved to 4 mm and the original moisture level preserved by keeping the soil in sealed plastic bags. After the soil box was filled, a 2 cm deep area of soil, corresponding to the blue area in Figure 6.2 B, was removed. This was then replaced with a soil-tracer mixture based on the same soil, with tracer concentration of approximately 100 g kg^{-1}. The soil box was wetted by placing in water to 1 cm above the sand-gravel interface for 24 hours and then removed and allowed to stand for 2 hours.

A cover was placed over the soil and a falling drop rainfall simulator (Armstrong et al. 2012) was run until the rainfall rate had stabilized at 40 mm h^{-1}. The cover was removed and time-lapse photography commenced. The soil box was exposed to rainfall for 3335 seconds after

which the cover was replaced and the rain stopped. Figure 6.2A shows the relative position of the camera, soil box, rainfall simulator and lights. The camera was positioned as close to vertical above the soil box as possible without obstructing the rainfall, allowing for near-orthoimages to be obtained.

6.4. Results

6.4.1 Validation of the intensity-based method

Figure 6.3A shows that it was possible to capture the desired area in a single photograph (~ 1.5 m x 1.5 m), while retaining a high degree of fine detail (millimetre resolution). A false colour image (Figure 6.3B) shows variations in tracer concentration that are not visible in the original. The data set consists of the nominal intensity of each pixel in the image. Throughout, intensity is presented without units, as the camera may generate interval, rather than ratio, data.

1

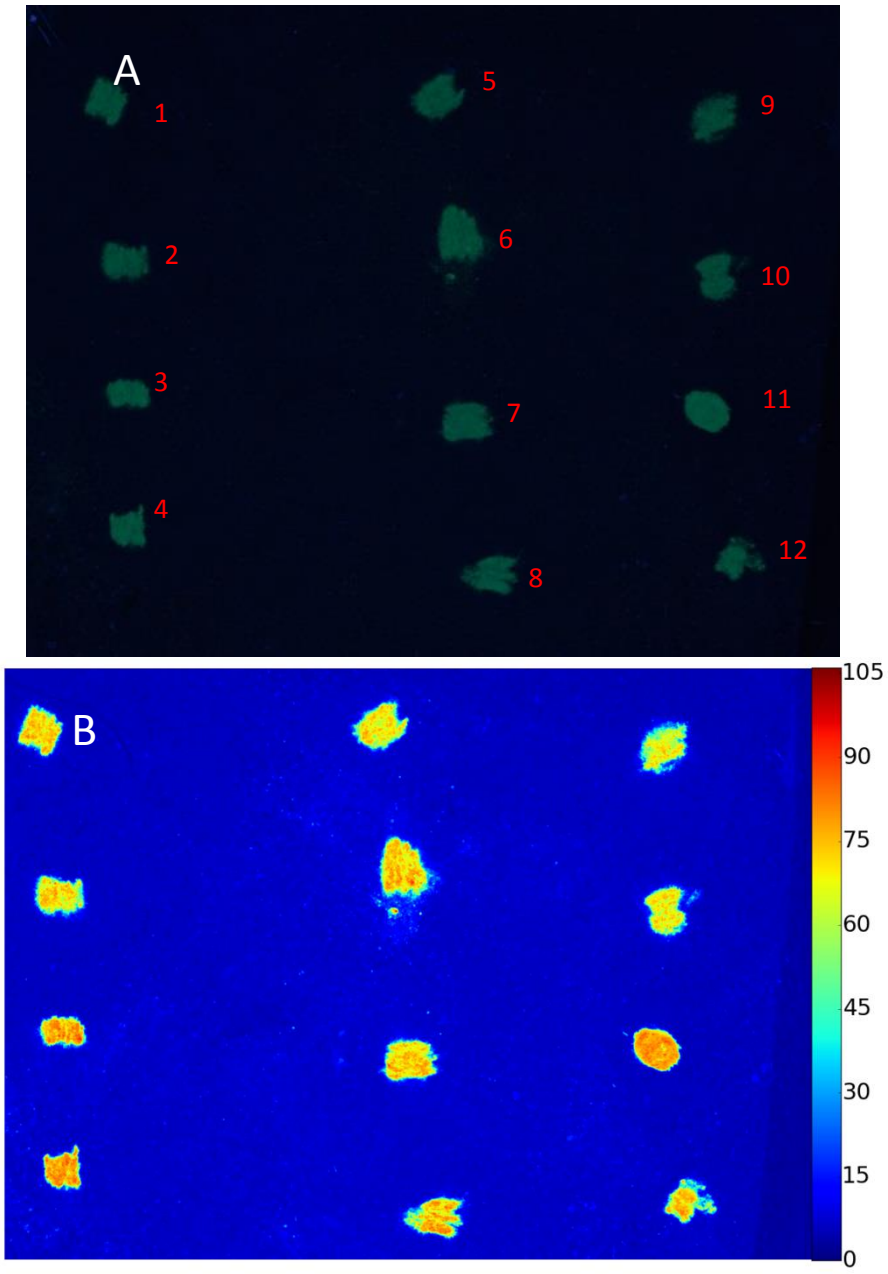

Figure 6.3. A) A true colour orthophoto of the soil surface (c. 1.5 m^2) with 12 tracer spots (100 g kg^{-1} tracer concentration) acquired to estimate spatial variation within and between patches. The spots are labelled 1-12 to allow comparison with Figure 6.4 B) Image A) after processing. The colour bar shows intensity of individual pixels. The nominal range is 0-254. For analytical work, the data are used as a matrix, but here have been converted to an image for ease of viewing. .

2

3

Assumption (i): Complex statistical testing has been avoided as it appears that the data distribution (i.e. the amount and direction of skew) varies between patches. For example, Figure 6.4 shows that some patches are positively skewed (e.g. spot 6), while some have very little skew (e.g. spot 3) and others are negatively skewed (e.g. spot 4).

The median intensity of the patches ranged from 67 to 79, the median of all the data points (spot All, Figure 6.4) is 74.0 and the mean all data points (spot All, Figure 6.4) is 73.4. The mean of the median values for each spot is 73.3, with a standard deviation of 3.8 and a standard error of 1.1. In addition, all the median intensities fall within ± 10% of the median of the whole data set (Figure 6.4B). Thus, I can have confidence that I can reproducibly evaluate the intensity of the tracer at a given concentration, taking into account all sources of variability, such as variations in lighting intensity, distance from the camera and the heterogeneity of the soil-tracer mixture.

Furthermore, the within-patch variation appears to be low, i.e. the interquartile range (IQR) for each patch is narrow relative to the overall spread of the data (Figure 6.4). Some variation between patches was seen; one explanation could be that some patches were located closer to the camera than others and would therefore appear brighter. However, when distance from camera is plotted against intensity (Appendix 3:SI Distance from camera, SI Figure 3) little, if any, relationship between is revealed.

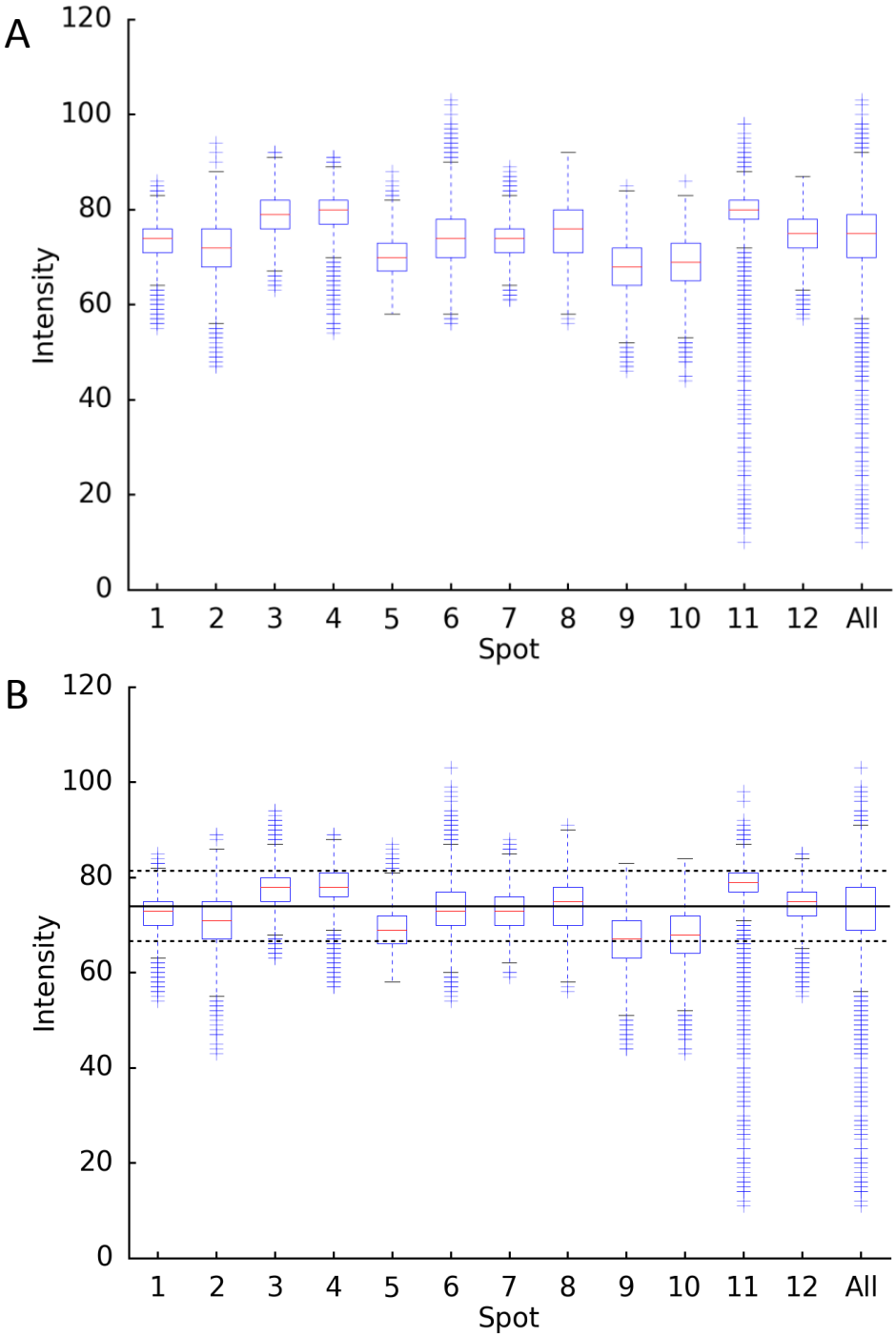

Figure 6.4. A) Variation within spots (patches) of tracer (1-12) compared to variations between spots (All). The red bar represents the median, the box represents the interquartile range, the whiskers represent the range and the crosses represent the outliers. B) as A), but with solid black line showing the median of all the data and the dashed lines showing ±10%. Note how all the median values are within this band with 7 spots below and 5 spots above the median. For nine spots (1, 2, 3, 4, 6, 7, 8, 11, 12) the entire interquartile range (50% of data) is within this band.

1

Assumption (ii): There was a small amount of variation between repeated images of the same patch (~ 3%), probably due to the JPEG compression process. This variation was consistent across all the patches, allowing me to accept assumption (ii). Nevertheless, it is expected that using RAW images would reduce this uncertainty, but doing so would make the image analysis process more computationally intensive, due to increased file size, and the images could not be viewed directly through standard software packages.

Assumption (iii): The data are summarised in Figure 6.5. For each concentration, the IQRs (representing 50% of the data points) for each discrete patch overlap. Thus, the observations made for assumption (i) (that the intensity is reproducible between tracer patches) is confirmed, but over a wider concentration range. In addition, there is no overlap of the IQRs for different tracer concentrations. It should be remembered that each box plot represents approximately 10,000 data points. Therefore, some overlap in the ranges of different concentrations of tracer, particularly at higher concentrations, is to be expected. For example, there is clear overlap in the range of tracer spots with concentration D and E. In these spots, there will be a few pixels with an extremely large amount of tracer and a few with very little tracer, therefore a pixel with a very high concentration of tracer for spot D could easily have the same concentration of tracer as a pixel with low concentration of tracer for spot E. This is simply because the tracer/soil mixture is not homogenous, particularly on the sub millimetre level. It is possible to clearly differentiate between the tracer patches of different concentrations and to identify which patches have the same concentration.

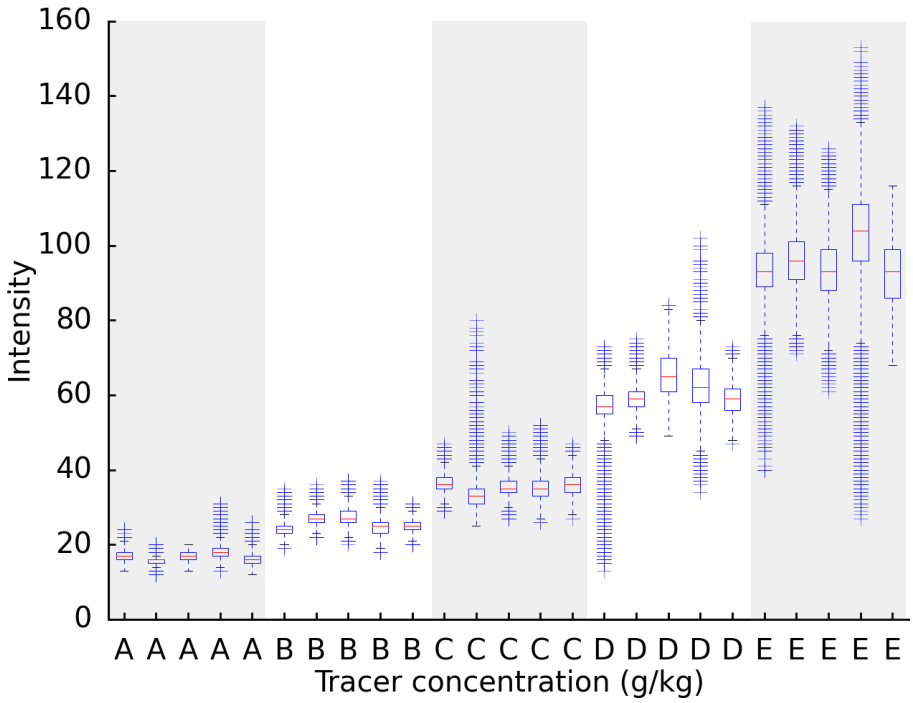

Figure 6.5. The variation between tracer spots of the same concentration compared to tracer spots of different concentration, where A is 3.97, B is 11.51, C is 19.85, D is 44.6 and E is 93.57 g kg-1.

Assumption (iv): It is possible to describe the relationship between the mean treatment tracer concentration and intensity using a straight line with a value of $R^2 = 0.99$ (Figure 6.6) allowing *Assumption* (iv) to be accepted. It is clear that the relationship is not truly linear as curvature can be seen in the graph, however as an approximation the linear fit is reasonable. It should also be noted that the application of an R^2 value to the line may not, strictly speaking, be appropriate as the uncertainty on each data point may not be the same. However, R^2 is a simple, commonly used and widely understood measure of fit for a straight line and therefore has been given as it may be useful to some readers. In conclusion, I have found that it is possible to use the tracer reproducibly and quantitatively.

6.4.2 Complex statistical testing (or lack of)

Complex statistical tests have been intentionally avoided throughout this thesis. This is not because they are difficult to perform, in fact there are a number of packages in Python which allow for them to be performed with ease, but rather it is hard to determine if they are appropriate, useful and aid understanding. In generally, as stated in 6.4.1, the data that I have gathered is non-normal, with some datasets exhibiting positive skew, others negative skew and other still very little skew. Due to the complex and unknown nature of the algorithms that the camera uses during data collection it is not clear if the datasets that have been collected would be expected to be normal or non-normal. Exploratory transformations were carried out on the certain sets of data to see if normal data could be obtained and no single transformation was found which could be applied to all data sets to allow for them to become normal. This is unsurprising as datasets are skewed in different directions and to different extents. The lack of normality suggests that the underlying assumptions of many standard parametric tests (i.e. that the data is normal) will be violated and therefore this calls into question the appropriateness and therefore meaning of these tests. The author is aware that there are non-parametric variants of most parametric tests, but the power of these tests is greatly reduced compared to the parametric version. This is not to say that these tests cannot be done, or that they have no meaning; rather that, in this case, the author suggests that the graphs displayed gave a more complete, true and comprehensible account of the data that a collection of statistical tests would. Furthermore, the author is keen to avoid a long debate about how appropriate a given test is or is not, as that is not the aim of the study and detracts from the key message. Specifically, there is no attempt to show if anything is statistically significant, therefore there is no need or use for tests which are designed for this purpose. Figure 6.5 is an excellent example of this, the concentrations that were tested were chosen arbitrarily, rather than because they should or should not be significantly different from one another. The concentrations used were selected to give users an impression the

capabilities of the technique rather than to define the techniques absolute limits. They may also be useful as a reference point for future users or further developments of these techniques. To this end very little is gained from saying the technique can or cannot statistically distinguish between tracer of concentration A and E when using 5 replicates of the tracer.

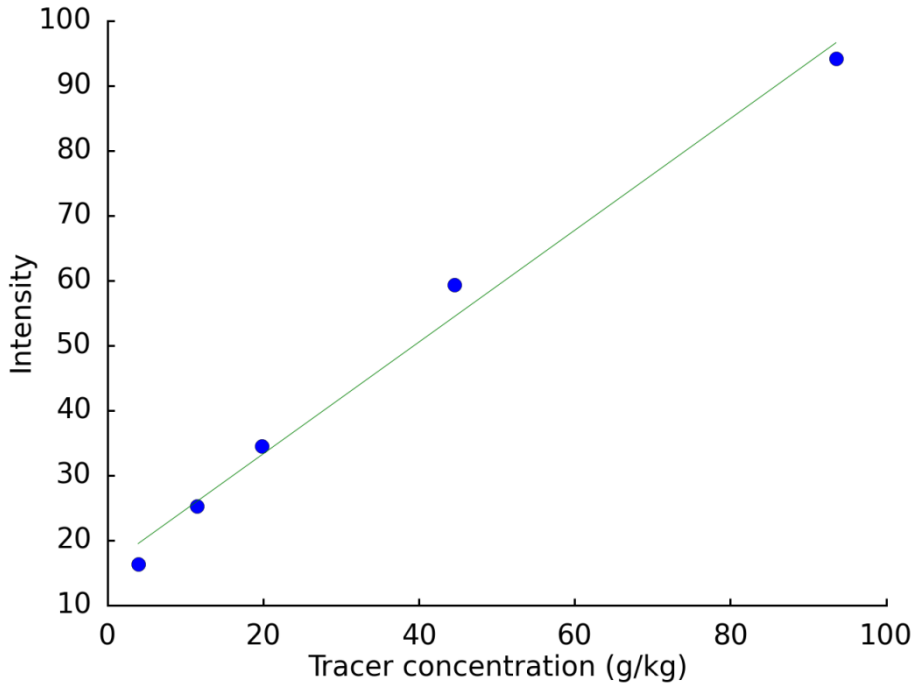

Figure 6.6. The relationship between the tracer concentration (g kg^{-1}) and the amount of light emitted from it. Each data point is the arithmetic mean of all data points from patches with the same concentration. The green line represents a linear line of best fit (R^2 0.99) y = 0.86x + 16.

6.4.3 Validation of the particle-based method

Figure 6.7 shows images of the TCSs and the particles that have been located. Overall, there is little to no variation between the number of particles counted in each of the 11 images of the individual TCS plates. The smallest variation was seen in TCS 1, in which 21 particles were found in every image, and the largest variation was seen for TCS 4, where the particle count ranged from 168 to 172, with a mean of 170 and a mode of 171. There appears to be some relationship between the number of particles counted and the uncertainty on the count number. When more particles are present, there is a greater chance that they will be touching, and hence may be counted as either 1 or 2 particles. Each image may differ from the others due to the algorithm used, giving rise to the small observed uncertainty.

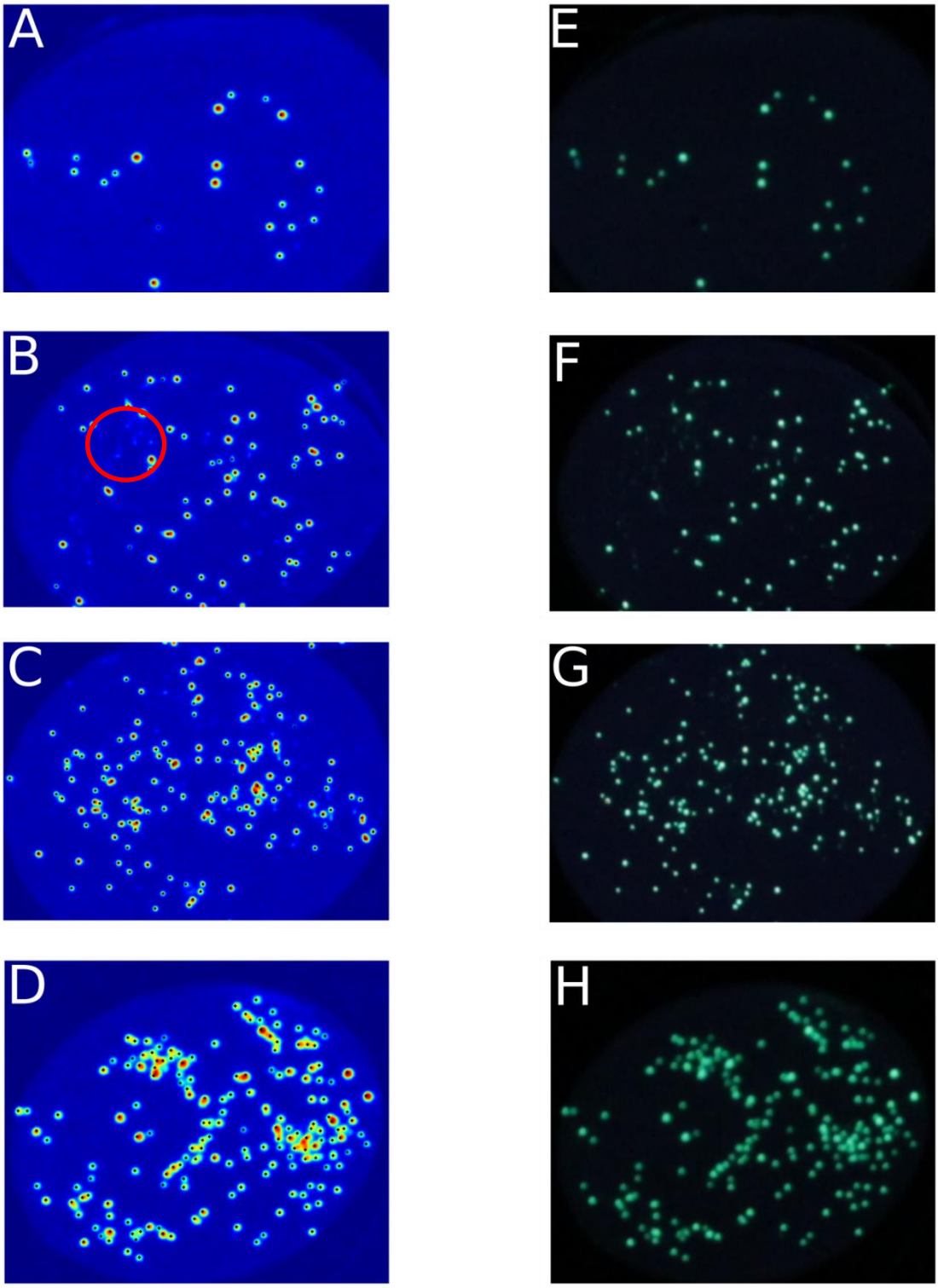

Figure 6.7. True and false colour images of the test counting samples (TCSs). A-D are false colour heat maps showing the green channel of the image and the black dots show the location of counted particles. E-H are the corresponding original images captured. Note how in some image (e.g. B) there is some background noise (highlighted by the red circle); this technique is able to distinguish between background and tracer particles effectively.

1 which is probably due to the shallow depth of field on the camera

It is worth remembering that this the methods discussed here differ from those in Chapter 5 in that they do not attempt to track the motion of an individual tracer grain and follow its movement. The images here just need to be of sufficient quality that grains can be counted in a reproducible manner to allow for accurate and precise numeration. The images, even with small amount of blur (see Figure 6.7H), are still very useable and the software can easily identify the particles, suggesting that the software is reasonably insensitive to image quality.

6.4.4 Quantitative real-time assessment of tracer movement

This experiment was designed to illustrate how the technique can be applied at a laboratory scale. It is designed to mimic a traditional soil box experiment where data are usually only collected after exposure to rainfall, highlighting how this technique acquires data throughout the rainfall event. The mean intensity of the sampling area containing the tracer (OTL) was plotted over the course of the experiment (Figure 6.8A). There is a rapid decline in intensity at the beginning of the experiment, which may be attributed to the formation of a film of water on the soil surface, reducing the amount of light from the tracer reaching the camera. There appears to be a step-change in intensity at 275 s, which results in the intensity value suddenly jumping 6 units between 1 image and the next. This step-change is reversed at 420 s and then there is another step up at 605 s (Figure 6.8A).

6.4.4.1 Artefact corrections

In order to investigate the cause of these abrupt changes the intensity of three other sampling areas (OCL 1 and 2 and below 3 area Figure 6.2B) were plotted (Figure 6.9). The OCL 1 and 2 are tracer-free controls which are located outside the soil box; therefore, any changes in the intensity are unlikely to be as a result of tracer movement. The below 3 (9-green; Figure 6.2B) sampling area is located in the soil box, however it is far away from the

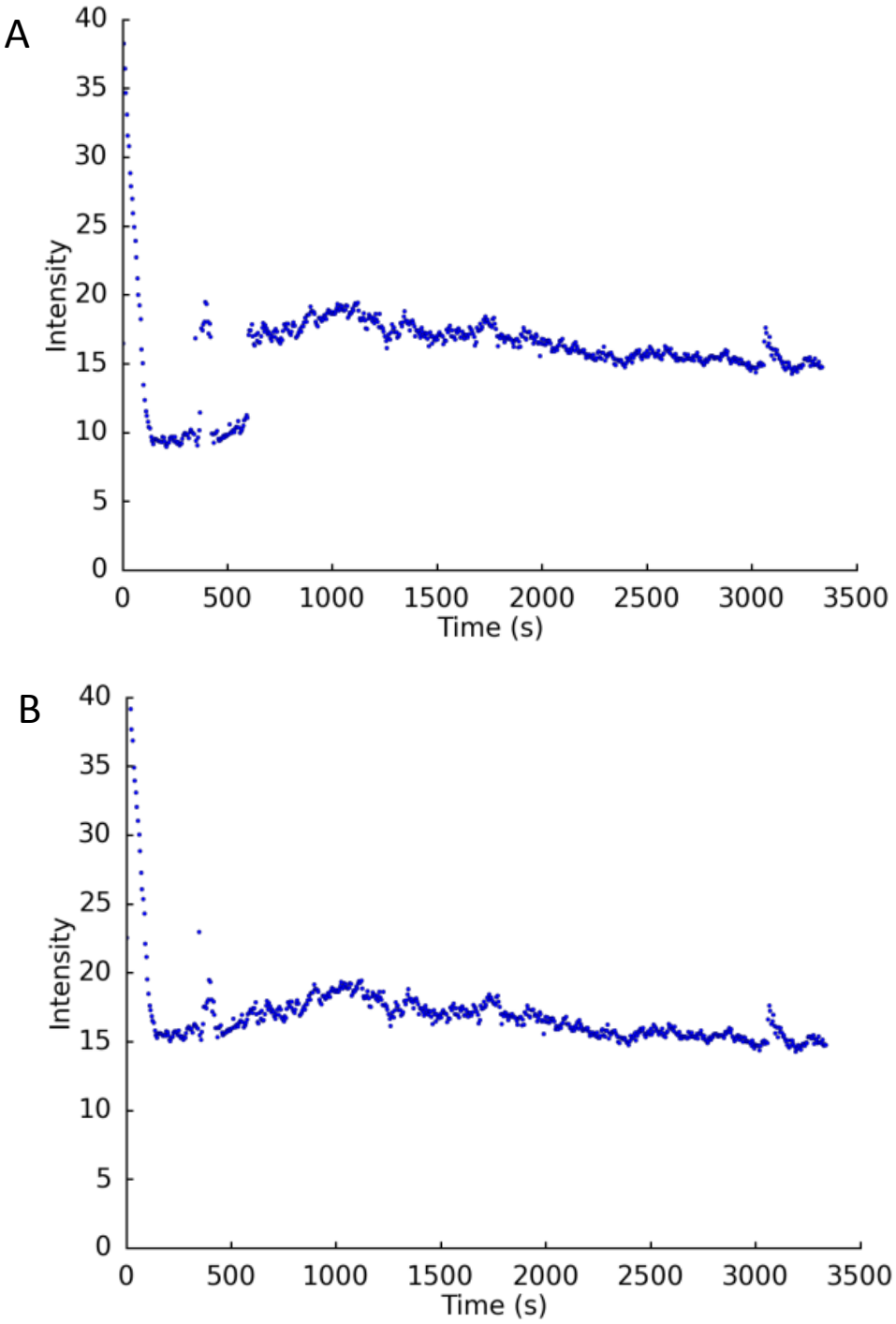

Figure 6.8. Changes in the intensity of the OTL area (Figure 6.2 B) (where the tracer was deposited at the start) over the course of the experiment for A) the raw data and B) after correction for artefacts. Images were recorded every 5 s.

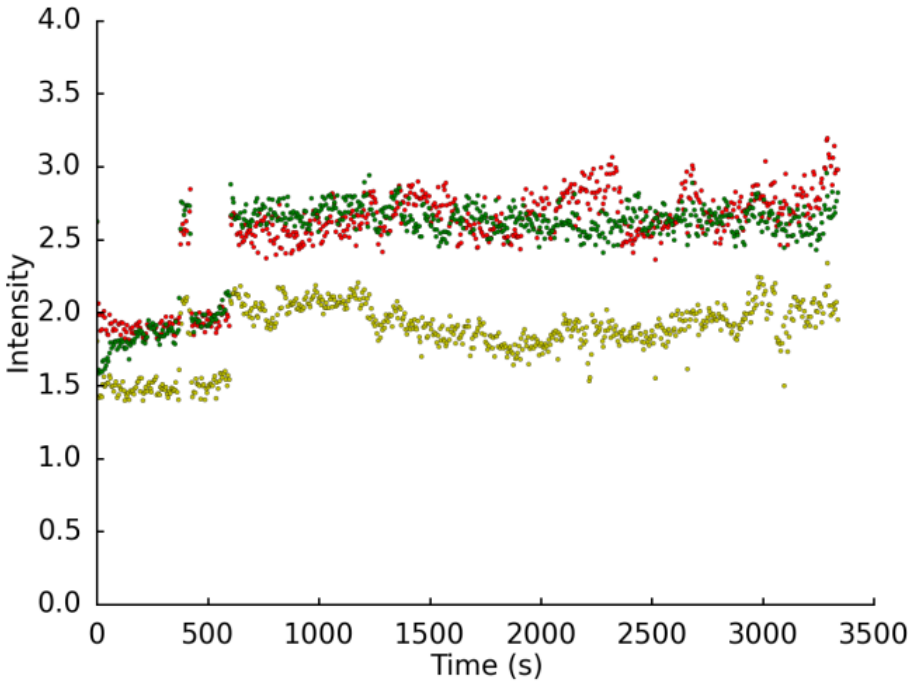

Figure 6.9. Raw data for area that should not contain any tracer. The yellow dots relate OCL 1 and the red dots relate OCL 2, both of which are located outside the soil box and therefore should not contain any tracer. The green dots relate to sampling area below 3 which is located far from the OTL and therefore should contain few, if any, tracer particles particularly when then step change occur. The physical areas that these relate to can been seen in Figure 6.2 B, the colour of the dots is the same as the colours of the rectangles.

OTL and it is likely that insignificant amounts of tracer were present when the step changes occurred. The step change was seen in all of these areas (OCL 1, 2 and below 3) and therefore has been considered an artefact; however, the cause of this artefact is not known. Changes in white balance, exposure time, exposure value or ISO value could be responsible for this step change, but inspection of the exchangeable image file format (Exif) data attached to the image found none. The lighting used was both current and voltage regulated in order to prevent any changes in lighting intensity, and forced air cooling was provided to keep the LEDs at a constant temperature. The lamps had been warmed to operating temperature before starting of imaging. No observable changes in lighting intensity were noted during the experiment. Assuming that the Exif data are correct and that there were no changes in lighting intensity, the most likely cause of the artefact is the JPEG compression used inside

the camera, which may have adjusted during the course of the experiment. A correction was applied based on the difference in mean intensity value when the step change occurred (Figure 6.8B). It has been suggested that the camera may be constantly changing its JPEG compression algorithm, and it is possible that constant minor alterations are taking place. For this reason, data from 2 OCL (optical control locations) used to monitor the intensity of blue light have been included (indicated by yellow and red dots in Figure 6.9), though only 2 clear step changes seem to occur. If there is constant minor adjustment to the JPEG compression it is likely that this results in minor changes to intensity, such as the range in intensity seen from 1,000 to 3,000 s in the yellow and red dots in Figure 6.9.

6.4.4.2 Comparison of particle-based and intensity-based methods

If there is an appropriate density of particles, it is possible to use both the particle-based and intensity-based methods to investigate changes in tracer concentration over time. Thus, two independent techniques can be used to quantify the amount of tracer in a single image, increasing the level of confidence in the analysis. It is worth remembering that both techniques use the same raw images and therefore any differences between the techniques are unlikely to be as result of differences in image resolution (i.e. pixel size or density). There is generally very good agreement between the two measurement techniques (Figure 6.10), as both data sets show the same pattern, with peaks at ~ 400 s and a dip at ~ 3100 s. When the two data sets were correlated, and a single anomalous data point removed, an R^2 value of 0.96 was obtained (n = 667) further indicating the excellent agreement between the two approaches (SI Method comparison).

The spread of the data is generally larger using the particle-based method and there is one peak at ~ 300 s that does not appear in the intensity data. Given that this peak consists of a single data point (unlike all other significant excursions), it is most likely to be an artefact, bearing in mind that all image analysis was fully automated.

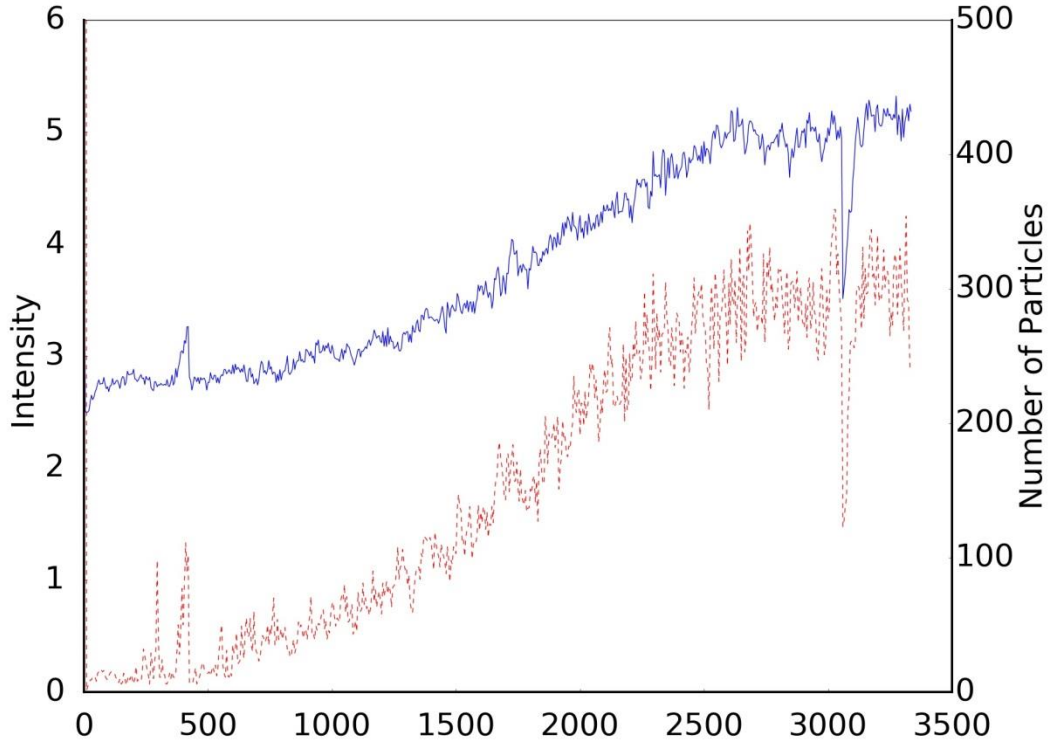

Figure 6.10. Comparison of the intensity-based and particle-based methods for quantifying tracer concentration over the course of the experiment. The solid blue line shows the tracer concentration as determined by the intensity of the tracer and the red dashed line by counting the number of particles. These data relate to below 1 (7-orange; Figure 6.2 B).

A further peak in intensity can be seen at approximately 400 s in the OTL (Figure 6.8), and in both intensity and particle number data relating to below 1 (7-orange; Figure 6.2 B) where the tracer was deposited (Figure 6.10). This peak is not seen in the areas right and left of OTL (4-black and 6-white; Figure 6.2 B) or in outside of the soil box (OCL 1 and 2; Figure 6.2 B, Figure 6.9 B). Noticeably, the peak occurs around the time of the step change, but is not a result of the correction process, i.e. the correction process removes the peak from the control areas, but not from areas where the tracer is located. Furthermore, although the particle-based and intensity-based data are both derived from the same images, they assess the amount of tracer in two distinct and independent methods. Nonetheless, both data sets indicate a peak in the same location and with the same relative magnitude, further providing

confidence in the results. Although detailed discussion of the putative causes of individual peaks and troughs is beyond the scope of this paper and this thesis some general comments can be made. There is a low concentration of tracer particles in area 7-orange (see Figure 6.2B) at the beginning of the experiment, as few tracer particles were placed in this location. However, there is a larger deposit of tracer just above this area. It therefore is possible that the tracer material will move down the slope into this area as rainfall progresses. It is also possible that the following set of circumstances is responsible for the data described in Figure 6.10: initially the tracer concentration is low due to the presence of very few tracer particles in this area before the experiment was started. As rainfall continued, soil, and therefore tracer, moved into the area from above. At the same time, there may be loss of soil, and therefore tracer, from the bottom of this area. However, as there is less tracer leaving than entering, there will appear to be a gain to tracer material in this area. As the experiment continues, tracer particles that have previously entered this area, will migrate down the area and the begin to leave. Towards the end of the experiment (after ~2500 s) the amount of tracer becomes more or less constant, suggesting that either movement of tracer is ceased or that the rate of movement is constant. As the area below (8-pink see Figure 6.2B) continued to gain tracer during this period it is more likely that the rate of transport of tracer into and out of this area becomes more constant.

6.5 Discussion

6.5.1 Uncertainties

The data presented here is designed to give some indication the scale and type of uncertainties that could be expected, rather than attempt to place an exact value on them. The exact nature of the uncertainties encountered can change based on a number of variables (such of distance of lighting and camera to the soil, light position, amount and nature of stray light, camera used etc.) and these can vary from experiment to experiment.

Thus, the method can be adjusted to balance ease of use versus precision and accuracy. Furthermore, future users can use similar tests to assess their experimental set-up, with the data presented here acting as a reference point. Nonetheless, much of the variation seen is due to the heterogeneous nature of the soil, rather than uncertainties associated with lighting, camera or image processing. In this respect, I feel that the technique has been optimised sufficiently for its intended application.

6.5.2 Limits of detection and quantification

When the concentration of tracer becomes low then the intensity-based method may not return useful results as the background noise in the image is larger than the fluorescence signal, however there is no clear point at which this occurs. The intensity-based method is dependent on a number of experimental factors including tracer size, camera resolution and lighting intensity. These will vary from experiment to experiment, making it hard to quantify a limit of detection outside a given experimental set-up. The maximum concentration of tracer in an area also has an effect on the limit of detection, as the camera sensor will be saturated for the bright object before it is able to register the dull object, i.e. part of the image will be overexposed. However, removing the bright object, either physically through shielding or through the image acquisition method (e.g. using high dynamic range methods, or zooming in on the lower intensity area), overcomes this issue. It is recommended that the limits of detection and quantification are experimentally determined, if these are required.

If insufficient fluorescence is present to use the intensity-based method, it may be possible to count the individual particles. This technique has a nearly infinite limit of detection as a single particle can be detected in any sized area. Practically, the user will define the point at which the images contain so little tracer that the results are not meaningful. For example, the user may decide that the detection limit is less than 10 particles m^{-2} and areas with lower concentrations could be considered to be tracer free.

6.5.3 Detecting and correcting for artefacts

Due to the volume of data collected during an experiment it is possible to detect and correct for artefacts, which could be missed with lower temporal resolution. The step change seen in Figure 6.8A is a prime example of this. Another aspect of the method that makes detection of artefacts easy is the large spatial area that can be sampled. Figure 6.9 shows data from three areas which would not be expected to have tracer in them and therefore clearly shows the artefact in question, however many more areas could have been analysed if further evidence should be required. Furthermore, areas of an image can often be analysed using two independent techniques; if a feature is only seen in one of these data sets then it raises questions about that feature. However, if a feature is seen in both techniques then this is good evidence that the feature results from tracer movement. The ease with which these two data sets can be generated and the flexibility with which the images can be processed combine to make a robust analytical approach. The system's ability to cope with the unexpected and still produce useful data is something which should not be underestimated, especially when undertaking one-off experiments.

6.5.4 Comparison to the two quantification techniques

There are relative advantages and disadvantages to using the intensity method rather than the particle counting method. One major advantage of the counting technique is that no calibration is required to translate this count number in a more common unit. It simply counts the number of particles, whereas the intensity method requires the use of a calibration curve to translate intensity into other units such as kg m^{-2}. However, the counting method is only useful when working at low concentrations of tracer and requires much more computing power, due to the way in which the particles are located, making this method much slower than the intensity method. The speed of the counting method scales geometrically with area assessed, making the intensity based method preferable for large areas, as the time it takes scales nearly linearly. The intensity method is simpler, as only the

area to be analysed needs to be defined, whereas the counting method requires the selection of parameters relating to particle size as well as filtering of the results to remove false positives. While this process is relatively simple, the user's skill has a great effect on the time required to identify the optimum parameters for a given image set.

6.5.5 Limitations

The method can only detect particles which are both exposed to blue light from the LEDs and are able to emit green light back to the camera. If sufficient water was covering a particle, or that water contains lots of particulates, then this could prevent a given particle from being detected. This type of event may explain the dip seen in Figure 6.10 at about 3,100 seconds. For example, if water was ponding above the area being sampled and then this pond broke its banks (in an action akin to "dam breaking") this could result in the rapid movement of water down the soil box. The water could cover a small proportion of particles for a short period of time making them invisible to the camera. Later, the water may drain away and the particles (assuming they were not washed away) would be uncovered and therefore able to be measured.

6.6. Conclusions

This chapter clearly shows that this technique is capable of recording high quality data relating to the movement of a soil tracer with exceptional temporal and spatial data. There may be scope to use this type of data in the design, parameterisation and evaluation of soil movement models. This technique also opens new possibilities for fundamental research. For example, it could be used to study dynamic systems such as the movement of soil in response to varying rainfall rates, as these types of studies are difficult with traditional sampling based methodologies. The ability of the technique to interpret the recorded images using two independent techniques allows for an easy assessment of the data quality to be made, and therefore allow a judgement to be made on how accurate and precise the data is.

Supporting information

The supporting information for this paper can be found in Appendix 3.

Chapter 7 qLift in action: A field trial about soil movement due to tillage

7.1 Abstract

qLift (quantitative LED-induced fluorescence tracing), a technique which allows for the concentration of a fluorescent tracer to be determined, has been shown to work effectively in a laboratory setting. This chapter shows how this technique can be adapted to operate in the field. In this case, the effect of tillage on soil movement in a field in northern Germany was investigated. Standard farming practices for the area were employed to simulate the effect of 7 years' worth of tillage. This trial represents the first time that these techniques have been used in a field setting and give an impression of the type and nature of data that this technique is able to capture while operating in the field. Previous laboratory uses of the technique have used rainfall as the driver for soil movement however this study shows that, with minor modifications, this technique is applicable of being used to monitor more than just rainfall-driven soil transportation.

7.2 Introduction

Arable and intensely grazed soils are some of the most at risk from erosion, and it is estimated that these lands erode 100-1000 times faster than the natural background rate (ITPS 2015). It has been estimated that 11% of the Earth's terrestrial surface is subject to soil erosion (Zhuang et al. 2015). The effects of soil erosion are long lasting and far reaching, and include increased flooding risk (Yin and Li 2001), land abandonment (Wood and Armitage 1997), the transport of contaminants such as metals (Quinton and Catt 2007) and pathogens (Tyrrel and Quinton 2003), and eutrophication of surface waters (Catt et al. 1998, Haygarth et al. 2005). Given that the affects of soil erosion are severe, it is not surprising that there has been a long history of studies which investigate the movement of soil and the effectiveness of

measure designed to counteract erosion. Most of these studies have been carried out by monitoring sediment yield at the outlet of a given area, for example field plot, hillside or catchment e.g. (Quijano et al. 2016, Zhang et al. 2016). While this approach has allowed for some insights into the process that are responsible for erosion are many limitations to this type of study. Firstly, little information is gained about the pathway by which soil is transported, and secondly the approaches offer very poor temporal resolution. In some cases, carrying out these studies requires disruption to the systems they are attempting to study by imposing artificial boundaries as well as removal of material such as soil and water

One response to this has been the use of tracers in erosion studies which can overcome some of the limitations of sediment yield studies. For example, tracers can allow for information about the pathway which sediment has taken to be obtained. There have been recent calls for the development of new tracing techniques (Stroosnijder 2005), and there has been some development of new tracing technologies such as Armstrong et al. (2012). Anecdotally, there is criticism of tracer techniques which have only been shown to operate in a laboratory setting. It has been suggested that true insight into soil movement processes requires field work to be carried out, and therefore tracing techniques that do not operate in the field are of limited value. While the validity of the assertion is in question, in can be argued that a tracing technique that can operate in the field as well as the laboratory is more powerful than one that is limited to just the laboratory.

This chapter demonstrates that it is possible to use the qLift to monitor the transport of the soil down a field slope in response to tillage. It gives an insight into the type and nature of the data that can be collected in the field by using this technique. While the majority of the data collection has been carried out without disturbance of soil from the study site, the technique was extended in order to monitor sub-surface movement of soil. This required the construction of soil pit which allows of images of the vertical profile of the soil to be collected

and therefore sub-surface tracer concentrations to be determined. It should be noted that although the soil was sampled from several vertical soil profiles, there was no need to remove and transport soil for analysis in laboratory, which reduced logistical costs and challenges.

7.3 Field trial methods

In order to demonstrate that this method works under field conditions, I applied the tracer and my image acquisition methods during a soil tillage experiment, conducted on rolling arable farmland in Northern Germany. The plot size was 20 m by 50 m, but I focussed on a subsection of this as other investigations were being carried out simultaneously. The field was tilled in the downslope direction only; the plot was orientated down the fall line of a gentle slope (~ 5-15^{o}). Each tillage event consisted of a first pass with a harrow and a second pass with a roller, carried out by a local farmer under conditions which are broadly representative of tillage practices in the area. In total, seven tillage events were undertaken in order to simulate seven years of tillage.

The tracer was deposited in a 1 x 0.3 x 0.3 m deep trench, 12 m from the top of the plot. Once the tillage was complete, imaging markers were placed down the plot at approximately 1 m intervals without walking on the plot. The images started 5 m above the original tracer location and extended 10 m downslope, and were collected at night to minimise the amount of background light. The location of each marker was recorded using a total station and each was used as a reference point to aid analysis of the images. To analyse the images, a 400 by 400 pixel area was taken starting at the corner of each marker.

The camera used was a Lumix GH4 operating at maximum resolution and recording images in JPEG format. The camera was controlled using the Panasonic imaging app using a Google Nexus 9. The lighting used was similar to that in Chapter 6, however it was powered using

lead acid batteries, as access to mains power was not possible in the field. More information about the camera and lighting set-up can be found in SI lighting.

In order to investigate the vertical profile of the tracer, five soil pits were dug to a depth of approximately 35 cm. These pits were photographed using the same type of lighting as shown in SI Lighting, but with only 1 LED to reduce the intensity of the lighting. The camera was placed in the pit approximately 40 cm from the pit wall on a small tripod. The pit was covered with black plastic to prevent natural light from coming in and the camera operated using the tablet as described above. These images were collected during the day.

7.4 Results

The purpose of the field experiment was to give an insight into the type of data that are likely to be collected, and to show how it might be analysed. Therefore, I have focussed here on methodological issues, rather than using the data to investigate physical processes.

7.4.1 Surface results

Figure 7.1 shows how the tracer concentration varies down slope, with an overall decline in intensity from 13 m onwards. It is likely that the sampling point near 16 m is artificially low as it was located in the tractor's tramlines, something which can be clearly seen when examining the photo-mosaic of the transect (SI Field trial). Overall, the results are what would be expected: there is downhill movement of the tracer. Using the intensity-based method it is possible to detect tracer up to eight metres from the original tracer location and further using the particle-based method (SI Field trial, SI Figure 5). The intensity-based method is simpler to execute and is computationally less intensive than the particle-based method; at this scale the former approach is less prone to sampling artefacts and additionally produces data that is commensurate with the scale of the study. The particle-based approach would be more appropriate when studying the fine detail of soil movement over mm to cm, or where the tracer concentration becomes very low. Nonetheless, the use of two separate automated

analysis methods combined with visual analysis of the images (SI Figure 6) give a high degree of confidence in the data.

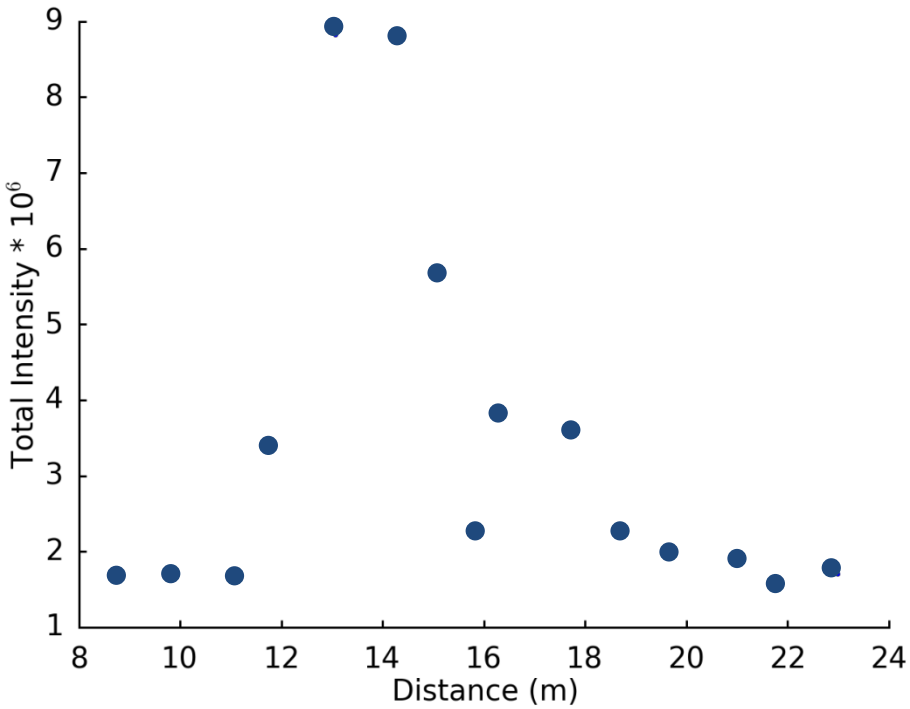

Figure 7.1. The total intensity of tracer in 400 × 400 pixel areas near markers approximately 1 m apart going down the slope. Total intensity was used as it more comparable to the particle-based method (SI Figure 5) that median or mean intensity.

One significant advantage of this non-destructive sampling approach is that data are acquired from the whole study area, at a scale that is not achievable through conventional destructive sampling methods and within a time-frame that would not be possible from high-resolution spot measurements. In addition, the resolution of the data is such that the images can be magnified and fine-scale details (mm to cm) can be detected. In other words, a single image, taking no more than 15 minutes to acquire, can be analysed at metre to millimetre scale, facilitating insights that are not otherwise achievable. (For reference, the data presented in Figure 7.1 took approximately 2 hours to collect).

7.4.2 Vertical distribution of tracer

By digging soil pits it is possible to image the vertical distribution of the tracer in the soil. Figure 7.2 shows the profile of the tracer as a function of depth for each of 5 pits, dug along a transect, together with false colour images of the areas analysed. The tracer profiles were generated by determining the mean intensity across every row of pixels, such that the vertical resolution is one pixel, with approximately 50-100 data points per vertical centimetre (depending on exact camera distance from the soil face).

As may be expected, it appears that less tracer is able to penetrate to depth in the soil down the slope (Figure 7.2), with evidence of this being that intensity of tracer at two fixed points (5 and 15 cm deep) is shown to decrease with distance down slope (Figure 7.3). Perhaps more interestingly, two distinct peaks are observed in the depth profiles, which may correspond to the position of the harrow blades. Both peaks seem to move up the profile going down slope. Thus, the harrow is seen to both move soil down slope and at the same time lift it from depth.

There is a high degree of variability within small spatial areas (both vertical and horizontally) within the soil profile, which can be seen clearly in the false colour images (Figure 7.2).

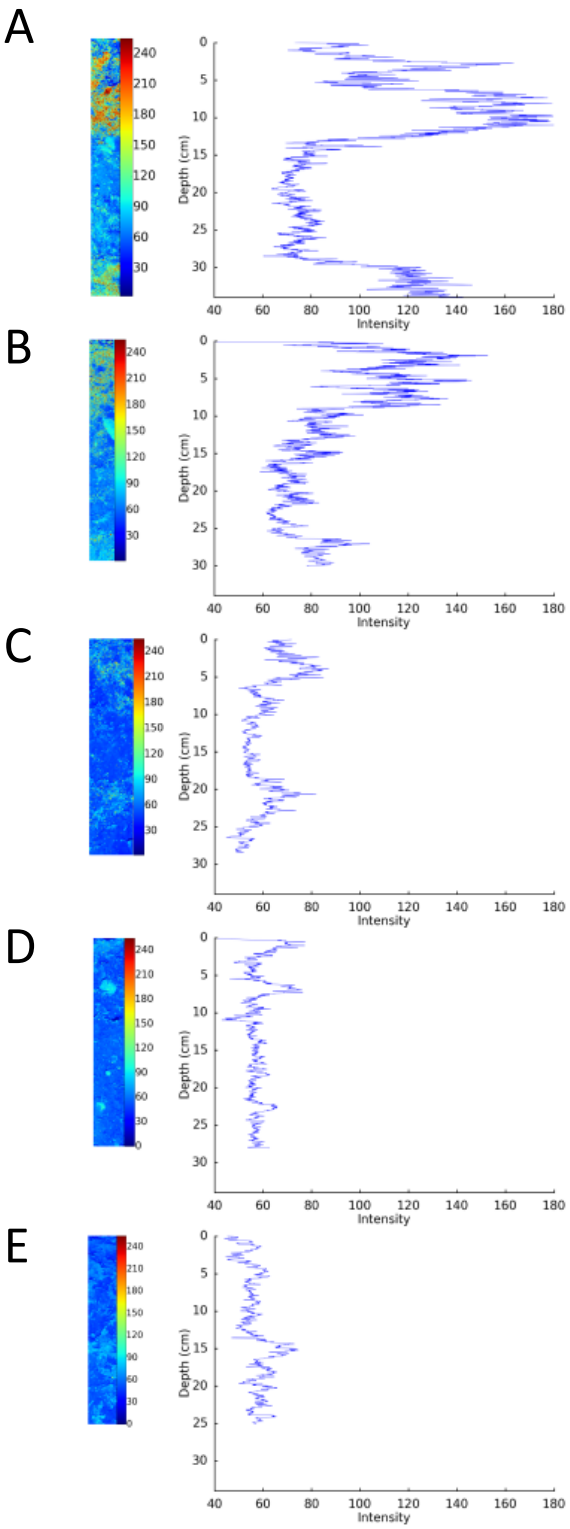

Figure 7.2. The vertical distribution of tracer in 5 soil pits down the slope. Distances given are down slope from a reference point. A) 5 metres; B) 7.5 m; C) 10 m; D) 12.5 m; and E) 15 m. The false colour images represent the areas analysed for each graph. The pale patches in the images are stones.

1

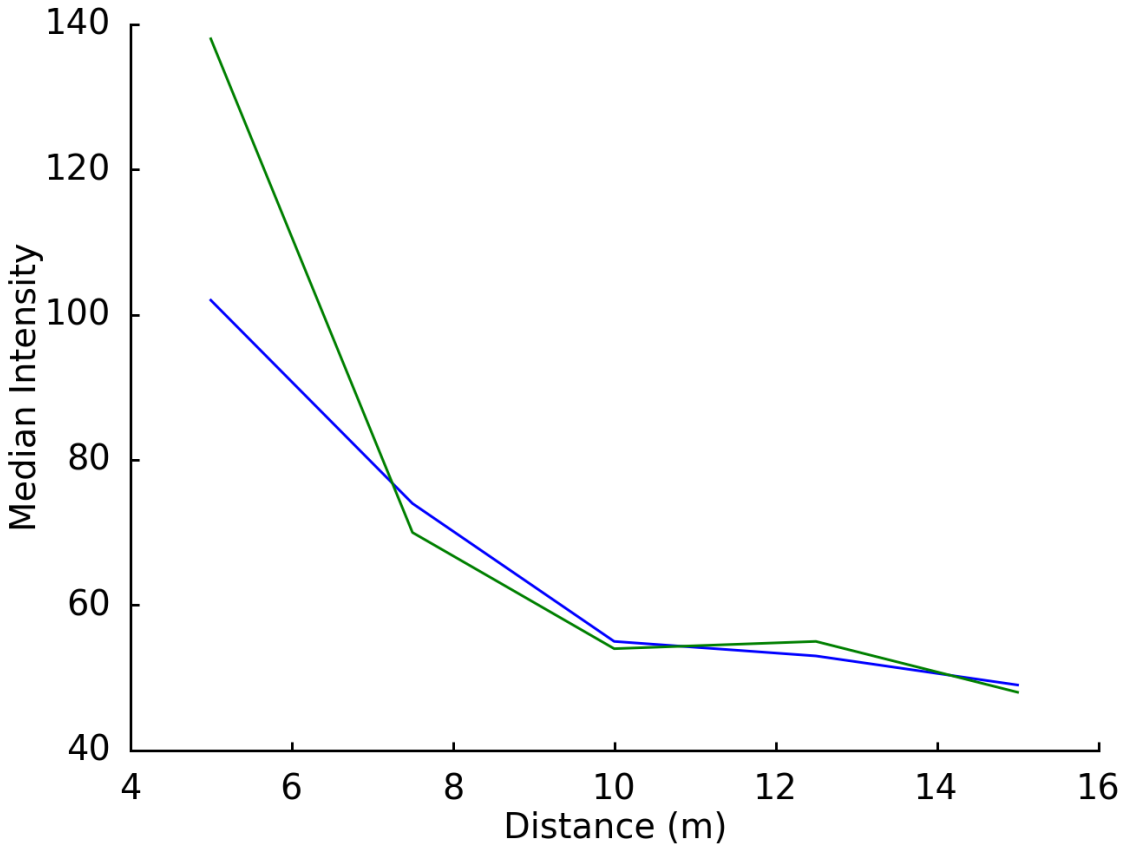

Figure 7.3. The median intensity of tracer at 5 cm (blue line) and 15 cm (green line) below the surface of the pit. Five pits were dug at 5, 7.5, 10, 12.5 and 15 m down slope from a reference point. A 100 by 100 pixel square was analysed with the top of the square being at the 5 or 15 cm mark, and the right-hand edge of the square being adjacent to the depth reference on the right-hand edge of the image.

Part of this variability is caused by the presence of small stones, which appear as patches of moderately high intensity compared to the background soil. I have made no attempt to correct for the presence of these features, however, adjustments to the image acquisition (e.g. f-stop, ISO and shutter speed settings) would reduce their contribution. Additional image post-processing could remove them altogether if necessary.

7.5. Discussion

As far as the authors are aware, this is the largest tracing study using florescent imaging of a tracer that has been undertaken. It conclusively demonstrates that this methodology is usable in plot scale outdoor studies under environmentally relevant conditions. There were

very few problems in scaling up from a soil box to plot scale and I cannot foresee any reason that this method cannot be used on larger areas if desired. The technique departs from traditional sampling based approaches and therefore offers new possibilities in soil science.

7.5.1 Speed and certainty

Two aspects which made this technique very suitable for the use in the field are the speed at which images can be taken and the instantaneous nature of the data acquisition. I was able to review an image in the field a fraction of a second after it was taken. Humans are very adept at being able to intuitively judge the quality of an image and this gave constant reassurance that I was collecting usable data. This is not something that is usually associated with traditional sampling techniques. It also gives the ability to adjust and adapt your experiment based on what you see. There were many examples of this, during the days I spent in Germany. Firstly, I had little idea as to how far the tracer would travel, so planning a sampling regime would have been difficult. Once the area had been tilled it was not possible to see the tracer with the naked eye so there were no visual clues as to how far it had travelled. However, once I got out the imaging apparatus I was able to quickly assess the extent of tracer movement allowing me to focus my efforts on areas of interest.

7.5.2 Benefits

One of the major benefits of this technique is removal of the need to physically sample the soil and doing so has a wide range of benefits. This offers access to higher quality data than was previously possible, due to the lack of disturbance to the soil system while collecting data, allowing a truer impression of movement to be gained. The spatial resolution of this technique is extremely high and nearly infinite. Cooper et al (2012) offer one of the few examples of high resolution tracing experiments that have been undertaken, sampling a ~14 x 6 m area using a 0.3 m grid to evaluate a new model. Doing this required taking over 600 samples by hand, making this technique impractical for studies of larger areas. The model

produced spatial resolved results of a similar type to those produced during this study undertaken in Germany. This suggests that the type of data produced from this method be helpful in the design, development and testing of existing and future soil models. It would also allow for these measurements to be taken without the need for laborious hand sampling and sample processing.

Guzman et al (2013) conclude that rapid and inexpensive sampling is a requirement of future tracing techniques, suggesting that magnetic and spectroscopic techniques are likely to afford this capability. The technique presented here could be thought of as being spectroscopic, with the camera being a spatially resolved spectroscope which operates in the visual range. Whether or not the technique is considered spectroscopic, it is certainly capable of rapid and inexpensive sampling which is both non-destructive and in situ. There have been moves in soil science towards rapid and inexpensive techniques; for example Vos et al (2016) suggested that using 'texture by feel' rather than traditional laboratory analysis could be used when particle size data are required, and offers monetary savings of 90%.

It should also be remembered that the techniques discussed here for data collection do not preclude more traditional approaches to tracer analysis. For example, it would have been possible to collect soil samples and then use conventional fluorimetry in a laboratory to determine the concentrations of tracer, if this was desired. The instantaneous nature of the images that were captured could have been used to inform a physical sampling campaign should this have been desired or required, although this was not carried in this trial.

7.5.3 Limitations

This method was designed to enable the investigation of the movement of soil particles across a soil surface. The method requires the tracer's particles to be exposed to light in order for fluorescence to occur and therefore an image be captured. This limits the technique to surfaces which can be exposed to light. Therefore, in order to image movement of the

tracer which was underneath the soil surface, pits must be dug. This was reasonably time consuming, but did allow for sub-surface movements of the tracer to be investigated by recording a vertical soil profile. The technique also requires darkness to be carried out effectively, and it has been commented that this limits the usefulness of the technique to night time. This is true to some extent, although, as on average, there is as much daytime as night time, this does not impose any more of a constraint than techniques that need to be carried out in the day. Furthermore, depending on the area that it being imaged it is possible to simply "black-out" the area that is being imaged as was done for the recording on the vertical soil pits. Images of the vertical soil profile were easily captured while the field was in direct sunlight.

7.6 Conclusions

Overall, this chapter clearly demonstrates that it is possible to use the qLift technique in the field. The high quality data, with high spatial resolution, that is created using this technique could be used in a variety of applications. There is also the possibility of using this technique on for mapping tracer locations in field-based experiments. Due to the speed at which images can be acquired and the ability to integrated the information into existing methodologies such as photogrammetry this could lead to the ability to investigate much larger areas than has been previous possible. Overall, I feel that this technique is well placed to help bring soil science into the 21st century and gain a deeper understanding of how soil systems behave.

Supporting information

The supporting information for this paper can be found in Appendix 3.

Chapter 8: Discussion

The aim of this discussion is to give an overall impression of how this thesis fits into existing work and the ability of the methods presented here to further our understanding of soil processes. Some mention of the limitations to the methods developed is also made. There is much discussion within the individual chapters that is not repeated here.

8.1 Scales and environments which can be investigated using these tracing methodologies

8.1.1 How the methods reported on in this thesis perform at varying spatial and temporal scales and environments

The methodologies presented here allow the same method to be used at a variety of scales, both temporally and spatially. For example, Chapter 5 demonstrates how sub-millimetre movements by soil particles can be detected, as well as how these movements can be resolved at sub-second time scales. Chapter 7 demonstrates how the same technology can be used on a plot in excess of 10 m in length to elucidate movement of tracer both horizontally and vertically in response to tillage. The environments which are being investigated are also very different; Chapter 5 details how the fluorescent sand tracer method can be used on a highly simplified and controlled environment, where rainfall, soil type and slope (among other things) can be easily controlled. In contrast, in Chapter 6, the same basic technique is used in an agricultural field where there is no control over environmental conditions. These chapters also illustrate how the fluorescent tracing method can be used to investigate different means of soil movement: water erosion in Chapter 5 and tillage in Chapter 6. The laboratory environments used here were all simplifications of real-life soil systems, although the systems investigated are larger and more realistic than those for which particle tracking experiments have been described previously, for example (Long et al. 2014). Field experiments in Chapter 6 demonstrated how the tracer could be deployed in a 'real' environmental setting. The techniques that have been developed are highly flexible which

allows them to operate well across this a wide range of temporal scales. For example, Chapter 5 demonstrates how data relating to the location of tracer particles can be captured every 0.02s (Chapter 5). In Chapter 4, a sub-second resolution was not desired, but rather a more coarse (seconds) resolution was all that was required. The technique was easily able to capture data relating to clay tracer location with images being captured every 7 seconds. If higher resolution data is captured than is desired or required, then it may be possible to reprocess the data at a lower resolution. For example, Figure 5.4 shows the speed of a particle with a 0.1 s time resolution, despite the data being originally collected at 0.02 s resolution. In terms of spatial resolution, the techniques also operate well across a range of scales. The HD video footage in Chapter 5 is sufficient for the sub mm resolution desired over a relatively small are, although using 4K or higher resolution camera would have allowed for a larger area to be imaged at the same resolution should this be desired or required. By varying the recording device used, it is possible to gain data at almost any scale and resolution, although large scale high resolution data is much harder and more expensive to obtain than low resolution small scale data. An anecdotal example of this would be when I captured single low quality, low resolution and small scale image of a soil box with tracer in it using a smartphone with a coloured glass filtered held over the lens. As this image was just used in a presentation to give an idea of how the system work, it was all that was required. At the other end of the scale I captured high resolution data (mm resolution) of larger areas (greater than 10 m^2) in Chapter 7 using a 16MP camera. The technique does not have an optimal resolution and preforms equally well at a many scales provided the appropriate equipment is used. This makes the technique presented here one of the most flexible methodologies that exists for understanding the movement of soil particles over a soil surface.

8.1.2 Highly resolved movement data and its uses in models

This thesis demonstrates that it is possible to collect empirical data regarding individual soil particle movement in response to rainfall (Chapter 5). For example, I have collected data

related to the speed and displacement of individual soil particles. This type of data may be useful in the design, development and evaluation of soil movement models.

Tucker and Bradley (2010) suggest that it should be possible to calculate the movement of soil particles from first principles, however, they suggest that doing so is not practical due to computational expense. They then go on to propose that the movement of soil could be treated as a 'random walk' and the modelling of such a walk would require process-level understanding of particle movement. They recommend that in order to do this one must measure transport coefficients such as "frequency, mean, and variance (or their heavy-tailed equivalents) [e.g., Ganti et al.,(2010)] of particle displacement". They conclude the paper by stating "By combining grain-scale experiments, field studies, and computer models, it may ultimately be feasible to develop a statistical physics basis for geomorphic transport laws, incorporating the full spectrum of local and nonlocal dynamics". The methods described in this thesis have the capability to deliver this type of data. Chapter 5 clearly shows that the particle tracing method is capable of operating at the grain-scale, and Chapter 6 shows the same method working at the field scale. The method has also been shown to deliver the type of data that Tucker and Bradley (2010) call for: distributions of speed and displacement of particles (Chapter 5; Figures 5.5, 5.8). In addition, the method offers the capability to provide particle movement data at sub-second temporal resolution (0.02 s in Chapter 5). As rainfall rates are likely to vary over second to minute scales, this method could allow me to gather previously unobtainable data on how changing rainfall intensity affects particle movement.

8.1.3 Temporal data and its use in models

Time resolved data on particle movement are important for validating soil erosion models (see Sections 2.8.4 for more details). My tracing method is able to deliver this type of time resolved data (e.g. Chapters 5 and 6). For example, Ma et al.'s (2008) model is capable of producing time resolved data regarding particle movement, and validation of the model

therefore requires time resolved particle movement data. They used a conventional approach to studying particle movement due to splash erosion, whereby they distributed 64 splash cups over a 5 × 5 m slope, with 16 being collected every 5 minutes. Not only was the time resolution rather coarse compared to that of Ma et al. model, but the sampling was unable to deliver key parameters e.g. they were unable to measure horizontal projected distance which is a key parameter in modelling transport of a given particle. Temporally resolved empirical data they (and other modellers) require for robust model testing could be provided by the methods shown in Chapters 5 and 6.

8.2 Size does matter

It could be said, at least for soil processes, that size does matter. It is well known that different sized particles are transported at different rates. It therefore follows that for any method to be successful at understanding the movement of soil, it must be able to operate at various particle sizes. The methods presented in this thesis are quite unique in that they are able to operate across a range of particle sizes. For example, Chapter 4 demonstrates that it is possible to use fluorescent imaging to track the smallest fraction of soil (clay), which has previous proved challenging. Doing this required the development of a novel tracer as no other suitable tracer was known. After successfully tracking the movement of clay, it became apparent that there was interest in being able to trace other fractions of soil such as the silt and sand fraction. With this in mind, the methods detailed in Chapters 5, 6 and 7 were developed to allow for other size ranges (such as silt and sand) to be traced using a commercially available tracer. Chapter 5 demonstrates that sand sized particles (~250 micron) can also be tracked, and in Chapter 6 silt sized particles (~70 microns) are tracked in a field trial. Tracers for other sized particles are available from Partrac (http://www.partrac.com/), and it is reasonable to believe that the methodologies described in this thesis would work for any size range of particles that they produce. It is known that

Partrac produce particles up to 400 µm, and larger sizes may be available upon request. However, there is still a small range of particle sizes (5-25 µm), which are hard to study. These particles are too small to be manufactured using the method developed by Partrac. Also they often lack the physical and chemical properties that would allow the methodology in Chapter 4 to be used. It would be interesting to see further work undertaken allowing the complete range of soil particle sizes to be investigated. Additionally, as these types of tracing technologies are in their infancy, there are limited data available to access the usefulness of the tracers in different soil types and for different erosive agents. For example, there are few, probably no, published data relating to the how well Partac's tracers perform in wind erosion studies. Further work where the clay tracer developed in Chapter 4 and Partrac's tracer (used in Chapters 5, 6 and 7) are used in different environments, for varying lengths of time and to study different erosive agents (i.e. wind, ice), should be considered.

8.3 Data rich soil erosion studies

Stroosnijder (2005) states that the lack of new technologies is one area that is currently holding back erosion studies. The tracing methods described in this thesis aim to help address this problem by providing a new way to collect and analyse erosion data. Stroosnijder comments on the fact that many models require large amounts of data and that it is *data* that are currently lacking. In fact, it often appears that studies try to collect the minimum number of samples to answer a given question, often based on practicalities, (for example, see Ma et al. (2008) in 8.1.2) rather than gain the best overall understanding of a system. The methods presented here offer a step towards data rich erosion studies, something which is difficult to achieve with most existing techniques due to time and resource constraints.

One of the key aspects that allows for the methods described here to move towards data rich studies is the removal of the need to physically sample soil to obtain tracer concentrations.

Sampling is a highly limiting process; both in terms of temporal and spatial resolution of data that can be collected, as well as in terms of money and time required. Leaving the current sampling-based paradigm behind offers a significant step towards providing soil scientists with data rich methods.

Data, however, are meaningless unless they can be interpreted in a useful way. Considering the huge amount of data that would be collected when the methods described in this thesis are deployed, there is a clear need to automation of data processing. This is why it was critical to develop data analysis tools alongside the development of the tracer imaging technologies. These tools allow for the large number of images that are collected to be processed in a reproducible and efficient manner, and make the data easier to interpret.

The data processing systems developed here use free and open access software, both to keep costs low and to allow for others to adapt the software to their own needs. Soil process studies are highly variable, and therefore it is very difficult to build comprehensive and effective software for every possible situation. To combat this, any software produced during this thesis has been written with flexibility in mind. It draws on many existing packages and libraries that are present in R and Python. Many of the manipulations that are carried out are basic matrix manipulations, such as averaging or summing. In the case of averaging there are many different options, such as mean (geometric or arithmetic), mode or median, and all of these options are easily available. It is this flexibility which has already allowed for the techniques to be adapted for different purposes. As an example, in Chapter 6, a technique was trialled for water driven erosion in the laboratory and then adapted for use in a tillage erosion field trial.

8.4 Method cost.

As stated in section 2.7.4 both the set-up and running cost of a method must be considered, with minimal cost being preferred. While there are costs associated with the methods

presented in this thesis, they are limited to a few thousand pounds in total. The equipment used to collect the images is readily available, and utilises consumer grade lighting, electronics and cameras.

The tracers that were used are also affordable. The clay tracer used in Chapter 4 is made from inexpensive montmorillonite clay and rhodamine, both of which are commercially available at minimal cost. Quotations from commercial companies suggest that it would be possible to produce the tracer at £20 kg^{-1}. Partrac's tracer (used in Chapters 5 and 6) is generally more expensive, but comes with the advantage of being available from a commercial supplier.

8.5 Assessment of the methods presented in this thesis

8.5.1 Tracer clay likeness

The novel clay tracer detailed in Chapter was based on the features an ideal tracer would have (Chapter 2). One of these features was that a tracer should mimic the behaviour of the material that it is attempting to trace. Assessment of how successfully this has been achieved is difficult, but it is reasonable to assume that the closer the material is (i.e. physical and chemical properties) to the material which it is designed to trace, the better it will perform. In this respect, the clay tracer should work very well, as it is made from the same material (natural clay) as the material that it attempts to trace. Testing how similar the chemical and physical properties of clay tracer are to native clay may be difficult depending on the property being tested. Some properties such as size are easily tested using a Mastersizer, (see SI 3 Tracer size in Appendix 1), and physical shape can be tested using a microscope (see Figure 4.3). Chemical properties such as cation exchange capacity could be tested using a standard cation exchange test. The addition of rhodamine to the clay is not expected to significantly alter the properties of clay, as it is assumed that it replaces the cations which are normally bound to the clay. The amount of rhodamine that is added is very small in

comparison to the amount of clay used, which means any changes in the clay's physical properties (for example density) will be minimal. Clays typically in size vary from <2 μm to <5 μm (Jackson et al. 1948) and it is therefore clear that the tracer described in Chapter 4 is of a size range which would be classified as clay (Chapter 4 SI 3: Tracer size).

8.5.2 Partrac's sand sized tracer

The sand size tracer used in Chapters 5, 6 and 7 that was produced by Partrac (http://www.partrac.com/) may offer a reasonable likeness to sand. The tracer uses a single particle of sand as a core for each tracer particle, which is then coated with a thin layer of fluorescent material. This fluorescent material will not have the same properties as the exterior of a sand particle, although there may be reasonable similarity. Sand contains quartz particles and comparison of these particles to the fluorescent tracer particle may help to evaluate their similarity to each other. The exterior of a quartz crystal is hard and reasonably inert properties which the fluorescent coating used by Partrac also possess. However, there are differences, as the fluorescent tracer particles are smooth and rounded, whereas quartz crystals are often irregularly shaped with angular edges.

8.5.3 Distinguishing the tracer from other material

The tracer must be easy to distinguish from non-tracer material and in this area the clay tracer performs well. There are few, if any, natural materials within soil which mimic the fluorescent properties of rhodamine, and the detection system is tuned to these fluorescent properties. The combination of monochromatic green excitation light (532nm) and the use of a filter to prevent light less than 570nm entering the camera, make the detection system very sensitive. The main reason for this high sensitivity is the lack of background noise as there are few, perhaps no, other materials commonly found in soil which will be detected by this system. The background that does exist comes from the high sensitivity of the CMOS sensors which are capable of detecting very low levels of light, eliminating background would be

extremely difficult due to the presence of stray light and the triggering of sensors by heat and other variables.

There have been times when other materials have been reflective enough to cause them to be confused with the tracer. This was observed then using the green Partrac tracer in the field (Chapter 6). The soil contained many rocks, some of which were reasonably large and therefore remained on the pit wall surface when small amounts of surrounding soil were picked away during preparation of the profile. This resulted in rocks that were reasonably clean, with large flat surfaces that were reflective. Some of the reflected light was able to bleed through the filters and activate the sensor. In this work, no effort was made to remove, or account for these features although a number of options are detailed in Chapter 6.

Rocks on the surface of the field presented less of an issue. This is probably because there are fewer of them; farmers tend to pick them up and remove them from fields as they break tilling and drilling equipment. Also, the rocks on the surface of the field had not been cleaned in the same way as those in the soil pits, which made them less reflective. Additionally, there was less light per unit area in the images of the soil surface than the images of the pit faces. The intensity of the lighting was reduced as much as possible for the pit images, but it was not possible to get the intensity as low as would have been desired. In general, for soil surfaces in the field, the opposite problem had been encountered; it was difficult to get enough light in the area to capture useful images so all the LEDs where hardwired to run at maximum brightness. In the future, with the use of PWM (pulse width modulation) it should be easy to accurately and cheaply control the brightness of the LEDs, which would allow for better images to be taken.

8.5.4 Ephemeral tracers

Guzman et al (2013) called for the development of “ephemeral” tracers, which means tracers that have a limited lifespan. Ephemeral tracers should exist in the environment for the time

taken required to perform a given study and then should degrade so that the area can be used again without background tracer being present. In some ways, the ability to undertake non-destructive in situ sampling, such as the methodology described here, removes this need. For example, if a study area had been used a year earlier and there was still tracer present on it then this could be quantified at the start of the experiment. Once the amount and location of tracer was known, more tracers could be added to certain areas if required. However, there is still merit in attempting to not fill the world with tracers that will last forever! The clay tracer described in Chapter 4 is likely to be an ephemeral tracer. Rhodamine B is known to photodegrade and it would be reasonable to expect the tracer to have degraded within a couple of years. The Partrac tracer is expected to be longer-lived, but similarly to all fluorophores, it will degrade over time.

8.6 Designing new tracing methodologies

8.6.1 Current tracing methods lack resolution

In Chapter 5, I state that desire to put soil into plastic bags is a major limiting factor to progress in soil science, and I still hold that belief. However, when this thesis is viewed as a whole, it becomes apparent that there is an even more overarching issue. Most, perhaps all, existing tracing methods lack spatial and temporal resolution that is commensurate with the spatial and temporal redistribution of soil. Chapters 4 and 5 demonstrate that soil is subject to redistribution on timescales of less than 1 minute and distances of less than 1 cm, however few, if any, methods operate at this resolution. If a system cannot be studied on the temporal and spatial scales at which it operates, then this is going to limit the depth of understanding that can be gained about a system. Boardman (2006) states that commonly used methods for quantification of soil loss result in measurements by weight ($t^{-1}\,ha^{-1}\,yr^{-1}$) or volume ($m^3\,ha^{-1}\,y^{-1}$). These measurements are not very satisfactory, as they fail to account for the material's pathway during redistribution.

8.6.2 Current method development

After reviewing the literature around tracer and tracing methodologies (Chapter 2) it became apparent that vast majority of tracer methodologies that are currently used are essentially opportunistic tracing methodologies, with ^{137}Cs and REEs being the classic examples. There *happened* to be a release of ^{137}Cs into the environment, and we *happened* to have a way of easily detecting ^{137}Cs, or we *happen* to be able to buy REE and we *happen* to be able to detect them using ICP-MS. From there, it seems that these methods have evolved by finding the path of least resistance between the tracer and detection method. Running a gamma detector in a field is difficult and expensive, so soil is put in plastic bags and brought to the detector (with the same being true for many other tracing techniques). It could be argued that current methods have evolved without much regard for the type of data that is required to gain a deeper understanding of soil movement, for example how far the redistributed material travels. Rather, these methods simply aim to glean any information possible about soil movement. There is nothing wrong with this approach and clearly a start must be made somewhere. However, perhaps it is time to start developing methods designed to operate on scales which are commensurate with soil redistribution.

8.6.5 Designing new tracing methodologies

There is an alternative way to approach tracing and this approach has helped shape this thesis (Figure 8.1). The ideas contained within Figure 8.1 were developed, in some form, as my PhD thesis progressed. However, complete crystallisation of them did not occur until well into the writing up stage of my thesis. They are, in some sense, my theories on how future soil tracing methods can be developed and draw on what I have learnt over the last 3 years. Perhaps it is best to view them as a speculative review of the overall findings of this PhD which focuses on method development. Until now, most of this thesis has focused on how my methods work and the data they can produce, whereas this section gives a speculative

formalisation as to how future methods in soil tracing could be designed. I will illustrate how this approach works, in a practical sense, with examples that draw from this thesis.

i) Firstly, a goal or issue to be investigated is identified; i.e. to understand the movement of individual particles on a soil surface, the aim of Chapter 5 in thesis.

ii) The type of data that is required to achieve the aim is elucidated. For example, highly temporally and spatially resolved data is required to monitor the movement of individual particles on a soil surface, as is a way of displaying it.

iii) Then there should be consideration for any constraints within which the method must operate, i.e. how much time and money is available to undertake these types of studies. For example, the cost of the tracer should be considered. The field trial in Chapter 6 gives an example of how erosion studies are often undertaken and therefore the constraints that a system must operate within. Here, two people were in the field for 4 days resulting in limited time and manpower to achieve the goal. These types of constraints are common in erosion studies, and therefore the methods in this thesis were designed to acquire data rapidly, and to be able to operate with minimal manpower.

iv) Now technologies which are capable of acquiring the desired data must be identified, and methods must be considered which will allow for the technology to be successful deployed. In this thesis, this process was assisted by a critical review of current tracing methods (Chapter 2). This identified that the combination of a digital camera and fluorescent tracers was likely to be capable of giving the desired data.

v) The final step was to create a proof of concept system that showed the method would deliver data which are of the required resolution and quality. Chapter 4 serves as a good example of this type of proof of concept.

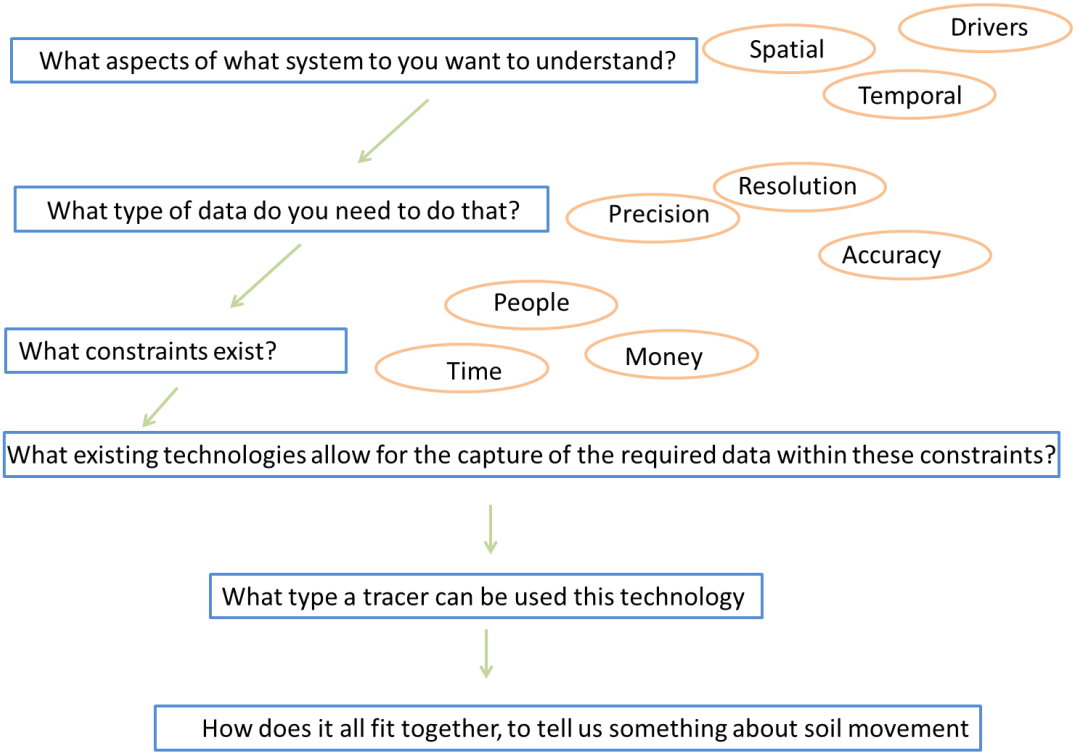

Figure 8.1. A graphical representation of the methodology that helped shape this thesis. The blue boxes shown give a statement for consideration and the orange circles give a selection of the type of things which may need to be considered.

8.6.6 Time for a synergistic view

Based on my experience in this PhD, the key to successful methodology design is to view the method as a whole, and the whole may be more than the sum of its parts. In a synergistic method, various elements of the method enhance each other rather than work against each other. For example, the use of a camera was key, as it captures data at the required resolution but also provides an easy-to-process format. In this way, the data acquisition part of the method is working with the data analysis part of the method. This contrasts sharply with many existing methods; in many existing methods the data acquired is of sub-optimal resolution and in a poor format, resulting in the requirement of more resources for the data analysis part of the method. A good illustration of how methods are often not designed synergistically is the ^{137}Cs method. In the ^{137}Cs method there are many steps between what is measured and the data that is required. Firstly, concentrations of ^{137}Cs are measured at various depths and locations in the study site, which requires collection of many samples for

which the ^{137}Cs activity concentration is subsequently measured. This results in a collection of spectra for each sample location with no inherent spatial metadata; to obtain location data, a GPS device can be deployed and depth data gathered using a ruler. This results in some digital data i.e. electronic spectra, and some analogue data such as depth data; none of which is inherently tied together. In comparison, images, such as those in Chapter 4, have inherent spatial information i.e. pixels, which have easily described locations using the rows and columns of the image. Pixel location was used to track the movement of clay (Chapter 4) and individual particles (Chapter 5). Equally, many cameras are capable of geo-tagging (such as the GH4 use in Chapter 6), which gives a GPS reference of where the image was taken and is stored in the EXIF data inside the image file. Temporally, almost all cameras record the time and date that a given image was captured, and I used this information to temporally resolve the movement of clay in Chapter 4. Also, the exact camera settings, such as ISO, shutter speed and f-stop used to take the image are also recorded, making it easy to select images that are taken with the same settings and are therefore more easily comparable. Furthermore, all these data are digital and contained within the image file itself, allowing easy access via graphical or command line programs. By contrast, the ^{137}Cs method spectra must be drawn together to create ^{137}Cs depth profiles. This can be achieved by comparing sample and reference sites profiles, with the difference between the sample and reference sites being (presumably) the result of soil movement. If a geographical method of examining the data is desired, then geographical data must be inputted and a map of soil redistribution made. Using the methods I have developed, it is possible to visually to compare images of the same site straight from the camera or to analyse various areas of the images using software I have created. Equally, as GPS data is contained within the image, GIS software can be used to overlay the image onto a map.

8.7 The need for darkness

It has been commented on by many that the need for the darkness is a considerable limitation of the method. However, this may not be as limiting as one would expect. Most tracing methods require collection of soil samples which, to be carried out effectively, requires light. Daylight generally works well for this, just as night-time generally works well for my methods and on average there are no more hours of light than there are darkness. There may be seasonal variation in the relative day length for a given area, if that area is located away from the equator. However, over the course of a year the number of hours of daylight and night will be roughly equal. If one wishes to collect soil samples at night then one must use artificial light, which can vary from using a handheld flashlight to large floodlights, depending on what is required. Equally, if one wishes to record fluorescent images in the daytime then the area must be "blacked-out". How difficult this is to achieve depends on the nature and area that one wishes to image, but the soil pits imaged in Chapter 7 (Figure 7.2) where imaged by placing a black cloth over the pit when the camera was inside. The pits where too small to frame the images using the viewfinder so this was done using a remote control on a tablet. Very little additional time was taken as a result of the need to use the black cloth. I would estimate that it took less than 1 extra minute per pit. There are circumstances where blacking out the area to be imaged is going to present significant challenges, such as if the movement of tracer in response to rainfall in the day (rather than in the night) is desired. However, I would argue that in the majority of cases, the solution is simple; just do the experiment at night. There may be cases where there is good reason for expecting soil movement during a night rainstorm to be different to that of a day rainstorm, but this is not likely to be the case most of the time. It would appear that the need for darkness is not really a limitation of the method any more than the need for daylight is for sampling based methods.

8.8 Concluding remarks

Clearly, much work has been undertaken using various existing tracing methods and much has been learnt. However, there is a limit to what can be understood without high resolution data which is commensurate with the temporal and spatial scales on which soil movements operate. The methods described in this thesis will hopefully open up the possibility for data rich soil movement studies. The data rich environment will allow for a better understanding of how soil redistribution processes operate, and could allow for the parameterisation and validation of many existing soil models.

Chapter 9: Conclusion

9.1 Thesis aims

9.1.1 Thesis aim one

One aim of this thesis was to "develop *in situ*, non-destructive fluorescence-based methods for the quantification of tracer on a soil surface" and this has been achieved, albeit in different ways, in every chapter. Chapter 4 tackles the issue of quantification of tracers on a soil surface by enabling quantification of the location of the tracer. This is a theme which continues on in Chapter 5, which shows it is possible to locate individual tracer particles to millimetre precision. Chapter 6 continues to build on this by allowing for the not only the quantitative determination of tracer particles' locations, but also by providing two independent methods for determining the concentration of tracer particles within a given area. Every chapter quantifies the tracer temporally as well as spatially, through the use of time lapse photography (Chapters 4 and 6) and videography (Chapter 5). The use of videography offers the highest level temporal resolution at a frame rate of 50 s^{-1}, although much higher resolutions are possible if a camera capable of higher frame rates is used.

9.1.2 Thesis aim two

The second aim of this thesis was to "test these methods in both laboratory and field-based scenarios". This has been achieved through extensive laboratory tests of both the clay tracer and the green Partrac (~250 µm) tracer and their associated methodologies. One of the main aims of the laboratory testing was to understand the uncertainties associated with the methodology. Generally, it was found that the uncertainties where small when compared to those that are often accepted in soil science. Chapter 6 shows that these methodologies can also be used in the field; in Chapter 6 the green Partrac tracer (~70 µm) was used in a field-based tillage erosion experiment. I have shown the methodologies are capable of operating at high temporal and spatial resolutions, which was previously unachievable.

9.1.3 Thesis aim three

The final aim of this thesis was to "investigate the motion of individual particles on a soil surface under simulated rainfall conditions at very high temporal and spatial resolutions". This was achieved in Chapter 5, where the movement of individual particles (~250 µm) was monitored at sub-millimetre and sub-second resolutions. Higher resolution data capture should be possible by using a higher resolution camera (for example, 4K vs HD) or a faster frame rate (for example 120 versus 50 frames s^{-1}), although if this more detailed information is of any practical value remains to be seen.

9.2 Further work

9.2.1 Quantitative clay tracer

During my PhD, it became clear that there was demand for a clay tracer that would allow for quantitative determination of clay tracer concentrations. The clay tracer used in Chapter 4 cannot be used for quantitative determination of tracer concentrations due to self-quenching of the fluorophore (rhodamine B). However, this self-quenching process does not occur with every fluorophore. For example, tris(bipyridine)ruthenium(II) chloride (Ru-BPY) may be able

to adhere to clays, as it has similar charge characteristics to rhodamine, and it may not self-quench. This would allow determination the concentration of clay tracer present using a similar method to intensity based method in Chapter 6.

9.2.2 Simultaneous detection of multiple soil fractions

The ability to trace multiple size fractions of soil simultaneously could also be useful. This could allow for a deeper understanding of the effect that size has on particle transport, as it would be possible to analyse the movement of different sized particles under identical rainfall conditions. There are two main ways in which this could be accomplished; using size and colour. To trace fractions of soil that are very different sizes, it may be possible to utilise their difference in size to distinguish between them. For example, the trackpy library that was used extensively in Chapters 5 and 6 comes returns a parameter relating to the size of the particle detected, and this could be used to group particles of similar sizes. Another option is to use different colours for different fractions of soil. If the correct colours are selected, it might be possible to record one fraction of soil in a given colour channel on the camera (e.g. blue), and another fraction in a different colour channel (e.g. red). Another option is to use multiple cameras and lights to sequentially image the area, with each camera and lighting combination being optimised to only record a certain tracer colour. As images can be acquired in a fraction of a second and some lights (such as LEDs) are capable of being switched on and off rapidly, it should be possible to maintain reasonable temporal resolution, especially if the lighting and cameras where electronically timed, for example using a Raspberry Pi.

9.2.3 Real time monitoring of vertical redistribution

Soils, in the real world, are 3-D environments in which particles are capable of moving in every direction. Therefore, for the most complete picture of soil movement to be obtained, the way in which soil moves vertically must also be considered. Steps were taken in this

direction in Chapter 6 through the use of soil pits to analyse the vertical distribution of soil after a tillage event. However, time resolved data has yet to be obtained and real time monitoring of vertical redistribution of soil could be considered one of the last remaining hurdles in tracing.

Real-time monitoring of vertical redistribution is possible, although it is unlikely to be a straightforward task. There are a number of ways in which this could be achieved, a selection of which are discussed here. Monitoring the vertical redistribution of soil in real time will require a method that does not need soil sampling to occur. I have identified two possible options for monitoring vertical distribution, detailed below.

The first is to use the methods that I have already developed and create a "work-around" that allows for (limited) aspects of vertical redistribution to be monitored. For example, a Perspex box containing the camera and lighting equipment could be inserted into the soil and hence would allow soil touching the box to be monitored in real time. There are serious limitations to this technique as the area that can be monitored would be small and considerable perturbation to the system would occur when installing such a box.

Another option is to design an alternative method specifically for monitoring the vertical redistribution of soil in real time. This may be the only option if the studies are to be optimised for imaging large areas. In principle, the methods presented in this thesis will work, however the detection method and the signature of the tracer will need to be changed for real-time monitoring of soil vertical redistribution. For example, signatures could be created using magnetic fields or high energy photons (gamma or x-rays), which can travel though soil. Nuclear magnetic resonance (NMR, also known as MRI [magnetic resonance imaging]) is routinely used in medical imaging and can give clear 3-D picture of living structures such as the brain. NMR uses magnetic spins of nuclei as a signature which is unique to each element, signatures of elements combine together, giving every compound a unique fingerprint which

can be easily identified. There are however, significant drawbacks to using NMR. The range of the instruments used is very limited, and powerful magnets are required to generate the signatures needed for identification. Soil will have a strong NMR signature and there will almost certainly be issues with separating the signature of soil from that of the tracer, although multinuclear NMR may make this process easier. Implementation in soil science is likely to be prohibitively expensive as the instrumentation alone runs to millions, without considering the rewriting of the image processing software. Alternatively, ground penetrating radar may be an option. This technique allows for the acquisition of 3-D data and is often used to find buried objects. A tracer that was designed to be highly reflective to radar would return a strong signal compared to the background soil. Existing imaging software should be reasonably easy to adapt and already allows for 3-D image. The time taken to acquire the images varies but there is clear potential for time resolved images. The size of particles that could be detected would be limited by the frequency at which the radar operated, and it is more likely that “clouds” of particles will be detected rather than individual ones. This is similar to the way in which “clouds” of metal strips are used to confuse radar guided missiles as the missile “sees” the cloud as a single large object rather than a collection of smaller ones. Nonetheless, tracking these clouds of particles throughout the soil system could offer many new insights into how soil moves. The cost of this system would be high compared to the camera system, but significantly lower than that of NMR and is probably not prohibitive. Ground based systems are cheapest (£10,000 upwards) and offer better sensitivity than airborne systems.

9.2.4 Large scale studies using drones

If studies are to be carried out a really large scales then land based measurement techniques used in this thesis are not capable of acquiring data fast enough. Using a drone that allows for airborne illumination and imaging could offer a good solution. Drones are capable of being flown 2 m above the ground, which is the height at which the images for the for the tillage

field trial (Chapter 6) where collected. The camera that was used in Chapter 6 is capable of being lifted by a commercially available drone, and a specialised gimbal exists that helps stabilize cameras to prevent image blur. The low f-stop (1.7) of the camera lens allows for a large amount of light to enter the camera which, combined with high ISO setting (800 - 6400), allows for shutter speeds be kept high, which would help keep images clear. The LED arrays that are used in the lighting system are capable of being powered by a drone battery and weigh very little. It is likely that the air flow from the drone rotors will be sufficient to cool the LEDs. Additionally, LEDs are capable of rapid pulsing which could allow for them to only emit light for a fraction of a second that is required to take a picture. This would reduce power consumption of the LEDs to a very low level.

9.3 In conclusion

Overall, this thesis demonstrates that there is a place for high resolution, data rich tracing methodologies in the future of soil science. There is merit in developing new tracing methodologies which involve the development of new instrumentation (i.e. modified cameras and special lighting rigs) as well as new ways of processing data to numerically and graphically represent the movement of individual particles over a soil surface.

Appendix 1- supporting information for: A novel fluorescent tracer for real-time tracing of clay transport over soil surfaces (Chapter 4)

Robert A. Hardy[1], *Jacqueline M. Pates*[1], *John N. Quinton**[1], *Mike P. Coogan*[2]

[1]Lancaster Environment Center, Lancaster University, Bailrigg, LA1 4YQ

[2]Chemistry Department, Lancaster University, Bailrigg, LA1 4YQ

* corresponding author: j.quinton@lancaster.ac.uk

Number of pages: 9

Number of figures: 4

Number of tables: 2

SI 1: Camera setup

The camera used was a Canon 500d fitted with an EF 50mm f/1.8 II lens. The camera was autofocused under artificial lights then switched to manual focus to prevent the camera from refocusing under low light conditions. A coloured glass filter (Optical Knight 570 nm 570FC5550 long-pass) was taped to the UV filter ring. Images were acquired using no flash and the following setting: exposure time 6 s, f-stop 1.8, ISO 800, RAW + JPEG at highest quality. An intervalometer (Shoot) with an interval of 7 seconds was used to acquire successive images.

SI 2: Laser lighting setup

The laser used was a 532 nm green laser with a nominal output of 75 mW driven by a 3.3 V DC power supply. Low voltage DC power was used on safety grounds. The laser diode was heat sunk in order to achieve more stable lighting.

The laser beam was passed through a diffuser (Thorlabs ED1-S20-MD), which has a very high efficiency (~ 90%) while providing near Lambertian diffusion. The diffuser was mounted on a bearing and rotated using an electric motor (Maplin sn35q) and a pulley system (Figure S1b). The diffuser was rotating at approximately 100 rpm. The rotating diffuser reduced the interference pattern often seen in laser light (Figure S2).

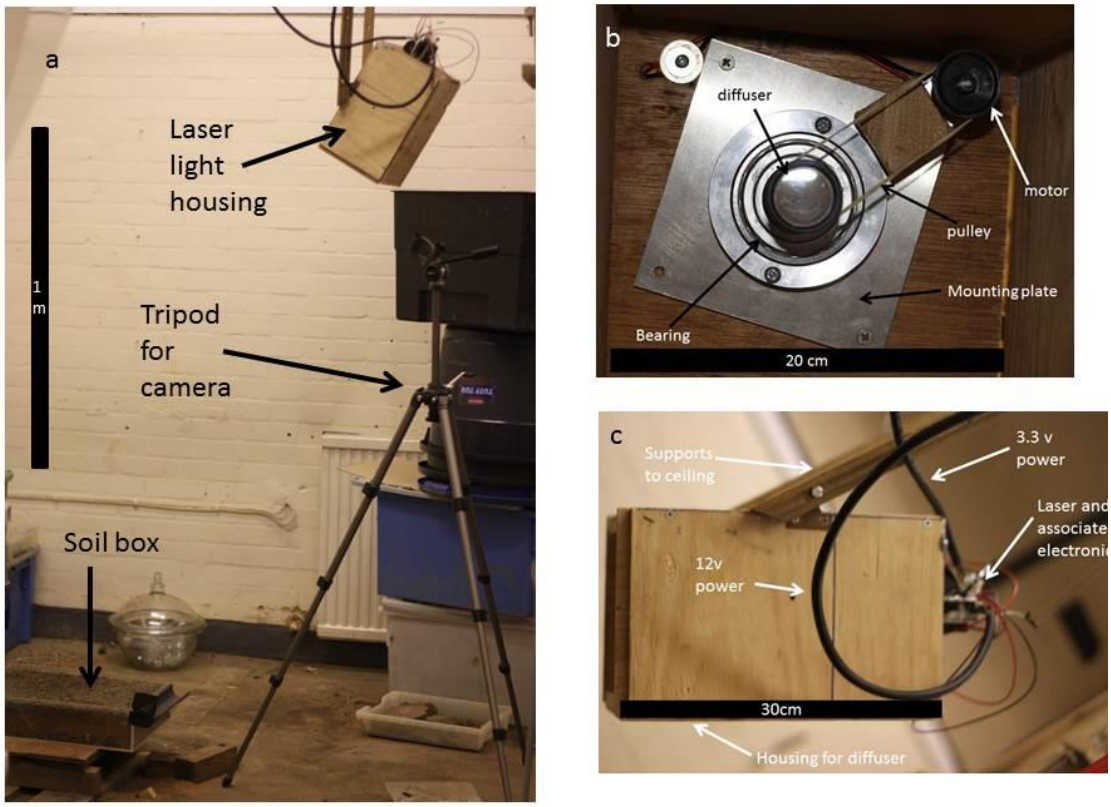

Figure S1: Lighting and camera set-up used to record images. a: Overall view of the set-up (rainfall simulator is just out of frame at top of image). b: Close-up of system used to rotate diffuser. c: Close-up of laser lighting housing.

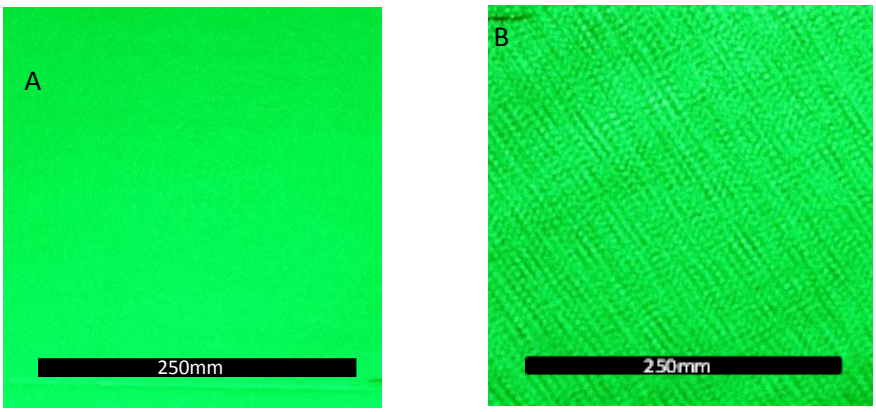

Figure S2: Images of the laser light used to illuminate the soil box. a: While the diffuser is rotating. b: Without rotating the diffuser.

SI 3: Tracer size

The size distribution of the clay particles was analysed before and after coating with Rhodamine. The data in Tables S1 and S2 suggests that addition of Rhodamine does not increase the size of the particles. The slight increase in the amount of clay-sized material (less than 2 μm) after tagging is thought to be due to the action of the ultrasonic bath used in synthesis, which causes some disaggregation of the clay particles.

The proportion of material in each size class was calculated from the cumulative data (Table S2). The normality of this new data set was tested using a Shapiro-Wilk test. The *p*-values were found to be 2.015×10^{-4} for the tracer and 1.182×10^{-5} for the clay before treatment; therefore the data were assumed to be not significantly different from a normal distribution. A *t*-test was performed, giving a *p*-value of 1.00. Therefore, it can be assumed that the two sets of data are not significantly different from one another.

Table S1: Size distribution of clay samples, before and after coating with Rhodamine.

Sample Name	**< 2.000 μm (%)**	**< 4.000 μm (%)**	**< 10.000 μm (%)**
Clay before tagging	51.46	77.35	91.44
Clay before tagging	51.51	77.33	91.44
Clay before tagging	51.53	77.30	91.43
Clay before tagging: mean ± SD	51.50 ± 0.03	77.330± 0.03	91.435 ± 0.009
Clay tracer	55.24	79.35	94.37
Clay tracer	55.28	79.39	94.37
Clay tracer	55.33	79.44	94.41
Clay tracer: mean ± SD	55.279 ± 0.045	79.392 ± 0.042	94.39 ± 0.02

Table S2: The percentage of material that is less than the given size fraction.

Size fraction (µm)	Clay before treatment (%)	Tracer (%)	Size fraction (µm)	Clay before treatment (%)	Tracer (%)
0.479	0	0.96	7.586	88.29	91.36
0.550	0	3.37	8.710	89.97	93.00
0.631	0	7.00	10.000	91.43	94.39
0.724	0	11.57	11.482	92.72	95.55
0.832	1.29	16.81	13.183	93.86	96.52
0.955	5.88	22.50	15.136	94.90	97.31
1.096	14.79	28.48	17.378	95.84	97.96
1.259	24.74	34.63	19.953	96.67	98.49
1.445	33.81	40.87	22.909	97.42	98.90
1.660	41.95	47.09	26.303	98.08	99.23
1.905	49.12	53.19	30.200	98.64	99.48
2.188	55.77	59.05	34.674	99.09	99.67
2.512	62.00	64.53	39.811	99.43	99.80
2.884	67.56	69.55	45.709	99.67	99.88
3.311	72.25	74.06	52.481	99.84	99.94
3.802	76.10	78.05	60.256	99.94	99.97
4.365	79.25	81.54	69.183	100	99.99
5.012	81.90	84.57	79.430	100	100
5.754	84.24	87.18	91.201	100	100

SI 4: Images

In order to make the images acceptable for publication some editing was required. JPEG images are not accepted so conversion into tiff format at 300dpi was required. The contrast was adjusted to compensate for differences between images viewed on the screen and in print. This was done to create images that were as reader-friendly as possible. All image analysis was carried out from the original images.

SI 5: Rapid imaging

Images can be taken in 0.8 s (Figure S3), using the same settings as described in SI 1: Camera setup, but with an ISO setting of 3200 and an exposure time of 0.8 s. The original images are very hard to interpret, but the false colour images clearly show where the tracer is. Increased noise is also present. Increasing the power of the laser should allow better quality rapid images to be produced if desired. The write speed of the camera also limits the number of images that can be recorded. Reducing the imaging resolution (to 2352 x 1568 pixels) and quality (standard) increases the number of images that can be recorded. Images cannot be captured in RAW mode.

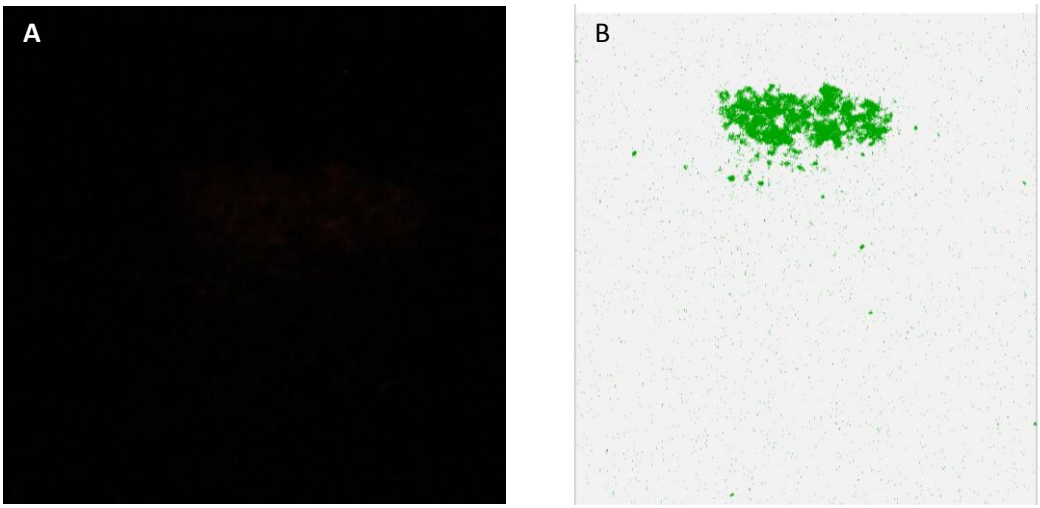

Figure S3: A demonstration of the image quality when sub-second exposure times are used. a: The true colour image. b: The false colour image.

SI 6: Image processing

The JPEG images (from the camera) are read using [R] and the package "jpeg", which reads the colour channels separately. The code selects the red image channel, as Rhodamine emits a mainly red light. The green channel contains some data, but it is very noisy, and the blue channel contains almost entirely noise. The red channel is read as a matrix, which then then has a noise suppression function applied to it. The user can define the extent of the noise suppression by adjusting the value of the object "noise_threshold", between the values 0 and 1. Experimentally it has been found that values in the 0.05 to 0.3 range work best. Higher numbers results in a greater degree of noise reduction, but care must be taken to avoid the addition of artefacts as a result of overly aggressive noise suppression. Any pixel with a value greater than "noise_threshold" is coloured green and anything less is coloured white. The matrix is converted to a raster class object (using the "raster" package) and cropped to the correct size. This raster image is then converted back into a matrix.

Using only the red channel from the JPEG images, a false colour image has been created (Figure 4), which shows presence or absence of tracer. The noise suppression level is set by adjusting the object "noise_threshold" as described previously. The images have then been combined into a time-lapse film using VirtualDub (version 1.10.4). Annotated code is available on request.

SI 7: Image acquisition time

On a Windows-based computer system the time that an image is taken can be determined from the file's properties. However, this only displays information with minute (rather than second) precision. mtime (modification time) was taken as the time the images were acquired as ctime (creation time) changes when the files are copied onto from one location to another. An annotated copy of the code used is in SI-

computer code. The program has not been tested on UNIX systems (i.e. Linux or Mac) and may not run correctly. Using mtime is only accurate if the images are not modified after they are created (for example opening and then saving the image can change the modification time).

SI 8: Computing requirements

Efforts have been made to allow the code to be run on the average desktop. A Dell Precision T3500 was used for the analysis presented here. The computer had an Intel Quad-Core Xeon processor (64 bit) with Hyper-Threading, although the usefulness of this feature is unknown as [R], generally, is single-threaded. The computer had 12 GB of RAM and was running Windows 7 Enterprise. The code was trialled on a 32 bit Dell Optiplex 390 (3.5 GB of RAM, Windows 7 Enterprise), but would often crash due to insufficient memory. If the error message "unable to allocate a vector of size…" is seen then a lack of memory is usually the issue. The version of [R] used was [R] x64 3.1.0. All packages were the most recent release from CRAN.

SI 9: Runoff

The runoff was analysed to determine if dissolved Rhodamine was responsible for the fluorescence seen in the images. The runoff was filtered, and the filters imaged using the standard settings (Figure S4). The images are not qualitatively different from those seen in Figure 4.

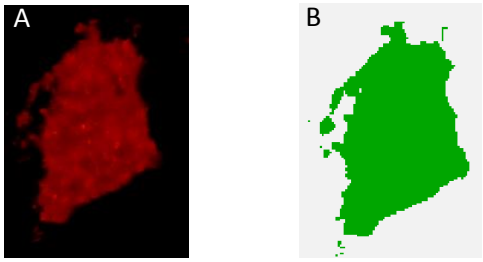

Figure S4: Particulate matter recovered from runoff. (A) True colour image showing the recovered tracer. (B) False colour image of the tracer.

SI 10: Tracking tracer spread

During the soil transport experiments, images were collected every 7 s. These were converted to false colour images, as described in SI 6: Image processing. Quantitative data about the movement of the tracer across the soil surface were then extracted from the images. The images were in matrix form, with a number representing each pixel.

SI 10.1: Tracer front

The tracer front is defined as the furthest extent of the tracer up and down slope on the soil surface. Each row in the image matrix was summed, and compared to a threshold value (object "tracer_threshold"), which was chosen to represent sufficient intensity to be considered tracer. Any positive value can be used as a threshold, but values from 50 to 150 have been shown to work well. The larger the number the greater the amount of tracer needed in a matrix row before that row is considered to have tracer in it. All of the matrix rows that have tracer in them were extracted and the largest and smallest row number found. These represent the tracer front at the top and bottom of the box. This function was then run on all of the images and the results are stored in a CSV file, containing the image names, the tracer front at the top of the box and the tracer front at the bottom of the box. Annotated code is available on request.

SI 10.2: Lateral spread

The lateral spread of the tracer was tracked in a similar way to the tracer front, but analysing column rather than row data. This analysis shows that the tracer does not just move down the slope, but also moves laterally. Annotated code is available on request.

SI 10.3: Tracer area

The area that the tracer occupied was estimated by counting the number of pixels that show tracer, i.e. those with a value (intensity) of greater than 0, giving the area of the image where tracer is present. The proportion of the image occupied by tracer, relative to the total image area, can also be calculated, which may be useful if images of different sizes are being compared. Annotated code is available on request.

Appendix 2 - Supporting information for: Using real time particle tracking to understand soil particle movements during rainfall events (Chapter 5)

Robert A. Hardy,[1] Michael R. James,[1] Jacqueline M. Pates,[1] and John N. Quinton[1]*

[1]Lancaster Environment Center, Lancaster University, Lancaster, LA1 4YQ, U.K.

* Corresponding author: John Quinton (j.quinton@lancaster.ac.uk)

Contents of this file

Text S1 to S2

Figures S1 to S2

Additional Supporting Information (Files uploaded separately)

Captions for Movies S1 to S1

Introduction

Here I provide more detail of certain aspects of the paper than was appropriate for the research article. In particular, there is information about the video of the particles moving and images extracted from this video which appear to show the particles "hopping".

Text S1.

Movie S1 is the raw video footage obtained during the experiment. It was shot in full HD at 50 frames per second, resulting in 5 minutes of footage requiring over 1Gb of space. Requiring viewers to download a file of this size was not considered practical so the video was compressed using ffmpeg by reducing the pixel count in the video, removing the audio channel and changing the file format. The original height of the video was 1080 pixels, which was reduced to 718 pixels, and the format was changed from .MTS to .MP4. These changes have resulted in some degradation of the images and therefore it is not recommended that this file is used for analysis. However, it has made the file smaller (less than 4 Mb) and therefore more suitable for displaying on the web. The blue dots that appear in the video are believed to be reflections of the blue illumination light used to stimulate fluorescence. Preprocessing the images removes these artefacts. When displayed in the default orientation the left-right axis on the screen is the uphill-downhill axis in the soil box, with the left-hand edge being the higher.

A clear example of a particle moving by various mechanisms (i.e. hopping and rolling) can be seen in the top right of the video from 4:12-4:45. Here the same particle makes repeated hops (both up and down slope), which are followed by rolls. These rolls are of various lengths; some are almost imperceptible, whilst other motions appear to span

many mm. I suggest that the longer rolls are the result of the particle interacting with shallow overland flow.

Captions for Movie S1

The raw video footage filmed during the experiment. The blue dots that appear after the rain has started appear to be pooled water on the surface reflecting the blue illumination lighting. Currently held at https://youtu.be/bdxngLIigLo

Text S2.

Figure S2 shows 4 consecutive frames from the video which have been cropped to show a single particle. The video was shot at 50 frames per second meaning that each frame represents the particle's position for no more than 0.02 s. The true time represented by the frame is unknown but is likely to be less than 0.02 s due to the time it takes the shutter to open and close. Based on the particle's size it has moved between 0.5 and 1 mm. There is strong evidence that it is one particle moving rather than a particle being uncovered while another is covered up. Firstly, given the small number of particles present it is highly unlikely that one particle will be covered at exactly the same time as another is uncovered. Furthermore, one dot appears to fade as the other strengthens in colour. There is also a slight streaking of colour between the two dots in the same way that a photograph can become streaked if an object moves while the shutter is open. Together, these pieces of evidence mean that it is highly likely that these two dots are the same particle.

There is also evidence that the particle travelled through the air rather than along the ground. The streaky line between two dots (most clearly seen in Figure S2b) is almost perfectly straight, something which is unlikely if the particle was travelling over a

rough surface like soil. In Figure S2c the same streak is present, although it has faded and the particle appears to have subtly changed direction (it is heading more towards the left than before). This observation is consistent with the particle striking the rough soil surface and starting to roll with the change in direction being caused by the uneven nature of the soil. This type of behaviour is observed multiple times during the experiment, with this example being one of the clearest.

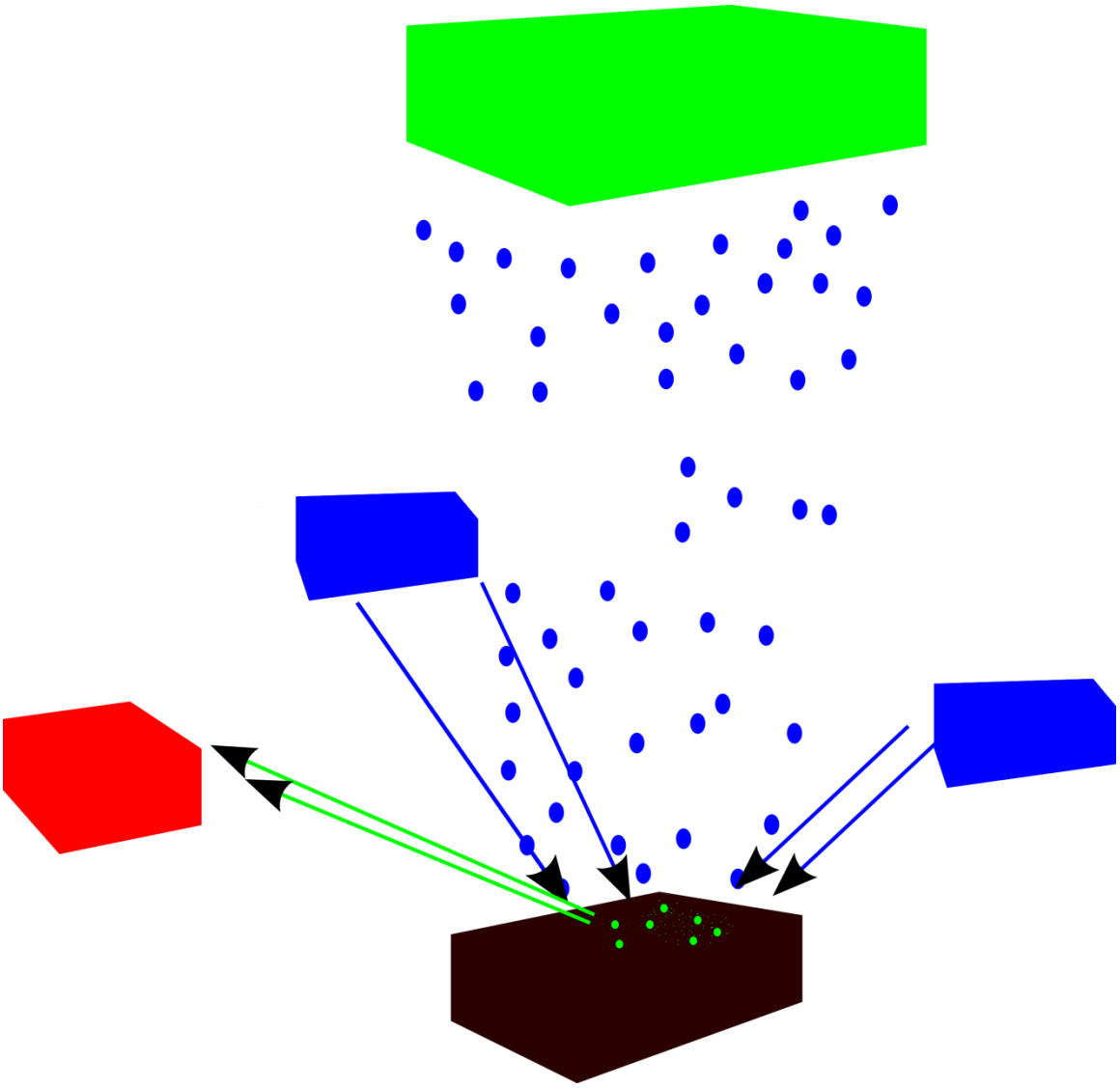

Figure S1. A schematic of the setup used to image the movement of the tracer. The brown box is the soil box, the blue rectangles are the lights with the blue arrows showing the direction of the light, and the blue dots are rain drops, which originate from the rainfall simulator (green box). The green arrows show the pathway of the green light emitted by the tracer, that is detected by the camera (red box).

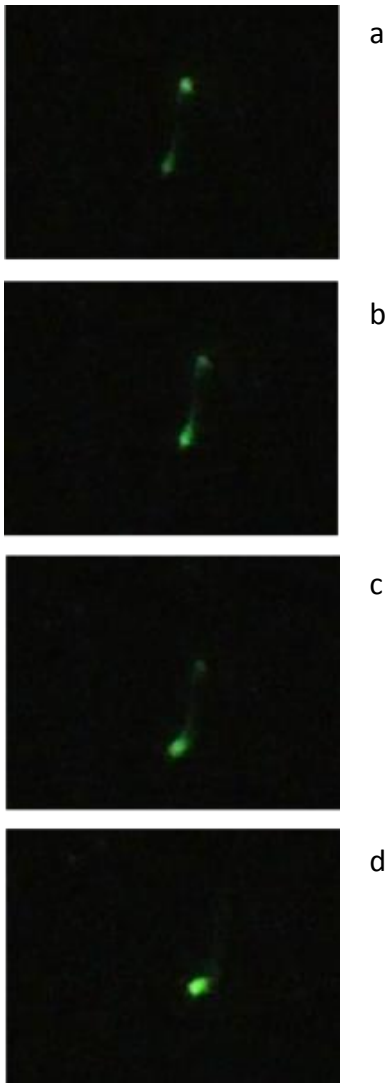

Figure S2. A hop shown frame by frame, in which the particle moves instantly from one location to another.

Appendix 3- Supporting information for: Quantitative LED induced fluorescence tracing (qLIFT): A tool for low cost high resolution soil tracing? (Chapter 6 and 7)

Lighting

Each lamp had four circular LED arrays, where each array had four LEDs, giving 16 LEDs on each lamp, and a total of 32 LEDS. Each circular LED array was driven by a dedicated constant current driver (12V at 0.7 W). The LED arrays mount was heat sunk using aluminium sheeting and cooled with forced air flow (SI Figure 1). The same lamps were used for all the imaging of soil on surface, however the orientation of the lamps when compared to the camera does vary mainly for practical reasons. The orientation in the field box trials can be seen in Figure 4 and in Figure SI 2. The camera and the lights were mounted on a lighting boom, two metres above and parallel to the ground. 12V lead acid batteries were used in the field in lieu of a 12V constant voltage supply that was used in the lab. The lamps and the camera were separated in the lab for greater flexibility but were mounted together in the field for greater portability. For imaging of the soil pits, 3 of the 4 LEDs were removed from the lamp to reduce the intensity of the lighting as the camera is much closer to the soil.

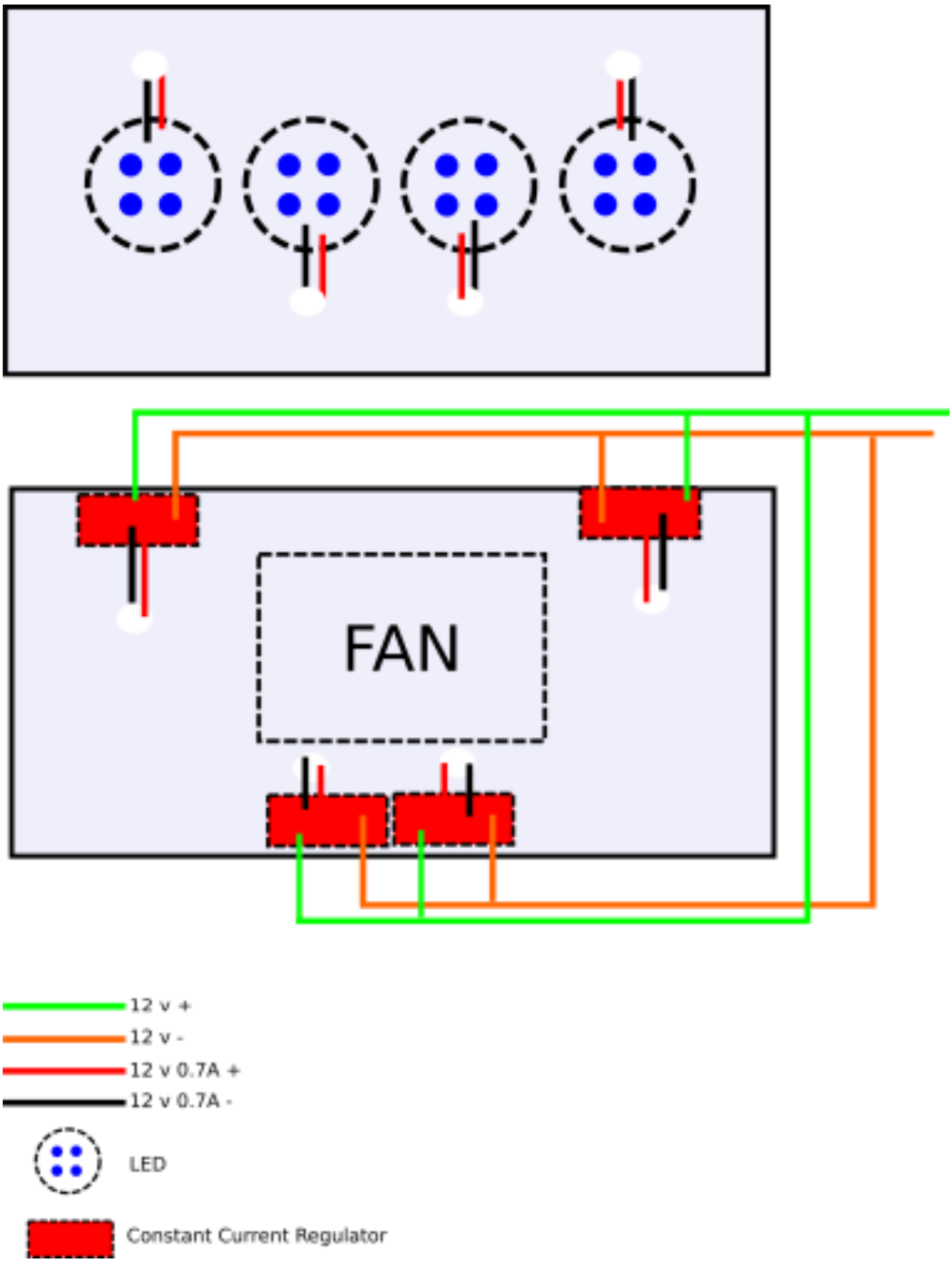

SI Figure 1. Schematic showing top and bottom of the LED lamps used to illuminate the area to be imaged. Diffusing plate not shown for clarity

Laboratory setup

SI Figure 2 gives an impression of the setup used in the Laboratory experiments. These conditions were designed to resemble a bare and recently tilled agricultural felid. This setup was used to take the images seen in Figure 6.2.

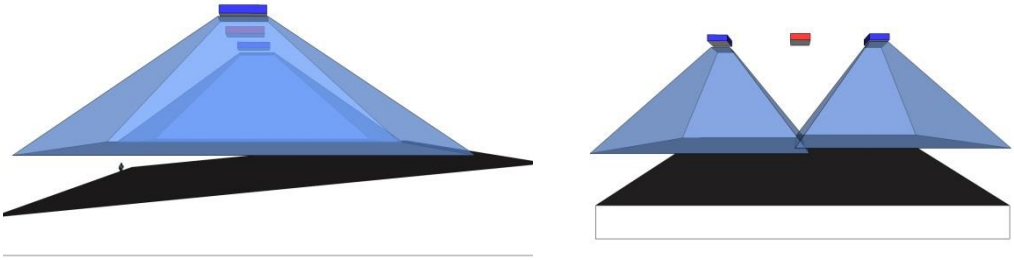

SI Figure 2. Schematic of the simulated field plot. Red box represents the camera, solid blue the LED lamps, and black the soil surface. The translucent blue area provides a schematic where the majority of the light falls. Not to scale.

Distance from camera

There appears to be no relationship between the distance from the camera that a spot is and the intensity of that spot, when an orthoimage is taken. The differences in distance are small but are representative of the differences likely to be seen in images produced using this methodology. If there is concern that there are differences in intensity due to distance from the camera of different objects in the same image then this test can then be repeated under the same conditions as the image was taken. This can give an idea as to the extent of the variation in intensity due to the difference in distance of the objects.

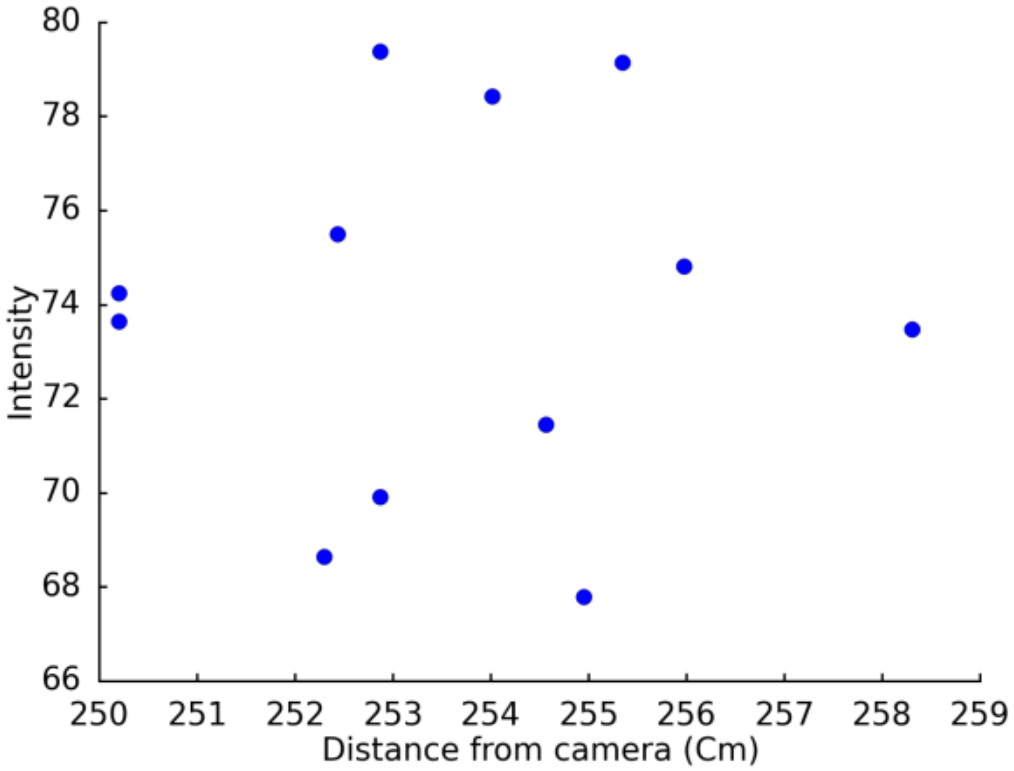

SI Figure 3. Variation of mean intensity of tracer spots with distance from camera. Note the lack of relationship.

Method comparison

Under certain conditions it is possible to assess the concentration of the tracer using both the particle counting method and the intensity method. SI Figure 3 shows one of these cases, where there is a clear linear relationship between the two sets of data. These are the same data as seen in the main text in Figure 12.

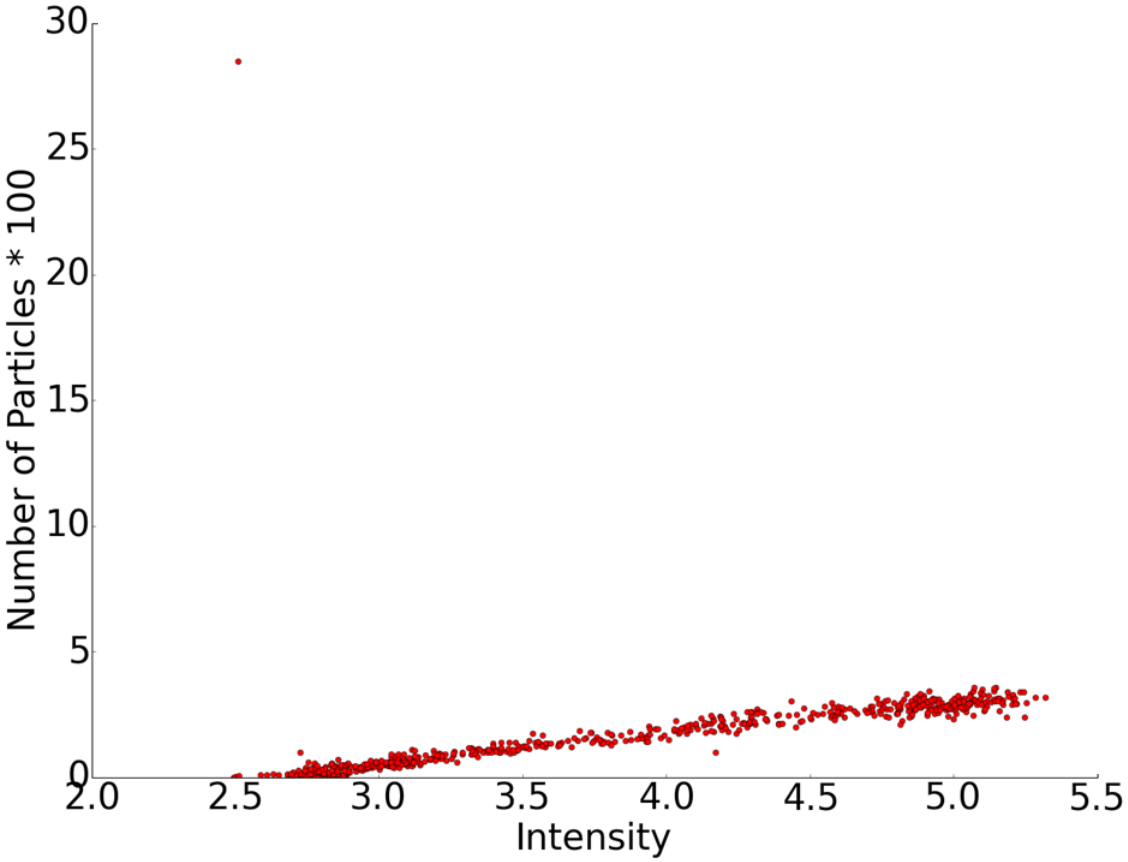

SI Figure 4. The relationship between intensity data and particle counting data. Note the strong linear relationship. The single large outlier is likely to be erroneous. It is likely that the outlier is the first point in the time series for which number of particles was abnormally high. This may be due to camera movement in the first few seconds of the experiment causing problems with the particle detection.

Field trial

The particle counting technique was applied to the same areas as the intensity method. The results suggest the method performed poorly in areas where there are a high concentration of particles. This is probably due to the lack of space between particles, which makes identification of individual particles difficult. As the concentration decreased the results look similar to those using the intensity method and there is a clear decline in the number of particle from 18 metres onwards. It appears that there is overlap in the concentrations of particles that the techniques are capable of analysing.

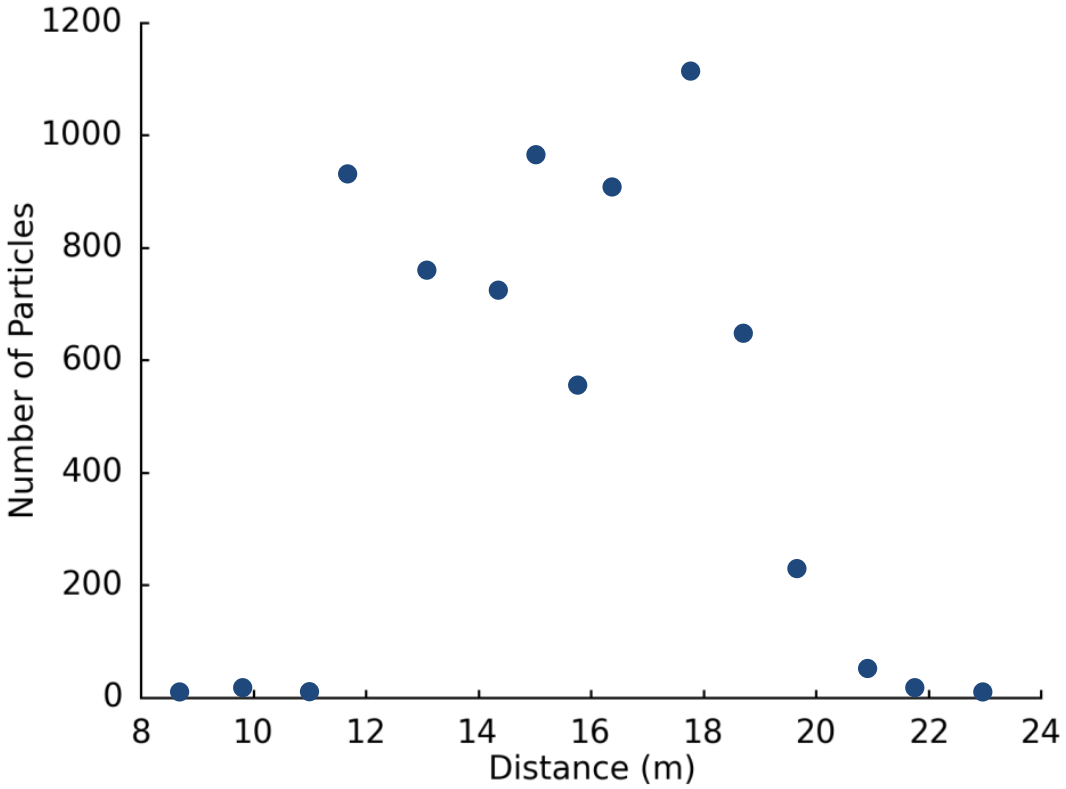

It was also possible to combine the images into a photomosaic to give an overall impression of the distribution of the tracer down the plot (SI Figure 6). These images have been degraded from the original image quality in order to make the file size manageable and therefore were not used for quantitative analysis. The false colour image (SI Figure 6 B) is not at the same resolution as the true colour image due to the image process that took place to obtain the image, therefore there may be small difference between the two images. These images should be treated as illustrative.

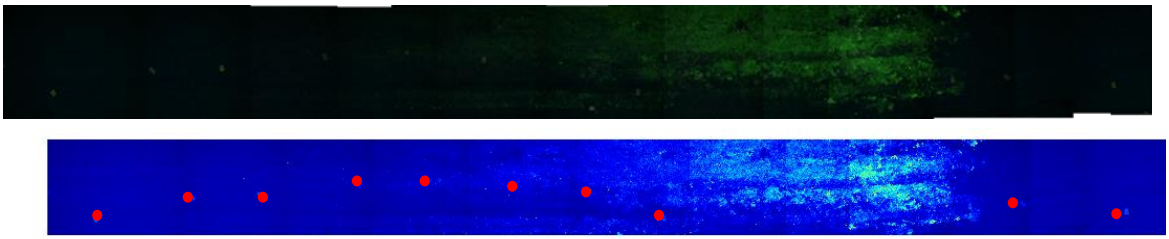

SI Figure 6. A) An illustrative photomosaic of the plot. The area photographed is about 15m long and 2m wide. The vertical banding is an artefact from the stitching together of images. B) as A) but in false colour with some of the markers that were placed in the field are highlighted using a red dot. These markers show the sampling locations used in Figure 11 and SI Figure 4, although it should be noted that some of the markers have not been shown when a marker is present in an area of high tracer concentration. This is to preserve the overall impression that the image gives

References

Akbarimehr, M. and R. Naghdi (2012). "Assessing the relationship of slope and runoff volume on skid trails (Case study: Nav 3 district)." Journal of Forest Science **58**(8): 357-362.

Armstrong, A., J. N. Quinton, B. C. P. Heng and J. H. Chandler (2011). "Variability of interrill erosion at low slopes." Earth Surface Processes and Landforms **36**(1): 97-106.

Armstrong, A., J. N. Quinton and B. A. Maher (2012). "Thermal enhancement of natural magnetism as a tool for tracing eroded soil." Earth Surface Processes and Landforms **37**(14): 1567-1572.

Bakker, M. M., G. Govers, C. Kosmas, V. Vanacker, K. van Oost and M. Rounsevell (2005). "Soil erosion as a driver of land-use change." Agriculture Ecosystems & Environment **105**(3): 467-481.

Beija, M., C. A. M. Afonso and J. M. G. Martinho (2009). "Synthesis and applications of Rhodamine derivatives as fluorescent probes." Chemical Society Reviews **38**(8): 2410-2433.

Black, K., J. Sloan and T. Gries (2013). Everything goes somewhere; tracking the movement of contaminated sediments in an industrialised estuary using dual signature sediment tracers. Tracer 6 - the 6th International Conference on Tracers and Tracing Methods. A. Haugan. Cedex A, E D P Sciences. **50**.

Black, K. S., S. Athey, P. Wilson and D. Evans (2007). "The use of particle tracking in sediment transport studies: a review." Geological Society, London, Special Publications **274**(1): 73-91.

Blake, W. H., D. E. Walling and Q. He (2002). "Using cosmogenic beryllium–7 as a tracer in sediment budget investigations." Geografiska Annaler: Series A, Physical Geography **84**(2): 89-102.

Bollinne, A. (1978). "Study of importance of splash and wash on cultivated loamy soils of Hesbaye (Belgium)." Earth Surface Processes and Landforms **3**(1): 71-84.

Bostick, B. C., M. A. Vairavamurthy, K. G. Karthikeyan and J. Chorover (2002). "Cesium adsorption on clay minerals: An EXAFS spectroscopic investigation." Environmental Science & Technology **36**(12): 2670-2676.

Bradshaw, C., L. Kumblad and A. Fagrell (2006). "The use of tracers to evaluate the importance of bioturbation in remobilising contaminants in Baltic sediments." Estuarine Coastal and Shelf Science **66**(1-2): 123-134.

Burkhardt, M., R. Kasteel, J. Vanderborght and H. Vereecken (2008). "Field study on colloid transport using fluorescent microspheres." European Journal of Soil Science **59**(1): 82-93.

Catt, J. A., K. R. Howse, R. Farina, D. Brockie, A. Todd, B. J. Chambers, R. Hodgkinson, G. L. Harris and J. N. Quinton (1998). "Phosphorus losses from arable land in England." Soil Use and Management **14**: 168-174.

Chasteen, T. G. "Relaxation mechanism for excited state molecules." Retrieved 22 Sept, 2016, from http://www.scimedia.com/chem-ed/quantum/jablonsk.htm.

Cloern, J. E., S. Q. Foster and A. E. Kleckner (2014). "Phytoplankton primary production in the world's estuarine-coastal ecosystems." Biogeosciences **11**: 2477-2501.

Collins, A. L., Y. S. Zhang, D. Duethmann, D. E. Walling and K. S. Black (2013). "Using a novel tracing-tracking framework to source fine-grained sediment loss to watercourses at sub-catchment scale." Hydrological Processes **27**(6): 959-974.

Cooper, J. R., J. Wainwright, A. J. Parsons, Y. Onda, T. Fukuwara, E. Obana, B. Kitchener, E. J. Long and G. H. Hargrave (2012). "A new approach for simulating the redistribution of soil particles by water erosion: A marker-in-cell model." Journal of Geophysical Research-Earth Surface **117**.

Dearing, J. A., R. I. Morton, T. W. Price and I. D. L. Foster (1986). "Tracing Movements of Topsoil by Magnetic Measurements - 2 Case-Studies." Physics of the Earth and Planetary Interiors **42**(1-2): 93-104.

Deasy, C. and J. N. Quinton (2010). "Use of rare earth oxides as tracers to identify sediment source areas for agricultural hillslopes." Solid Earth **1**(1): 111-118.

Debus, B., D. Kirsanov, I. Yaroshenko, A. Sidorova, A. Piven and A. Legin (2015). "Two low-cost digital camera-based platforms for quantitative creatinine analysis in urine." Analytica Chimica Acta **895**: 71-79.

Delon, G., D. Terwagne, S. Dorbolo, N. Vandewalle and H. Caps (2011). "Impact of liquid droplets on granular media." Physical Review E **84**(4): 046320.

Dhawale, N. M., V. I. Adamchuk, S. O. Prasher, R. A. V. Rossel, A. A. Ismail and J. Kaur (2015). "Proximal soil sensing of soil texture and organic matter with a prototype portable mid-infrared spectrometer." European Journal of Soil Science **66**(4): 661-669.

Diaz, C. A., Y. Xia, M. Rubino, R. Auras, K. Jayaraman and J. Hotchkiss (2013). "Fluorescent labeling and tracking of nanoclay." Nanoscale **5**(1): 164-168.

Duke, M. J. M., A. F. Plante and W. B. McGill (2000). "Application of INAA in the characterisation and quantification of Dy-labeled ceramic spheres and their use as inert tracers in soil studies." Journal of Radioanalytical and Nuclear Chemistry **244**(1): 165-171.

Elimelech, M. (1995). Particle deposition and aggregation : measurement, modelling, and simulation. Oxford England ; Boston, Butterworth-Heinemann.

Ellison, W. D. (1944). "Studies of raindrop erosion." Agric. Eng. **25**: 131-136.

Foufoula-Georgiou, E., V. Ganti and W. E. Dietrich (2010). "A nonlocal theory of sediment transport on hillslopes." Journal of Geophysical Research: Earth Surface **115**(F2).

Furbish, D. J., E. M. Childs, P. K. Haff and M. W. Schmeeckle (2009). "Rain splash of soil grains as a stochastic advection-dispersion process, with implications for desert plant-soil interactions and land-surface evolution." Journal of Geophysical Research: Earth Surface **114**(F3): n/a-n/a.

Furbish, D. J., K. K. Hamner, M. Schmeeckle, M. N. Borosund and S. M. Mudd (2007). "Rain splash of dry sand revealed by high-speed imaging and sticky paper splash targets." Journal of Geophysical Research: Earth Surface **112**(F1): n/a-n/a.

Gerino, M., R. C. Aller, C. Lee, J. K. Cochran, J. Y. Aller, M. A. Green and D. Hirschberg (1998). "Comparison of different tracers and methods used to quantify bioturbation during a spring bloom: 234-thorium, luminophores and chlorophyll a." Estuarine Coastal and Shelf Science **46**(4): 531-547.

Govers, G. and G. Rauws (1986). "Transporting capacity of overland flow on plane and on irregular beds." Earth Surface Processes and Landforms **11**(5): 515-524.

Guzman, G., V. Barron and J. A. Gomez (2010). "Evaluation of magnetic iron oxides as sediment tracers in water erosion experiments." CATENA **82**(2): 126-133.

Guzman, G., J. N. Quinton, M. A. Nearing, L. Mabit and J. A. Gomez (2013). "Sediment tracers in water erosion studies: current approaches and challenges." Journal of Soils and Sediments **13**(4): 816-833.

Hardy, R. A., J. M. Pates, J. N. Quinton and M. P. Coogan (2016). "A novel fluorescent tracer for real-time tracing of clay transport over soil surfaces." CATENA **141**: 39-45.

Haygarth, P. M., L. M. Condron, A. L. Heathwaite, B. L. Turner and G. P. Harris (2005). "The phosphorus transfer continuum: Linking source to impact with an interdisciplinary and multi-scaled approach." Science of the Total Environment **344**(1–3): 5-14.

Heng, B. C. P., G. C. Sander, A. Armstrong, J. N. Quinton, J. H. Chandler and C. F. Scott (2011). "Modeling the dynamics of soil erosion and size-selective sediment transport over nonuniform topography in flume-scale experiments." Water Resources Research **47**.

Hijmans, R. J. (2014). Raster: Geographic data analysis and modeling. http://CRAN.R-project.org/package=raster

Homenauth, O. P. and M. B. Mcbride (1994). "Adsorption of aniline on layer Silicate clays and an organic soil." Soil Science Society of America Journal **58**(2): 347-354.

Hudson, N. W. (1965). The influence of rainfall on the mechanics of soil erosion: with particular reference to Southern Rhodesia MSc Thesis, University of Cape Town

ITPS, F. a. (2015). Status of the World's Soil Resources (SWSR) – Main Report. F. a. A. O. o. t. U. Nations and a. I. T. P. o. Soils. Rome, Italy, FAO and ITPS.

Jackson, M. L., S. A. Tyler, A. L. Willis, G. A. Bourbeau and R. P. Pennington (1948). "Weathering Sequence of Clay-Size Minerals in Soils and Sediments. I. Fundamental Generalizations." The Journal of Physical and Colloid Chemistry **52**(7): 1237-1260.

Jarvis, N. J., K. G. Villholth and B. Ulen (1999). "Modelling particle mobilization and leaching in macroporous soil." European Journal of Soil Science **50**(4): 621-632.

Jomaa, S., D. A. Barry, A. Brovelli, G. C. Sander, J. Y. Parlange, B. C. P. Heng and H. J. Tromp-van Meerveld (2010). "Effect of raindrop splash and transversal width on soil erosion: Laboratory flume experiments and analysis with the Hairsine-Rose model." Journal of Hydrology **395**(1-2): 117-132.

Katsuragi, H. (2011). "Length and time scales of a liquid drop impact and penetration into a granular layer." Journal of Fluid Mechanics **675**: 552-573.

Kimoto, A., M. A. Nearing, X. C. Zhang and D. M. Powell (2006). "Applicability of rare earth element oxides as a sediment tracer for coarse-textured soils." CATENA **65**(3): 214-221.

Kinnell, P. I. A. (1988). "The Influence of Flow Discharge on Sediment Concentrations in Raindrop Induced Flow Transport." Australian Journal of Soil Research **26**(4): 575-582.

Kinnell, P. I. A. (2005). "Raindrop-impact-induced erosion processes and prediction: a review." Hydrological Processes **19**(14): 2815-2844.

Knapen, A., J. Poesen, G. Govers, G. Gyssels and J. Nachtergaele (2007). "Resistance of soils to concentrated flow erosion: A review." Earth-Science Reviews **80**(1-2): 75-109.

Lakowicz, J. R. (2006). Principles of fluorescence spectroscopy. New York, Springer.

Lal, R. (2003). "Soil erosion and the global carbon budget." Environment International **29**(4): 437-450.

Leguedois, S., O. Planchon, C. Legout and Y. Le Bissonnais (2005). "Splash projection distance for aggregated soils: Theory and experiment." Soil Science Society of America Journal **69**(1): 30-37.

Lisle, I. G., C. W. Rose, W. L. Hogarth, P. B. Hairsine, G. C. Sander and J. Y. Parlange (1998). "Stochastic sediment transport in soil erosion." Journal of Hydrology **204**(1–4): 217-230.

Long, E. J., G. K. Hargrave, J. R. Cooper, B. G. B. Kitchener, A. J. Parsons, C. J. M. Hewett and J. Wainwright (2014). "Experimental investigation into the impact of a liquid droplet onto a granular bed using three-dimensional, time-resolved, particle tracking." Physical Review E **89**(3): 032201.

Long, K. D., H. Yu and B. T. Cunningham (2014). "Smartphone instrument for portable enzyme- linked immunosorbent assays." Biomedical Optics Express **5**(11): 3792-3806.

Ma, T., C. H. Zhou, T. X. Zhu and Q. G. Cai (2008). "Modelling raindrop impact and splash erosion processes within a spatial cell: a stochastic approach." Earth Surface Processes and Landforms **33**(5): 712-723.

Mabit, L., M. Benmansour and D. E. Walling (2008). "Comparative advantages and limitations of the fallout radionuclides Cs-137, Pb-210(ex) and Be-7 for assessing soil erosion and sedimentation." Journal of Environmental Radioactivity **99**(12): 1799-1807.

Mabit, L., K. Meusburger, E. Fulajtar and C. Alewell (2013). "The usefulness of 137Cs as a tracer for soil erosion assessment: A critical reply to Parsons and Foster (2011)." Earth-Science Reviews **127**(0): 300-307.

Mahler, B. J., P. C. Bennett and M. Zimmerman (1998). "Lanthanide-labeled clay: A new method for tracing sediment transport in karst." Ground Water **36**(5): 835-843.

Mccarthy, J. F. and J. M. Zachara (1989). "Subsurface Transport of Contaminants - Mobile Colloids in the Subsurface Environment May Alter the Transport of Contaminants." Environmental Science & Technology **23**(5): 496-502.

Milori, D., L. Martin-Neto, C. Bayer, J. Mielniczuk and V. S. Bagnato (2002). "Humification degree of soil humic acids determined by fluorescence spectroscopy." Soil Science **167**(11): 739-749.

Morgan, R. P. C. (2005). Soil erosion and conservation. Malden, MA, Blackwell Pub.

Morgan, R. P. C., J. N. Quinton, R. E. Smith, G. Govers, J. W. A. Poesen, K. Auerswald, G. Chisci, D. Torri and M. E. Styczen (1998). "The European Soil Erosion Model (EUROSEM): A dynamic approach for predicting sediment transport from fields and small catchments." Earth Surface Processes and Landforms **23**(6): 527-544.

Mukai, H., A. Hirose, S. Motai, R. Kikuchi, K. Tanoi, T. M. Nakanishi, T. Yaita and T. Kogure (2016). "Cesium adsorption/desorption behavior of clay minerals considering actual contamination conditions in Fukushima." Sci Rep **6**: 21543.

Nearing, M. A. and J. M. Bradford (1985). "SINGLE WATERDROP SPLASH DETACHMENT AND MECHANICAL-PROPERTIES OF SOILS." Soil Science Society of America Journal **49**(3): 547-552.

Nearing, M. A., L. Deerascough and J. M. Laflen (1990). "Sensitivity analysis of the Wepp Hillslope Profile Erosion Model." Transactions of the Asae **33**(3): 839-849.

Nefzaoui, E. and O. Skurtys (2012). "Impact of a liquid drop on a granular medium: Inertia, viscosity and surface tension effects on the drop deformation." Experimental Thermal and Fluid Science **41**: 43-50.

Nielsen, M. H., M. Styczen, V. Ernstsen, C. T. Petersen and S. Hansen (2011). "Distribution of bromide and microspheres along macropores in and between drain trenches." Vadose Zone Journal **10**(1): 345-353.

Ollesch, J., S. L. Drees, H. M. Heise, T. Behrens, T. Bruning and K. Gerwert (2013). "FTIR spectroscopy of biofluids revisited: an automated approach to spectral biomarker identification." Analyst **138**(14): 4092-4102.

Parsons, A. J. and I. D. L. Foster (2011). "What can we learn about soil erosion from the use of Cs-137?" Earth-Science Reviews **108**(1-2): 101-113.

Parsons, A. J., Y. Onda, T. Noguchi, J. Patin, J. Cooper, J. Wainwright and N. Sakai (2014). "The use of RFID in soil-erosion research." Earth Surface Processes and Landforms **39**(12): 1693-1696.

Parsons, A. J., J. Wainwright and A. D. Abrahams (1993). "Tracing sediment movement in interill overland-flow on a semiarid grassland hillslope using magnetic-susceptibility." Earth Surface Processes and Landforms **18**(8): 721-732.

Pelletier, J. D. (2012). "Fluvial and slope-wash erosion of soil-mantled landscapes: detachment- or transport-limited?" Earth Surface Processes and Landforms **37**(1): 37-51.

Petrofanov, V. L. (2012). "Role of the soil particle-size fractions in the sorption and desorption of potassium." Eurasian Soil Science **45**(6): 598-611.

Pimentel, D., C. Harvey, P. Resosudarmo, K. Sinclair, D. Kurz, M. Mcnair, S. Crist, L. Shpritz, L. Fitton, R. Saffouri and R. Blair (1995). "Environmental and Economic Costs of Soil Erasion and Conservation Benefits." Science **267**(5201): 1117-1123.

Plante, A. F., M. J. M. Duke and W. B. McGill (1999). "A tracer sphere detectable by neutron activation for soil aggregation and translocation studies." Soil Science Society of America Journal **63**(5): 1284-1290.

Poesen, J., B. v. Wesemael, G. Govers, J. Martinez-Fernandez, P. Desmet, K. Vandaele, T. Quine and G. Degraer (1997). "Patterns of rock fragment cover generated by tillage erosion." Geomorphology **18**(3): 183-197.

Polyakov, V. O. and M. A. Nearing (2004). "Rare earth element oxides for tracing sediment movement." CATENA **55**(3): 255-276.

Polzehl, J. and K. Tabelow (2007). "Adaptive smoothing of digital images: the R package adimpro." Journal of Statistical Software **19**(1): 1-17.

Pryce, O. (2011). Development of environmental tracers for sediments and phosphorus. Environmental science, Lancaster University.

Quijano, L., S. Begueria, L. Gaspar and A. Navas (2016). "Estimating erosion rates using Cs-137 measurements and WATEM/SEDEM in a Mediterranean cultivated field." Catena **138**: 38-51.

Quinton, J. N. and J. A. Catt (2007). "Enrichment of heavy metals in sediment resulting from soil erosion on agricultural fields." Environmental Science & Technology **41**(10): 3495-3500.

Quinton, J. N., J. A. Catt and T. M. Hess (2001). "The selective removal of phosphorus from soil: Is event size important?" Journal of Environmental Quality **30**(2): 538-545.

Reeuwijk, L. P. v. (2002). Procedures for Soil Analysis. Technical Paper no. 9. (First edition 1986) (Second edition 1987) (Third edition 1992) (Fourth edition 1993). (Fifth edition 1995). (Sixth edition 2002). Wageningen, The Netherlands., ISRIC.

Rinnan, R. and Å. Rinnan (2007). "Application of near infrared reflectance (NIR) and fluorescence spectroscopy to analysis of microbiological and chemical properties of arctic soil." Soil Biology and Biochemistry **39**(7): 1664-1673.

Ritchie, J. C. and J. R. McHenry (1990). "Application of radioactive fallout caesium-137 for measuring soil erosion and sediment accumulation rates and patterns: A review." J. Environ. Qual. **19**(2): 215-233.

Rossel, R. A. V., R. N. McGlynn and A. B. McBratney (2006). "Determing the composition of mineral-organic mixes using UV-vis-NIR diffuse reflectance spectroscopy." Geoderma **137**(1-2): 70-82.

Royall, D. (2001). "Use of mineral magnetic measurements to investigate soil erosion and sediment delivery in a small agricultural catchment in limestone terrain." CATENA **46**(1): 15-34.

Sadeghi, S. H. R., M. B. Seghaleh and A. S. Rangavar (2013). "Plot sizes dependency of runoff and sediment yield estimates from a small watershed." CATENA **102**: 55-61.

Sauer, M., J. Hofkens and J. Enderlein (2011). Handbook of fluorescence spectroscopy and imaging : from single molecules to ensembles. Weinheim, Wiley-VCH.

Selvam, P. P., S. Preethi, P. Basakaralingam, N.Thinakaran, A. Sivasamy and S. Sivanesan (2008). "Removal of rhodamine B from aqueous solution by adsorption onto sodium montmorillonite." Journal of Hazardous Materials **155**(1–2): 39-44.

Shapiro, L. G. and G. C. Stockman (2001). Computer vision. Upper Saddle River, NJ, Prentice Hall.

Sharpley, A. N., S. J. Smith, B. A. Stewart and A. C. Mathers (1984). "Forms of phosphorus in soil receiving cattle feedlot waste." Journal of Environmental Quality **13**(2): 211-215.

Smith, J. T. and N. A. Beresford (2005). Chernobyl :catastrophe and consequences. Chichester, UK, Springer.

Stevens, C. J. and J. N. Quinton (2008). "Investigating source areas of eroded sediments transported in concentrated overland flow using rare earth element tracers." CATENA **74**(1): 31-36.

Stroosnijder, L. (2005). "Measurement of erosion: Is it possible?" CATENA **64**(2–3): 162-173.

Sumner, M. E. (2000). Handbook of soil science. Boca Raton, Fla, CRC Press.

Sverdrup, H. U., M. W. Johnson and R. H. Fleming (1942). The oceans, their physics, chemistry, and general biology. New York,, Prentice-Hall, inc.

Syers, J. K., T. D. Evans, J. D. Williams and J. T. Murdock (1971). "Phosphate sorption parameters of representative soils from Rio Grande Do Sul, Brazil." Soil Science **112**(4): 267-&.

Tauro, F., S. Grimaldi, A. Petroselli and M. Porfiri (2012). "Fluorescent particle tracers for surface flow measurements: A proof of concept in a natural stream." Water Resources Research **48**(6): W06528.

Team, R. C. (2013). R: A Language and Environment for Statistical Computing. http://www.R-project.org/

Tedetti, M., C. Guigue and M. Goutx (2011). Utilization of a Submersible Ultra-Violet Fluorometer for Monitoring Anthropogenic Inputs in the Mediterranean Coasts. Dordrecht, Springer.

Trackpy, C. (2010). Trackpy: Fast, Flexible Particle-Tracking Toolkit.

Tucker, G. E. and D. N. Bradley (2010). "Trouble with diffusion: Reassessing hillslope erosion laws with a particle-based model." Journal of Geophysical Research-Earth Surface **115**: F00a10.

Tyrrel, S. F. and J. N. Quinton (2003). "Overland flow transport of pathogens from agricultural land receiving faecal wastes." Journal of Applied Microbiology **94**: 87s-93s.

Urbanek, S. (2013). tiff: Read and write TIFF images. http://CRAN.R-project.org/package=tiff

van Dijk, A. I. J. M., A. G. C. A. Meesters and L. A. Bruijnzeel (2002). "Exponential Distribution Theory and the Interpretation of Splash Detachment and Transport Experiments." Soil Science Society of America Journal **66**(5): 1466-1474.

Van Rompaey, A. J. J., G. Govers, E. Van Hecke and K. Jacobs (2001). "The impacts of land use policy on the soil erosion risk: a case study in central Belgium." Agriculture, Ecosystems & Environment **83**(1–2): 83-94.

Vanhoof, C., V. Corthouts and K. Tirez (2004). "Energy-dispersive X-ray fluorescence systems as analytical tool for assessment of contaminated soils." Journal of Environmental Monitoring **6**(4): 344-350.

Ventura, E., M. A. Nearing and L. D. Norton (2001). "Developing a magnetic tracer to study soil erosion." CATENA **43**(4): 277-291.

Vos, C., A. Don, R. Prietz, A. Heidkamp and A. Freibauer (2016). "Field-based soil-texture estimates could replace laboratory analysis." Geoderma **267**: 215-219.

Wainwright, J., A. J. Parsons, E. N. Muller, R. E. Brazier, D. M. Powel and B. Fenti (2008). "A transport-distance approach to scaling erosion rates: I. Background and model development." Earth Surface Processes and Landforms **33**(5): 813-826.

Wainwright, J., A. J. Parsons, E. N. Muller, R. E. Brazier, D. M. Powell and B. Fenti (2008). "A transport-distance approach to scaling erosion rates: 2. Sensitivity and evaluation of MAHLERAN." Earth Surface Processes and Landforms **33**(6): 962-984.

Wainwright, J., A. J. Parsons, E. N. Muller, R. E. Brazier, D. M. Powell and B. Fenti (2008). "A transport-distance approach to scaling erosion rates: 3. Evaluating scaling characteristics of MAHLERAN." Earth Surface Processes and Landforms **33**(7): 1113-1128.

Walling, D. (2003). Usig envioremental radionuclides as traces in sediment budgets investigation. Erosion and sediment transport:measurement in rivers. J. Bogen, TFergus and D. Walling. wallingford. **IAHS publication 283:** 57-78.

Walling, D. E., Q. He and W. Blake (1999). "Use of (7)Be and (137)Cs measurements to document short- and medium-term rates of water-induced soil erosion on agricultural land." Water Resources Research **35**(12): 3865-3874.

Waters, J. C. (2009). "Accuracy and precision in quantitative fluorescence microscopy." The Journal of Cell Biology **185**(7): 1135-1148.

Wood, P. J. and P. D. Armitage (1997). "Biological effects of fine sediment in the lotic environment." Environmental Management **21**(2): 203-217.

Woods, S., P. P. J. Haydock, K. Evans, R. C. Robinson and T. C. K. Dawkins (1999). "Use of fluorescent tracer techniques and photography to assess the efficiency of tillage incorporated granular nematicides into potato seed-beds." Soil and Tillage Research **51**(1–2): 17-23.

Xia, X. Q., Y. Q. Mao, J. Ji, H. R. Ma, J. Chen and Q. L. Liao (2007). "Reflectance spectroscopy study of Cd contamination in the sediments of the Changjiang River, China." Environmental Science & Technology **41**(10): 3449-3454.

Yang, D. W., S. Kanae, T. Oki, T. Koike and K. Musiake (2003). "Global potential soil erosion with reference to land use and climate changes." Hydrological Processes **17**(14): 2913-2928.

Yasunari, T. J., A. Stohl, R. S. Hayano, J. F. Burkhart, S. Eckhardt and T. Yasunari (2011). "Cesium-137 deposition and contamination of Japanese soils due to the Fukushima nuclear

accident." Proceedings of the National Academy of Sciences of the United States of America **108**(49): 19530-19534.

Yin, H. and C. Li (2001). "Human impact on floods and flood disasters on the Yangtze River." Geomorphology **41**(2–3): 105-109.

Young, R. A. and R. F. Holt (1968). "Tracing soil movement with fluorescent glass particles." Soil Science Society of America Proceedings **32**(4): 600-602.

Zhang, Q., W. P. Ball and D. L. Moyer (2016). "Decadal-scale export of nitrogen, phosphorus, and sediment from the Susquehanna River basin, USA: Analysis and synthesis of temporal and spatial patterns." Science of The Total Environment **563–564**: 1016-1029.

Zhang, X. C., J. M. Friedrich, M. A. Nearing and L. D. Norton (2001). "Potential use of rare earth oxides as tracers for soil erosion and aggregation studies." Soil Science Society of America Journal **65**(5): 1508-1515.

Zhang, X. C., M. A. Nearing, V. O. Polyakov and J. M. Friedrich (2003). "Using rare-earth oxide tracers for studying soil erosion dynamics." Soil Science Society of America Journal **67**(1): 279-288.

Zhang, X. C., G. H. Zhang, B. L. Liu and B. Liu (2016). "Using cesium-137 to quantify sediment source contribution and uncertainty in a small watershed." Catena **140**: 116-124.

Zhu, W. J., C. H. Lu, F. C. Chang and S. W. Kuo (2012). "Supramolecular ionic strength-modulating microstructures and properties of nacre-like biomimetic nanocomposites containing high loading clay." Rsc Advances **2**(15): 6295-6305.

Zhuang, Y., C. Du, L. Zhang, Y. Du and S. Li (2015). "Research trends and hotspots in soil erosion from 1932 to 2013: a literature review." Scientometrics **105**(2): 743-758.